DEVELOPMENT OF EXTRACTANTS FOR THE MUTUAL SEPARATION OF LANTHANIDES AND ACTINIDES

By
A.S. SUNEESH
CHEM02201104003

Indira Gandhi Centre for Atomic Research
Kalpakkam

A thesis submitted to the

Board of Studies in Chemical Sciences
In partial fulfillment of requirements
for the Degree of

DOCTOR OF PHILOSOPHY

of

HOMI BHABHA NATIONAL INSTITUTE

August, 2016

Homi Bhabha National Institute

Recommendations of the Viva Voce Committee

As members of the Viva Voce Committee, we certify that we have read the dissertation prepared by "**Shri. A.S. Suneesh**" entitled "**Development of extractants for the mutual separation of lanthanides and actinides"** and recommend that it may be accepted as fulfilling the thesis requirement for the award of Degree of Doctor of Philosophy.

N. Sivaraman 18/9/17
Chairman – Dr. N. Sivaraman **Date:**

Antony. m p 18.9.2017
Guide / Convener – Dr. M.P. Antony **Date:**

K. A. Venkatesan 18/9/17
Technical Adviser - Dr. K.A. Venkatesan **Date:**

Ashok Khanna
Examiner - Prof. Ashok Khanna **Date:** 18/9/17

Member 1- Dr. C. Mallika C Mallika **Date:** 18.09.17

Member 2- Dr. Sharat Chandra **Date:** 18/9/17

Final approval and acceptance of this thesis is contingent upon the candidate's submission of the final copies of the thesis to HBNI.

I/We hereby certify that I/we have read this thesis prepared under my/our direction and recommend that it may be accepted as fulfilling the thesis requirement.

Date: 18.9.2017

Place: Kalpakkam

Antony. m p
Guide - Dr. M.P. Antony

STATEMENT BY AUTHOR

This dissertation has been submitted in partial fulfillment of requirements for an advanced degree at Homi Bhabha National Institute (HBNI) and is deposited in the Library to be made available to borrowers under rules of the HBNI.

Brief quotations from this dissertation are allowable without special permission, provided that accurate acknowledgement of source is made. Requests for permission for extended quotation from or reproduction of this manuscript in whole or in part may be granted by the Competent Authority of HBNI when in his or her judgment the proposed use of the material is in the interests of scholarship. In all other instances, however, permission must be obtained from the author.

Suneesh S

A.S. Suneesh

DECLARATION

I, hereby declare that the investigation presented in the thesis has been carried out by me. The work is original and has not been submitted earlier as a whole or in part for a degree / diploma at this or any other Institution / University.

Suneesh S

A.S. Suneesh

List of Publications arising from the thesis

Journal

1. "Mutual separation of americium (III) and europium (III) using glycolamic acid and thioglycolamic acid", A.S. Suneesh, K.A. Venkatesan, K.V. Syamala, M.P. Antony, P.R. Vasudeva Rao, *Radiochimica Acta*, **2012,** 100, 425-30.

2. "Development and demonstration of americium (III)-europium (III) separation using diglycolamic acid", A.S. Suneesh, R. Kumaresan,S. Rajeswari, P.K. Nayak, K.V. Syamala, K.A. Venkatesan, M.P. Antony, P.R. Vasudeva Rao, *Separation Science and Technology,* **2013**, 48, 1998-2006.

3. "Chromatographic separation of americium (III) from europium (III) using alkyl diglycolamic acid", A.S. Suneesh, K.V. Syamala, K.A. Venkatesan, M.P. Antony, P.R. Vasudeva Rao, *Separation Science and Technology*, **2015**, 50, 1213-1220.

4. "Diglycolamic acid modified silica gel for the separation of hazardous trivalent metal ions from aqueous solution", A.S. Suneesh, K.V. Syamala, K.A. Venkatesan, M.P. Antony, P.R. Vasudeva Rao, *Journal of Colloid and Interface Sciences*, **2015**, 438, 55-60.

5. "Novel Diglycolamic Acid Functionalized Iron Oxide Particles for the Mutual Separation of Eu (III) and Am (III)", A.S. Suneesh, R. Jain, , K.A. Venkatesan, M.P. Antony, BM Bhanage, P.R. Vasudeva Rao, *Solvent Extraction and Ion Exchange*, **2015**, 33, 656-670.

6. "Magnetic Assisted Separation of Trivalent F-Elements from Dilute Nitric Acid Medium", A.S. Suneesh, R. Jain, , K.A. Venkatesan, M.P. Antony, BM Bhanage, P.R. Vasudeva Rao, *Separation Science and Technology*, **2015**, 50, 2041-2050.

7. "Diglycolamic acid anchored on polyamine matrix for the mutual separation of Eu (III) and Am (III)", A.S. Suneesh, K.V. Syamala, K.A. Venkatesan, M.P. Antony, P.R. Vasudeva Rao, *Radiochimica Acta*, **2016**, 104, 11-21.

Conferences

1. Bis(2-ethylhexyl)diglycolamic acid for the mutual separation of europium(III) and americium(III) from citric acid- nitric acid medium, A.S. Suneesh, K.V. Syamala, K.A. Venkatesan, M.P. Antony, P.R. Vasudeva Rao, In: Symposium of emerging trends on separation science and technology (SESTEC). SVKM Mithibhai College, Mumbai, India, P.N. Pathak, R.M. Sawant, P.K. Mohapatra, A. Goswami, K.L. Ramakumar (eds), (2012) p-87

2. Glycolamic acids for lanthanide-actinide separation, A.S. Suneesh, K. A. Venkatesan, K. V. Syamala, M. P. Antony, P. R. Vasudeva Rao, In: International conference on vistas in chemistry (ICVC): IGCAR Kalpakkam, India, V. Ganesan, S. Antonysamy, Kitheri Joseph (eds) (2011), p-161.

3. Effect of additives on the mutual separation of lanthanides and actinides usnig glycolamic acids, A.S. Suneesh, K. V. Syamala, K. A. Venkatesan, M. P. Antony, P. R. Vasudeva Rao, In: International conference on vistas in chemistry (ICVC): IGCAR Kalpakkam, India, V. Ganesan, S. Antonysamy, Kitheri Joseph (eds) (2011), p-198.

4. Demonstration of Eu(III)-Am(III) separation in a 20-stage mixer-settler using diglycolamic acid, A. S. Suneesh, R. Kumaresan, S. Rajeswari, P. K. Nayak, K. V. Syamala, K. A. Venkatesan, M. P. Antony, P. R. Vasudeva Rao, In: Nuclear and Radiochemistry Symposium (NUCAR)-2013, Govt. Model Science College, Jabalpur, India, R. Tripathy, G.A. Rama Rao, B.S. Tomar, K.L. Ramakumar (eds), (2013), p 193.

5. N,N-Bis-octyldiglycolamic acid impregnated resins for americium (III)- europium (III) separation, A.S. Suneesh, K. V. Syamala, K.A. Venkatesan, M.P. Antony, P. R. Vasudeva Rao, In: Emerging Trends in Separation Science and Technology(SESTEC), D.K. Singh, P.K. Mohapatra, B.S. Tomar, A. Goswami, K.L. Ramakumar (eds). BARC, Mumbai, India. P-145

6. A novel glycolamic acid functionalized silica for the separation of americium (III) from europium (III), A.S. Suneesh, K. V. Syamala, K.A. Venkatesan, M.P. Antony, P. R. Vasudeva Rao, In: Emerging Trends in Separation Science and Technology(SESTEC), D.K. Singh, P.K. Mohapatra, B.S. Tomar, A. Goswami, K.L. Ramakumar (eds). BARC, Mumbai, India. P-33

7. Surface Characterization of Novel Diglycolamic Acid Functionalized Iron Oxide Particles by Raman Spectroscopy and Scanning Electron Microscopy, A.S. Suneesh, R. Kumaresan, K.A. Venkatesan, M.P.Antony, P. R. Vasudeva Rao, In: DAE-BRNS, 5th Interdisciplinary Symposium on Materials Chemistry, (ISMC-2014), December 9 – 13, 2014, Bhabha Atomic Research Centre, Mumbai – 400085, INDIA (p-153)

8. Extraction behavior of lanthanides in diglycolamic acid functionalized-polyamine matrix, G.G.S. Subrahmanian, K. V. Syamala, A.S. Suneesh, K.A. Venkatesan, M.P. Antony, In: Emerging Trends in Separation Science and Technology (SESTEC-2016), IIT Guwahati, India, May 17-21, 2016, A.C.Deb, S. Sodaye, M.S.Murali, T. Banarjee, P.K. Mohapatra, K.L.Ramakumar (eds), pp-58

Suneesh S

A.S. Suneesh

DEDICATION

Dedicated to Chachu & Sachu

Science is organized knowledge. Wisdom is organized life.
…..Immanuel Kant

ACKNOWLEDGEMENTS

I express my sincere thanks to my Ph.D supervisor Dr. M.P. Antony, for his guidance, constant support, and valuable suggestions to improve the quality of work throughout the tenure.

I take immense pleasure in thanking Dr. K.A. Venkatesan, for his keen assessment of work, support, guidance, valuable suggestions and constant encouragement.

I am pleased to express my deep sense of gratitude to Dr. S. Antonysamy, Former Dean, HBNI (Chemical Sciences, IGCAR Campus), Dr. N. Sivaraman, Dean, HBNI (Chemical Sciences, IGCAR Campus) & Doctoral committee chairman and doctoral committee members, Dr. Sharat Chandra and Dr. C. Mallika for valuable suggestions and critical evaluation of work progress.

I profoundly thank Dr. G. Paneerselvam for recording samples for XRD, Dr. N. Ramanathan for FT-IR spectra, Dr. T.S. Lakshmi Narasimhan for TG-DTA samples, Dr. R. Kumar for providing facility for radioactive tracer counting, Dr. B.M. Banage for SEM-EDX spectra and Shri. G.G.S. Subramanian for ICP-OES analysis. I also acknowledge SAIF-IIT Madras for providing NMR spectra.

I wish to record my special thanks to Smt. K.V. Syamala and Shri. Rakesh Jain for helping me in experiments.

I also wish to thank all my lab members, Shri. B. Robert Selvan, Dr. R. Kumaresan, Shri. P.K. Nayak, Dr. Alok Rout, Shri. G.G.G.Subramaniam, Smt. Amutha subha, Smt. R. Rama, Shri. Murali Krishna and Shri. K. Ramaswami for their kind help and support.

I wish to express my hearty thanks for all the members of Irradiated Fuel Studies Section, Dr. G. Panner Selvam, Smt. S. Rajeswari, Smt. T. Prathibha, Shri. G.G.S. Subramanian, Shri. T. Kalayarasu, Shri. A. Amalraj, Shri. R. Karunakaran, Shri. T. Bapuji, Smt. Amrutha Sen and Shri. Karunanidhi, for their kind support.

CONTENTS

Chapter 2: Experimental

Chapter 3: Development of materials for Ln(III)-An(III) separation by liquid-liquid extraction mode

Chapter 4: Develpment of diglycolamic acid-impregnated resins for the mutual separation of Eu(III) and Am(III)

Chapter 5: Diglycolamic acid anchored on polyamine resin for the mutual separation of Eu(III) and Am(III)

Chapter 6: Silica functionalized diglycolamic acids for Ln(III)-An(III) mutual separation

Chapter 7: Magnetic solid phase separation for the mutual separation of lanthanides and actinides

Chapter 8: Summary and scope of future studies

SYNOPSIS

1. Introduction

Nuclear energy is highly promising due to the high energy output and cost-competitiveness as compared to fossil fuel resources and other renewable sources such as wind, solar, hydel power etc [1]. Nuclear energy is essentially the power produced due to fission of super heavy elements such as uranium or plutonium. The amount of energy released per gram of uranium is 8000 times more than per gram of fossil fuel based plants [2]. In the present situation, nuclear power plants contribute 11 % of the total energy production in the world and 3 % of the total energy production in India. Though, nuclear energy has several advantages such as minimal emission of green house gases, high energy output etc., the radiotoxicity risk associated with the radioactive waste produced during reactor operation is a major challenge to the nuclear energy based power production.

Reprocessing and re-use of reactor produced plutonium and depleted uranium in future reactor facilitates the maximum utilization for the fissile content of natural uranium [3]. Recovery of plutonium and depleted uranium from spent fuel is generally performed by an industrially well-established PUREX (Plutonium Uranium Recovery by EXtraction) process. PUREX process is essentially an aqueous reprocessing method, involving dissolution of spent nuclear fuel in nitric acid medium and the recovery of fissile elements such as uranium and plutonium by the liquid-liquid extraction by a solution of 1.1 M tributyl phosphate (TBP) in *n*-dodecane. The aqueous product (PUREX raffinate) discarded after this process, known as “high-active waste” (HAW), is a complex mixture of several alpha-emitters such as americium, curium and neptunium, fission products, corrosion products of structural materials and the additives etc. Among the radionuclides present in HAW, long living alpha emitters such as americium, curium and neptunium, which are known as minor actinides, contribute to the maximum level of radiotoxicity.

Partitioning and Transmutation (P&T) is being considered as a viable strategy for the safe management of HAW [4]. It is based on the separation of minor actinides and long-lived radiotoxic fission products from HAW and transmutation into stable or innocuous products in advanced fast reactors. Partitioning of minor actinides from HAW by the current practice, liquid-liquid extraction, usually results in the co-extraction of trivalent lanthanides due to the similarity in chemical and extraction properties of lanthanides and minor actinides [5]. Since lanthanides act as neutron poisons that reduce the efficacy of transmutation process, the separation of lanthanide from minor actinides or vice-versa is necessary prior to transmutation. However, mutual separation of lanthanides and actinides is the most challenging task at the back end of fuel cycle due to the identical extraction chemistry of these elements in reprocessing streams [6, 7]. Moreover, the high concentration of nitric acid (3–4 M) prevailing in HAW also complicates the separation procedure to a great extent. However, some studies have been reported in the literature for the separation of ^{241}Am and ^{243}Cm actinides directly from PUREX raffinate. The methods include 1-cycle SANEX (Selective ActiNide Extraction), GANEX (Group ActiNide Extraction), TRUSPEAK (Trans-Uranic extraction + trivalent lanthanide actinide extraction by Phosphorous based Extractants and Aqueous Komplexing agents) approaches and SMART (Single-cycle method for partitioning of trivalent actinides using completely incinerable reagents from nitric acid medium) [5].

Another possible option for trivalent actinide partitioning is a two-cycle approach [6-8] which involves the separation of trivalent actinides and lanthanides together from the PUREX raffinate in the first cycle followed by lanthanide (Ln)-actinide (An) separation. The nitric acid concentration in the product stream varies from 0.1 M to 0.001 M. Several methods based on solvent extraction have been reported in literature for the separation of lanthanides (Ln) from actinides (An) in the aqueous raffinate obtained after the separation of americium and curium [6-8]. Kolarik *et al.* [6] studied the selective separation of Am(III) from Eu(III) using triazines such as 2,6-ditriazolyl- and 2,6-ditriazinylpyridines, from 1- 2 M nitric acid medium. Dithiophosphinic acid (DPAH), commercially available as cyanex 301, and their derivaties are explored for lanthanide-actinide separation [7]. Among the various DPAH investigated orthotrifluoromethylphenyl dithiophosphinic acid, was shown to exhibit a separation factor (=D_{Am}/D_{Eu}) of 105 from 0.005 M nitric acid medium containing 1 M sodium nitrate. TALSPEAK [8] is another promising technique exploits differential complexing abilities of bis-2-ethylhexyl phosphoric acid (HDEHP), present in organic phase and diethylenetriamine-N,N,N',N'',N'''-pentaacetic acid (DTPA) present in aqueous phase towards lanthanides and actinides. However, each process has its own limitations. For example, phosphorous and sulfur based reagents are not completely incinerable, whereas nitriazine based reagents are poorly soluble in paraffinic solvents. In view of this, the development of advanced reagents and simplified process for the mutual separation of lanthanides and actinides are desirable.

2. Scope of the present study

The present work involves the synthesis of various diglycolamic acid based extractants and their evaluation for the mutual separation of lanthanides and actinides. Diglycolamic acid is acid derivative of diglycolamide. Diglycolamides are the popular reagents for the separation of trivalent lanthanides and actinides from concentrated nitric acid medium (3-4 M nitric acid). A couple of alkyldiglycolamic acids have been developed and studied the feasibility of using them for the mutual separation of lanthanides and actinides. The features that make diglycolamic acids unique among the class of extractants used for the mutual separation of lanthanides and actinides are (a) diglycolamic acids are CHON based. and (b) high solubility of diglycolamic acid based extractants in n-dodecane or paraffinic diluents. Third-phase formation, extractant diluent non-compatibility etc are the major limitations of liquid-liquid extraction. In contrast to the liquid-liquid extraction methods, the studies on the mutual separation of lanthanides and actinides using solid phase extraction methods are very limited. This is essentially due to the lack of availability of adsorbents suitable for lanthanide-actinide separation. Solid phase extraction is a promising technique for the separation of metal ions from aqueous solution owing to its simplicity, robustness, regenerating ability and can be easily engineered into plant scale levels and technologically demonstrated [9]. In fact, solid phase extraction is suitable for the separation of micro-quantities of radionuclides present in a large volume of feed solution, as in the present case. Initially ligand impregnated resins were used for variety of applications. Wide variety of ligands can be impregnated in the form of solid phase extractants (SPE). In connection with this, diglycolamic acids were impregnated on polymeric resins and studied the feasibility of using them for the mutual separation of lanthanides and actinides. These diglycolamic acid impregnated resin offered high extraction of Eu(III) with superior Eu(III)/Am(III) separation. However, due to the poor chemical stability of these impregnated resins, ligand-chemically linked solid phase extractants (SPEs) (or also known as anchored resins) have been used at later stage.

The anchored resins have several advantages such as (i) wide variety of functional groups can be incorporated in polymer matrix using organic reactions, (ii) physical properties of polymer matrix can be finely tuned to suit particular applications, and (iii) they can withstand normal experimental conditions such as feed acidity, radiation environment etc. In this context, a polyamine resin modified diglycolamic acid, PA-DGAH was synthesized and used for the mutual separation of lanthanides and actinides. Employment of this organic solid support for the treatment of radioactive liquid solutions suffers from drawbacks of swelling and the chemical and radiolytic degradation [10]. Also the contaminated spent ion exchange resins require further treatment for final disposal. To overcome the problems associated with radiolytic degradation and disposal of spent organic resins, chemically inert inorganic solid supports such as silica grafted with various organic compounds have been studied for the efficient removal of metal ions from waste streams. The advantage of utilizing the inorganic solid support is that it can be vitrified or ceramized to an unleachable solid form for final disposal [11, 12]. In view of this, a silica anchored diglycolamic acid, Si-DGAH was developed for the mutual separation of lanthanides and actinides. However, these functionalized materials also have some drawbacks such as small particle size, choking of the column during engineering-scale operation, etc. These problems can be easily avoided by the use of magnetic solid-phase separation (MSPS) methodology [13].

MSPS is emerging as a promising technique for the separation of toxic and radiotoxic metal ions from various aqueous streams. In the MSPS technique, the magnetic particles (MPs) are added to the waste solution to extract the target metal ion and the MPs are then separated from the solution by means of an external magnetic force. Since this method uses the application of an external magnetic field, the particle size of the adsorbent can be lowered considerably for efficient and rapid extraction of metal ions from waste solution. In this context, an iron oxide (Fe_3O_4) particle functionalized with diglycolamic acid (Fe-DGAH) was developed for the mutual separation of Am(III) and Eu(III).

3. Organization of the thesis

This thesis is divided into eight chapters.

Chapter 1 deals with a brief introduction to reprocessing of spent nuclear fuel, the safe management of HAW, partitioning and transmutation and need of lanthanide-actinide separation. This chapter provides a detailed literature survey on various strategies proposed for the safe management of HAW. This chapter also provides introduction to various class of extractants, methodology for separations of metal ions and the scope for further developments.

Chapter 2 details the various chemicals and reagents used for the synthesis of various diglycolamic acids, impregnation of diglycolamic acids on to polymeric resins, anchored resins, silica diglycolamics acid based adsorbents and magnetic adsorbents. This includes synthesis purification and characterization of these organic solvents and adsorbents by various spectroscopic techniques such as NMR, FT-IR, mass spectrometry, TG-DTA, elemental analysis, XRD, SEM-EDX, Raman etc. An introduction to description of various experimental tools used for characterization such as NMR, FT-IR, mass spectrometry, TG-DTA, elemental analysis, XRD, SEM-EDX, Raman are discussed. Methodologies adopted for the measurement of radioactivity of various radioisotopes using sodium iodide thalium (NaI(Tl)) detector, high purity germanium detector (HpGe) are discussed. Usage of inductively coupled plasma-optical emission spectroscopy (ICP-OES) for the determination of concentration of various metal ions presents in HAW, and thereby the distribution ratio measurements etc., are also explained.

Chapter 3 deals with the evaluation of two diglycolamic acid based extractants bis(2-ethylhexyl)diglycolamic acid (HDEHDGA) and the thio-derivative bis(2-ethylhexyl)thiodiglycolamic acid (HDEHSDGA) for the mutual separation of Ln(III) and An(III). The mutual separation of Eu(III) and Am(III) was demonstrated in a counter-current mixer-settler by employing the optimized conditions. The extractants, bis(2-ethylhexyl)diglycolamicacid (HDEHDGA) and bis(2-ethylhexy)thiodiglycolamic acid (HDEHSDGA) were synthesized and characterized by ^{1}H and ^{13}C nmr, mass and IR spectroscopy. The extraction behaviour of $^{(152+154)}$Eu(III) and ^{241}Am(III) from nitric acid medium by a solution of HDEHDGA (or HDEHSDGA) in n-dodecane(n-DD) was studied for the mutual separation of actinides and lanthanides. The effect of various parameters such as the pH, concentrations of HDEHDGA, HDEHSDGA, sodium nitrate, N,N,N',N'-tetrakis(2-pyridylmethyl)ethylenediamine (TPEN) and diethylenetriaminepentaacetic acid (DTPA) on the separation factor (SF) of americium(III) over europium(III) and vice versa was studied, and the conditions needed for the preferential separation were optimised. The results show that HDEHDGA exhibits higher extraction for $^{(152+154)}$Eu(III) and HDEHSDGA shows the superior selectivity for ^{241}Am(III). In order to develop a large scale separation method for the mutual separation of lanthanides and actinides, a mixer setller demonstration run was performed with HDEHDGA. Though, HDEHSDGA offered high separation factors of the order of ~3000, HDEHDGA was chosen for the mixer-settler demonstration runs owing to the fact that sulfur containing extractants are less stable towards high radiation background. Based on the optimized conditions, the feasibility of separating Am(III) from Eu(III) present in simulated feed solution was investigated in a 20- stage mixer-settler. Quantitative extraction of Eu(III) and Am(III) in 0.1 M HDEHDGA/n-DD was achieved in 3-4 stages, whereas the selective back extraction of Am(III) was achieved in ~20 stages upon contacting the loaded organic phase with a stripping formulation composed of DTPA-citric acid at pH 1.5. The results confirmed the possibility of using diglycolamic acid for the separation of trivalent actinides from the chemically similar lanthanides, which is indeed necessary for transmutation of minor actinides present in HAW.

Chapter 4 describes the development of the extraction chromatographic method developed for clean and mutual separation of Eu(III) and Am(III) present in dilute nitric acid medium. For this purpose, we synthesized some new alkyl diglycolamic acid derivates with alkyl group varied from butyl to decyl and impregnated in a PS-DVB resin

(Tulsion ADS 400). The alkyl derivatives of diglycolamic acid (alkyl = butyl to decyl) were synthesized and characterized by ^{1}H and ^{13}C nmr, and IR spectroscopy. The diglycolamic acids were impregnated in Tulsion ADS 400 for the chromatographic separation of hazardous Am(III) and Eu(III). The extraction behaviour of Am(III) and Eu(III) in the impregnated resin was studied as a function of various parameters such as aqueous phase pH, concentration of diglycolamic acid, and diethylenetriaminepentaacetic acid (DTPA) etc. The distribution coefficient (K_d) of Am(III) and Eu(III) in the resin phase increased with increase in pH of aqueous phase and loading of DGAA in the resin. The concentration of DTPA needed for efficient separation of Am(III) from Eu(III) was optimized and the performance of the resin under dynamic extraction conditions was assessed by following the breakthrough curve in the column study using octyl derivative of diglycolamic acid. The conditions needed for the elution of Am(III) alone from the column was performed using 0.001 M DTPA solution at pH 2.5. The study confirmed the feasibility of separating Am(III) from Eu(III) using HDODGA by extraction chromatography.

Chapter 5 describes the development of a polymeric resin prepared by anchoring of diglycolamic acid to an organic polyamine matrix and studies on the extraction behavior of Am(III) and Eu(III) from dilute nitric acid medium. Diglycolamic acid was anchored on a polyamine matrix and the product (PA-DGAH) was characterized by ion-exchange capacity measurement, TG-DTA and FT-IR spectroscopy. The extraction behavior of Am(III) and Eu(III) in PA-DGAH was studied from dilute nitric acid medium to examine the feasibility using the anchored adsorbent for their mutual separation. The effect of various parameters such as the duration of equilibration, concentration of europium, nitric acid and diethylenetriaminepentaacetic acid (DTPA) in aqueous phase on the distribution coefficient (K_d) of Am(III) and Eu(III) was studied. The distribution coefficient decreased with increase in the concentration of nitric acid. Rapid extraction of metal ions in the initial stages of equilibration followed by the establishment of equilibrium occurred within 4 hours. The data on the rate of uptake of Am(III) and Eu(III) were fitted into pseudo-first order and pseudo-second order rate equation. The extraction isotherm was fitted to Langmuir and Freundlich adsorption models and the apparent europium extraction capacity was determined. The mechanism of extraction was elucidated and the conditions needed for efficient separation of Am(III) from Eu(III) was optimized using DTPA. The study indicated the possibility of using PA-DGAH for the separation of Eu(III) from Am(III) with high separation factors.

Chapter 6 describes the development of diglycolamic acid functionalized silica gel (Si-DGAH) for the separation of Am(III) and Eu(III) from aqueous nitric acid medium. The surface of the silica gel was modified with diglycolamic acid moieties and the product (Si-DGAH) was characterized by elemental analysis, TG-DTA, ^{1}H and ^{29}Si NMR and scanning electron microscopy (SEM). The adsorption behavior of hazardous americium (III) and europium (III) in Si-DGAH was studied from aqueous nitric acid medium to examine the feasibility using the modified silica for the separation of Am(III) and Eu(III) from aqueous wastes. In this context, the effect of various parameters such as the duration of equilibration, and concentrations of europium, nitric acid, sodium nitrate and diethylenetriaminepentaacetic acid (DTPA) in aqueous phase, on the distribution coefficient (K_d) of Am(III) and Eu(III) was investigated. The distribution coefficient of ~103 mL.g^{-1} (>99.9% extraction) was obtained for both Am(III) and Eu(III) at pH 3, and the K_d values decreased with increase in the concentration of nitric acid. Rapid kinetics of extraction in the initial stages of equilibration, followed by the establishment of equilibrium occurred within 30 minutes. The extraction data were fitted in to Langmuir adsorption model and the apparent europium extraction capacity was determined.

Europium loading capacity of the sorbent was determined at various feed pH by column method. The study indicated the possibility of using diglycolamic acid-modified silica for the separation of Eu(III) and Am(III) from aqueous wastes.

Chapter 7 deals with the development of two magnetic solid phase adsorbents Fe-DGAH and Fe-SDGAH. Fe-DGAH and Fe-SDGAH were synthesized and characterized by TG-DTA, X-Ray diffraction, ^{1}H NMR, and scanning electron microscopy (SEM). The extraction behavior of Am(III) and Eu(III) in Fe-DGAH (or Fe-SDGAH) was studied from dilute nitric acid medium to examine the feasibility using Fe-DGAH (Fe-SDGAH) for the mutual separation of trivalent actinides and lanthanides. For this purpose, the effect of various parameters such as the duration of equilibration, concentrations of europium, nitric acid and diethylenetriaminepentaacetic acid (DTPA) in the aqueous phase on the distribution ratio (K_d) of Am(III) and Eu(III) was studied. The distribution ratio of ~104 mL.g^{-1} was obtained for both Am(III) and Eu(III) at pH 3 by using Fe-DGAH, and it decreased with an increase in the concentration of nitric acid. A separation factor of Eu(III) over Am(III) of ~150 was achieved in the presence of DTPA. However, Fe-SDGAH showed selectivity towards Am(III) with a Am(III)/Eu(III) separation factor of ~3. Rapid sorption of metal ions in the initial stages of equilibration followed by the establishment of equilibrium occurred within 2h. The sorption data were fitted to the Langmuir adsorption model, and the apparent europium sorption capacity was determined to be ~50 mg.g^{-1} for Fe-DGAH and ~11 mg.g^{-1} for Fe-SDGAH. The study indicated the feasibility of using Fe-DGAH particles for magnetic separation of Eu(III) from Am(III) with high separation factors.

Chapter 8 summarizes the results and conclusions obtained in the present work. This chapter also discusses about scope for the future work in this field.

REFERENCES

1. M.V. Ramana, The power of promise: Examining nuclear energy in India. Penguin UK, (2012)
2. http://www.world-nuclear.org/information-library/economic-aspects/economics-of-nuclear-power.aspx
3. J. L. Swanson, "PUREX Process Flow sheets", In: Science and Technology of Tributyl phosphate, Eds. W.W. Schulz, L.L. Burger, J.D. Navratil, K.P. Bender, CRC Press Inc. Boca Raton, p 55, 1984.
4. Implications of Partitioning and Transmutation in Radioactive Waste Management. IAEA Technical Reports Series, STI/DOC/010/435, 2004.
5. S.A. Ansari, P.N. Pathak, P.K. Mohapatra, V.K. Manchanda, Aqueous partitioning of minor actinides by different processes. Sep. Purif. Rev. 40 (2011) 43-76.
6. B.A. Moyer, editor. Ion exchange and solvent extraction: a series of advances. CRC Press; 2009.
7. Z. Kolarik, U. Müllich, F. Gassner, F.: Selective extraction of Am(III) Over Eu(III) by 2,6-ditriazolyl- and 2,6-ditriazinylpyridines, Solvent Extr. Ion Exch. 17 (1999) 23-32.
8. D.R. Peterman, M.R. Greenhalgh, R.D. Tillotson, J.R. Klaehn, M.K Harrup, T.A. Luther, J.D. Law: Selective extraction of minor actinides from acidic media using symmetric and asymmetric dithiophosphinic acids. Sep. Sci. Technol. 45 (2010) 1711–1717.
9. K.L. Nash: The chemistry of TALSPEAK: a review of the science. Solvent Extraction and Ion Exchange. 33 (2015) 1-55.
10. L.R. Van Loon, W. Hummel: Radiolytic and chemical degradation of strong acidic ion-exchange resins: Study of the ligands formed. Nucl. Tech. 128 (1999) 359–371.

11. F. Frizon, C. Cau-dit-Coumes: Cementation of ILW ion exchange resins: Impact of sulfate ions released by radiolysis on hydrated matrix. J. Nucl. Mater. 359 (2006) 162–173.
12. W. Lutze, R.C. Ewing:. Radioactive waste forms for future, North-Holland, Oxford, 1988.
13. K. A. Arteaga, J.A. Rodriguez, E. Barrado. Magnetic solids in analytical chemistry. Anal. Chim. Acta 674(2010) 157–165.

LIST OF FIGURES

LIST OF TABLES

Chapter 1: Introduction

Electricity plays its pivotal role in the development of a country and it serves as one of the basic requirements of everyday life [1]. Being the fourth largest economy in Asia, the electricity requirement of India has been catered so far predominantly by the coal-fired thermal power plants [2]. India has more than 200 GWatt installed electricity-plants, mainly coal-fired power plants and few hydel power plants [2]. However, the demand for energy by the year 2050 is estimated to be roughly 1000 GWe [2-4]. Though, India shares fourth largest coal reserves in the world, and also hold its position among the top petroleum importing countries, it requires additional sources of energy to meet this target [2, 3]. The use of fossil fuels (coal and petroleum products) pose several environmental concerns such as generation of green house gas, carbon particulates etc. Moreover, the fossil fuel reserves are declining at a faster pace with increase of energy demand. Other renewable energy resources such as wind, solar, tidal powers etc. also contribute to the energy requirement to some extent. However, there is always uncertainity in the development of renewable energy technologies. Therefore, the nuclear energy option for meeting the future energy demand is inevitable. Nuclear energy has got several advantages such as minimal green house gas production and enhanced energy production as compared to fossil based fuels. At present, nuclear power plants contribute only 3 % of the total energy demand in India [2, 3]. The contribution of nuclear energy needs to be increased from the present 3 % to at least 25% in coming years for a sustained development of our nation.

1.1. Nuclear fuel cycle and types of nuclear reactors

All the nuclear power plants currently operating in the world are based on nuclear fission[*] reaction. Many types of nuclear reactors have been designed and built to convert the heat produced from a nuclear fission to electrical energy [5]. Several process steps, starting from mining of uranium to final waste disposal, are associated with the production of electricity in nuclear reactors. They are collectively known as nuclear fuel cycle [6]. The process steps starting from mining of uranium to fuel loading into nuclear reactor is collectively called as “front end of the nuclear fuel cycle” and from discharging of spent fuel to waste management is called as “back end of the nuclear fuel cycle”. The fuel that is discharged from a nuclear reactor, known as ‘spent nuclear fuel (SNF)’. It contains un-used (or depleted) uranium (U), plutonium (Pu) and several radionuclides known as “fission products”(FPs), formed by fission reaction. The uranium and plutonium can be recovered from the spent fuel and reused as fuel in future reactors. World-wide two different management strategies have been employed for the management of spent nuclear fuel [6-8]. (1) The SNF is either reprocessed to recover uranium and plutonium for fueling future reactors, known as ‘closed fuel cycle option’, or (2) simply considered as waste and stored in geological repositories, called as the ‘open fuel cycle option’. Figure 1.1 illustrates the various stages involved in closed fuel cycle option.

The major advantages of closed fuel cycle option are given below.

1. Maximum utilization of fissile element through the recyling of uranium and plutonium (produced from thermal reactors) in fast reactors.
2. Reduction of radioactive waste volume and radiotoxicity by reprocessing and P&T.
3. A reduction in the proliferation of nuclear materials.

---

[*] Nuclear fission is the process in which a large nucleus splits into two or more smaller nuclei with the release of energy (200 MeV) along with the release of few neutrons.

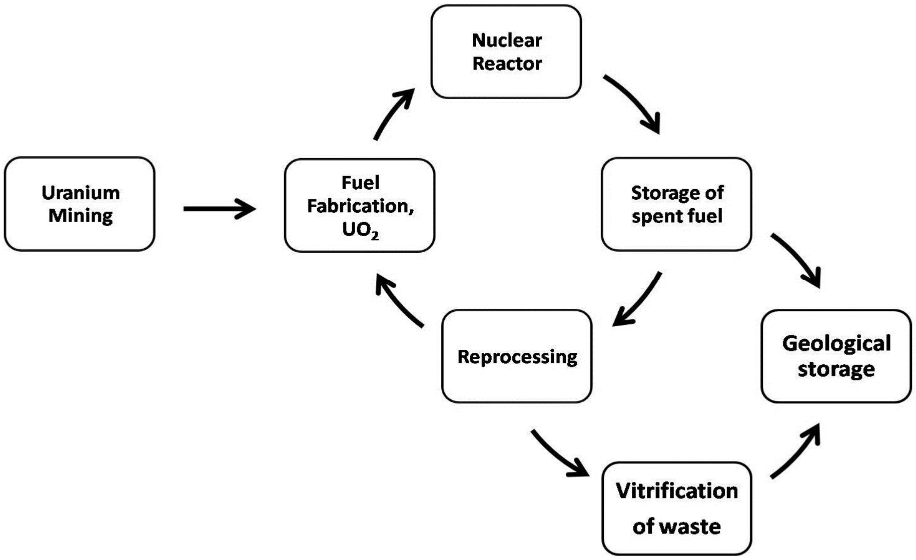

Figure 1.1. Illustration of closed nuclear fuel cycle

Envisaging the potential of utilizing available uranium in India to its maximum level and to utilize the massive thorium reserve, Dr. Homi Jehangeer Bhabha, father of Indian nuclear programme, charted a three stage nuclear power programme to meet the nation's energy demand [9]. The first stage came on track with the building up of natural uranium fueled Pressurized Heavy Water Reactors (PHWRs). The second stage is based on setting up of Fast Breeder Reactors (FBRs) that utilizes the plutonium recovered from the reprocessing of spent fuel of PHWRs. A 40 MW_t Fast Breeder Test Reactor (FBTR) is in operation at Kalpakkam since 1985[10] to demonstrate the second stage. In fast reactors it is proposed to use thorium as blanket. The fissile ^{233}U produced from fertile element thorium (Th) is then utilized in the third stage of Indian power programme. A 30 kW_t Indian reactor, KAlpakkam MINI reactor (KAMINI) uses ^{233}U as fuel [11]. In addition to this, Advanced Heavy Water Reactors (AHWRs) are also conceptualized to employ ^{233}U as fuel [12].

1.2. Nuclear reactions in the reactor

Uranium (^{235}U, natural abundance 0.7 %) is used as fuel in thermal reactors such as PHWR, pressurized water reactor (PWR), boiling water reactor (BWR) and light water reactor (LWR) etc, whereas combination of uranium and plutonium (^{239}Pu,) is used as fuel in fast breeder reactors (FBR). In thermal reactors, fission is caused by thermal neutrons (neutrons having energy of the order of ~0.025 keV) and in fast reactors, fission is caused by fast neutrons (neutrons having energy of the order of 1 to 2 MeV). In addition, another fissile element of uranium, ^{233}U, (obtained from activation of ^{232}Th, a naturally occurring fertile element) also undergoes fission reaction in the presence of thermal neutrons. When the fissile element captures neutrons, fission takes place and the nuclei divide usually into smaller nuclei. The amount of energy released per unit mass of fissile material is known as burn-up of the fuel. Depending upon the type of nuclear reactor and composition of fuel, the burn-up and fission products formed would vary. It is observed that for the fission of ^{235}U or ^{239}Pu results in the generation of fission products with mass ranging from 80-110 and 120-160. Among them, the FP that are having mass numbers around 90 and 140 has particularly high fission yields. Major FPs and their half-life are shown in table 1.1 [13, 14].

Table 1.1. Major long-lived fission products produced by fission of ^{235}U fission and their half-life

FP	Half life/ years
^{147}Pm	2.6
^{135}Cs	2.3×10^{6}
^{137}Cs	30
^{90}Sr	28
^{99}Tc	211×10^{3}
^{93}Zr	1.5×10^{6}
^{126}Sn	1×10^{5}
^{79}Se	6.5×10^{4}
^{106}Ru	1
^{129}I	15.7×10^{6}

Fission is also accompanied by the emission of two or three neutrons which results in the formation of several activation products such as plutonium (^{238}Pu, ^{239}Pu, ^{240}Pu, ^{241}Pu etc), americium (^{241}Am, ^{243}Am etc), curium (^{242}Cm, ^{244}Cm, ^{245}Cm etc.), and neptunium (^{237}Np, ^{239}Np) as shown in figure 1.2. A list of such activation (or transmutation) products and their half-life is showed in table 1.2 [13, 15]. Among these activation products Np, Am, and Cm are called minor actinides (MA) as their concentration in the fuel is very less.

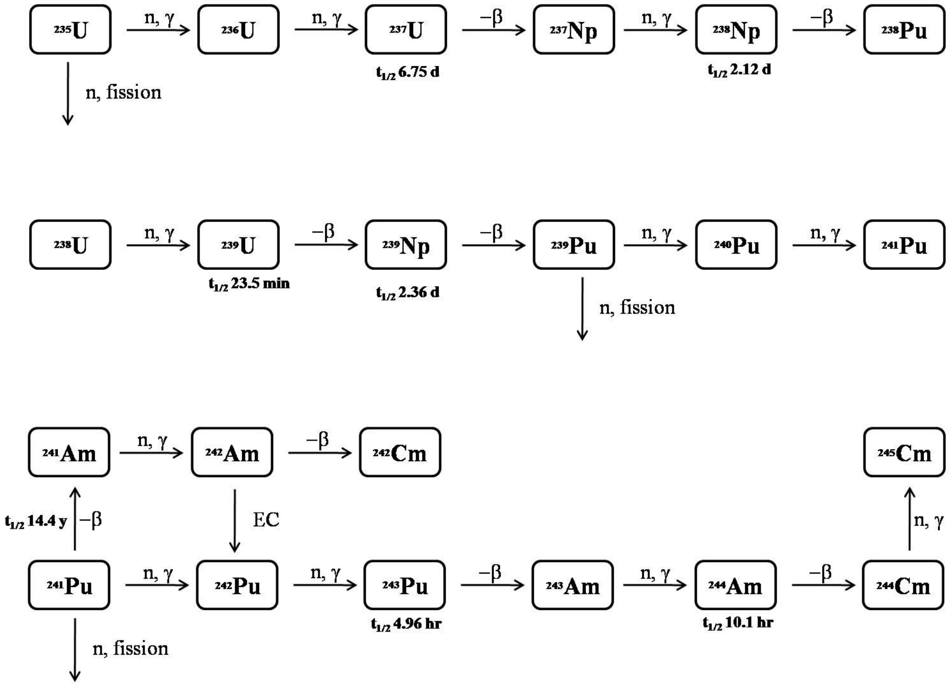

Figure 1.2. Major activation reactions of uranium and plutonium

Table 1.2. Major transmutation products produced from uranium and plutonium and their half-life and specific activity[†]

Transmutation product	Half-life	Energies of primary Emission/ MeV	Specific activity /Ci/g
^{237}Np	2.14×10^6 y	α, 4.78	7×10^{-4}
^{238}Np	2.1 d	β, 0.25, 1.24, 0.332,	2.6×10^5
^{239}Np	2.3 d	β, 0.427	2.3×10^5
^{238}Pu	87.4 y	α, 5.49	17.2
^{239}Pu	2.4×10^4 y	α, 5.15	6.13×10^{-2}
^{240}Pu	6580 y	α, 5.16	0.227
^{241}Pu	14.9 y	β, 4.9	99
^{242}Pu	3.87×10^5 y	α, 4.9	3.82×10^{-3}
^{241}Am	433 y	α, 5.48	3.43
^{242}Am	16 h	β, 0.63-0.67	8.11×10^5
^{242m}Am	144 y	α, 5.2 & I.T.	10.3
^{243}Am	7370 y	α, 5.27	0.2
^{242}Cm	162 d	α, 6.11	3.32×10^3
^{243}Cm	32 y	α, 5.79	45.9
^{244}Cm	18 y	α, 5.8	80.9
^{245}Cm	8265 y	α, 5.36	0.177
^{246}Cm	4655 y	α, 5.39	0.312
^{247}Cm	1.56×10^7 y	α, 4.87	9.28×10^{-5}
^{248}Cm	3.39×10^5 y	α, 5.05	4.24×10^{-3}
^{249}Cm	64 m	β, 0.9	1.18×10^7
^{250}Cm	1.74×10^4 y	α	8.2×10^{-2}

[†] Specific activity: Specific activity is the activity per quantity of a radionuclide and is a physical property of that radionuclide. Activity is a quantity related to radioactivity. The SI unit of activity is the Becquerel (Bq).

1.3. Radiotoxicity[‡] of spent nuclear fuel

The radioactive wastes, even in low concentrations, are hazardous and its disposal requires isolation into stable form [16]. The long term radiotoxicity associated with the spent fuel is predominantly due to the presence of long-lived alpha emitting actinides such as: plutonium, neptunium, americium, curium etc. and fission products such as: Cs (^{133}Cs, ^{137}Cs), I (^{131}I, ^{135}I), Sr (^{90}Sr), Zr (^{93}Zr), Mo (^{99}Mo), Ru (^{103}Ru, ^{106}Ru), Xe, Kr, ^{147}Pm etc (see table 1.1). Figure 1.3 shows the variation in the relative radiotoxicity of different components of spent nuclear fuel with time [17]. The radioactivity due to natural level (uranium ore) is represented as reference level in this figure. The idea of waste management is aimed at reducing the radioactivity of spent nuclear waste to the reference level. Radiotoxicity of the spent fuel discharged immediately from the reactor is dominated by various short lived radionuclides such as I, Zr, Cs, Pd, Ru etc [13]. After the decay of short-lived isotopes, the major contributors of radiotoxicity are long lived ^{137}Cs and ^{90}Sr, which contributes the radiotoxicity for 300 years [13, 14]. After 300 years, the major contribution of radiotoxicity could be due to the presence of alpha nuclides such as Pu (^{238}Pu, ^{239}Pu, ^{240}Pu, ^{242}Pu), Am (^{241}Am, ^{243}Am), Np (^{237}Np), Cm (^{243}Cm, ^{244}Cm) etc [13, 15]. If plutonium and depleted (un-used) uranium is recovered by reprocessing, the major radiotoxity of the resultant radioactive waste could be due to minor actinides (MAs) and fission products (FPs), ^{137}Cs and ^{90}Sr.

Plutonium and depleted uranium are chemically separated from spent nuclear fuel by a process known as reprocessing. This process involves several steps such as cutting and chopping of fuel pin, dissolution of spent fuel in concentrated nitric acid, followed by recovery of uranium and plutonium from the aqueous solution by a using liquid-liquid

---

[‡] Radiotoxicity is a measure of how nocuous a radionuclide is to health. It is depending up on the type and energy of rays, absorption in the organism, residence time in the body, etc. Radiotoxicity of spent fuel is expressed in terms of mSv/tonne of fuel. Relative radiotoxicity is defined as ratio of the radiotoxicity of the spent fuel to radiotoxicity due to uranium ore.

separation process. Details about reprocessing are described in section 1.5. The aqueous radioactive waste (also known as raffinate) rejected after the extraction of uranium and plutonium is known as high-active waste (HAW) [13], which contains significant quantities of lanthanides and minor actinides (Am, Cm and Np, please see table 1.2). The radiotoxicity of HAW obtained after reprocessing is due to americium, curium, and neptunium. Partitioning and transmutation (P&T) [18, 19] strategy is an accepted method to remediate the radiotoxicity of HAW. P&T involves the separation of minor actinides from HAW, followed by transmutation of them in to short-lived or stable isotopes. Details of P&T are explained in section 1.7

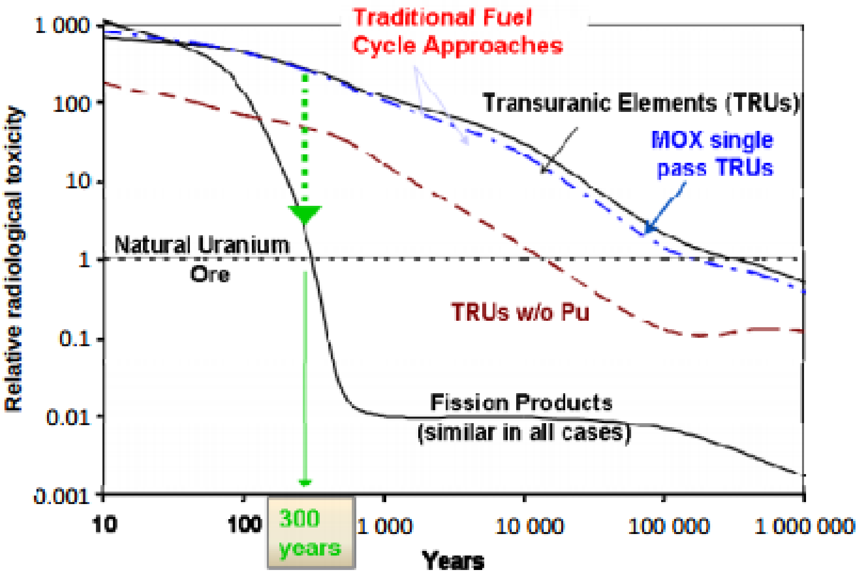

Figure 1.3. **Relative radiotoxicity of different components in the spent nuclear fuel from a light water reactor irradiated to 60GWd/Te natural U with respect to the radiotoxicity of the corresponding uranium ore [15].**

1.4. Classification of waste.

Radioactive wastes are categorized into various classes according to the physical, chemical, radiological and biological properties as well as origin of waste. According to the origin and physical form, it is primarily classified into various forms like solid, liquid or gaseous. Reprocessing of spent fuel often results in liquid form of radioactive wastes. According to the concentration of radioactive elements present in the liquid waste streams, the waste is commonly classified as exempt waste (<37 Bq/L), low-level waste (37–3.7×10^{6} Bq/L), intermediate-level waste (3.7×10^{6}–3.7×10^{11} Bq/L) and high-level waste (above 3.7×10^{11} Bq/L) [20].

1.5. Reprocessing of spent nuclear fuel

The spent nuclear fuel discharged from nuclear power reactors contains substantial amounts of fissile element, plutonium and un-used uranium. The purpose of reprocessing is to recover plutonium and un-used uranium and use them in fast reactors. The spent nuclear fuel can be reprocessed in two ways: aqueous reprocessing method (Plutonium Uranium Reduction EXtraction (PUREX)) or non-aqueous reprocessing (pyrochemical process) methods [21]. Though, Pyrochemical process has attractive features such as less number of process steps, lower volumes of waste generated and easier waste management etc, it has several limitations compared to aqueous reprocessing such as lower separation factors for fission products, need for remote operation, need for sophisticated equipment, need for high purity inert atmosphere to enable handling of hygroscopic salts and reactive metals, high temperature operation etc [21, 22].

Due to the simplicity in the operation and several years of operational experience, aqueous reprocessing methods (PUREX process) have been followed for reprocessing of spent fuel. This process involves the chemical separation of plutonium and uranium from spent nuclear fuel by a liquid-liquid separation process.

1.6. Plutonium Uranium Reduction EXtraction (PUREX) process

Plutonium Uranium Reduction EXtraction (PUREX) process is a liquid-liquid extraction process which uses tri-*n*-butyl phosphate (TBP) diluted with n-dodecane as solvent to extract uranium and plutonium. Because of the the ability of actinides in tetravalent states and hexa valent states to form strong solvation type complexes with TBP resulted in the separation of actinides from fission products. PUREX process consisting of the following steps [23].

1. Initial cooling of the spent fuel to remove short-lived fission products such as Zr, Nb, Ru, I, etc.
2. Decladding of the fuel[§], dissolution in nitric acid and adjustment of the valance state of Pu to Pu(IV) and U to U(VI) making it amenable for solvent extraction.
3. Solvent extraction of U(VI) and Pu(IV) by 1.1 M TBP in *n*-dodecane.
4. Scrubbing of loaded organic phase once or twice with different concentration of nitric acid to remove the unwanted fission products.
5. Partitioning of Pu(IV) by selective reduction in organic phase to Pu(III), which goes with aqueous phase and subsequent stripping of U(VI) with dilute nitric acid.
6. Final purification of U and Pu and to use the fuel in future (fast reactors) reactors.
7. Treatment of the solvent for its reuse in the process.

PUREX process thus provides fissile element plutonium and un-used uranium, which can be further employed in fast reactors.

[§] Decladding: Process meant to separate the clad material. Clad is the solid support material for the nuclear fuel.

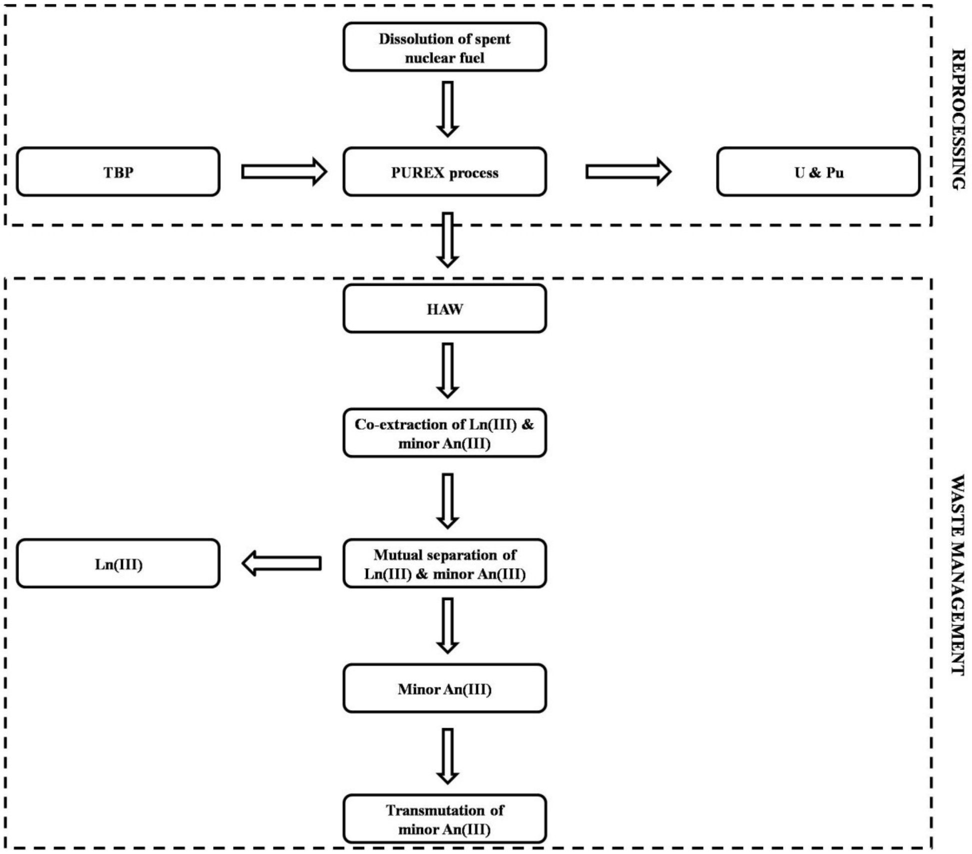

Figure 1.4. Reprocessing and waste management of spent nuclear fuel

1.7. P&T strategy.

The aqueous waste (also known as high active waste: HAW) resulted from the aqueous reprocessing of spent nuclear fuel poses long term challenges to the environment and mankind due to the presence of long-lived alpha emitters such as MAs (americium, curium and neptunium) [24-28]. This is because radiotoxicity due to MA is very high. Currently, HAW is vitrified in the form of borosilicate glass and stored in deep geological repositories [26, 28-31]. However, this practice needs long term surveillance as the half-lives of MA are very high. On the other hand, the partitioning (P) of MAs from HAW, and their subsequent transmutation (T) into stable or short-lived products by using fast reactors or accelerated driven systems (ADS) reduces the radiotoxicity of HAW to a large extent, and simplifies the management of HAW [18,19]. Details of transmutation reactions are explained in section 1.11.

1.8. Partitioning of minor actinides

The partitioning of MAs[**] from HAW involves the separation of trivalent actinides from their chemically similar trivalent lanthanides present in HAW. These lanthanides are formed as fission products in significant quantities as compared to trivalent actinides [13, 14]. Moreover, the high concentration of nitric acid (3-4 M) prevailing in HAW also complicates the separation procedure to a great extent. However, some studies have been reported in the literature for the separation of ^{241}Am and ^{243}Cm actinides directly from PUREX raffinate. The methods include 1-cycle selective actinide extraction (SANEX), group actinide extraction (GANEX) and transuranic extraction-transuranium elements extraction by phosphours based reagents and aqueous Komplexing agents (TRUSPEAK) approaches [32-35]. These methods employ combination of neutral extractants such as N,N,N',N'-tetra-octyldiglycolamide (TODGA), triazine derivatives, carbomylmethylphosphine oxide (CMPO) and acidic extractants such as N,N-diethylhexylphosphoric acid (HDEHP), di-isodecylphosphoric acid (DIDPA) etc. [32-35] for the selective separation of trivalent actinides directly from PUREX raffinate.

The current practice of trivalent actinide partitioning is a two cycle approach [36-39]. It involves the separation of trivalent actinides and lanthanides together from the PUREX raffinate in the first cycle by using neutral extractants such as CMPO, TODGA, N,N,N',N'-tetra-2-ethylhexyldiglycolamide (TEHDGA), and tri-octylphosphine oxide (TOPO) etc, followed by lanthanide (Ln)-actinide (An) separation [36-39]. The product

---

[**] Though MAs refers to americium, curium and neptunium, minor actinide partitioning refers to partitioning of americium and curium only. Neptunium, due to its complicated chemistry and it does not exist in trivalent state; it is generally being separated along with plutonium in PUREX process, or discarded along with various short-lived fission products.

obtained in the first cycle serves as feed solution for the mutual separation of An(III) and Ln(III) [40]. The nitric acid concentration of the above aqueous product varies from 0.1 M to 0.001 M.

Several methods based on solvent extraction have been reported in literature for the separation of lanthanides (Ln) from actinides (An) from the TRUEX product [40-42]. Methods reported so far for the separation of lanthanides from actinides are discussed in section 1.10.

1.9. Need of mutual separation of lanthanides and actinides[††]

HAW contains large amount of fission products and minor actinides at 3-4 M nitric acid medium [13]. Since MAs exists in trivalent state, it is in-extractable by TBP. It it require a multi-dentate ligand for effective complexation [13]. This is because TBP contains only one donating site (P=O) for complexing with the metal ion. Therefore, neutral ligands such as carbomylmethylphosphine oxide (CMPO), malonamides, diglycolamides etc have been identified as popular candidates for the complexation of Am(III) and Cm(III) [36-39]. Majority of the lanthanides formed as fission products also exhibit +3 oxidation state and posses similar chemical and extraction behavior as that of trivalent actinides (An(III)) [13, 43, 44]. However, the presence of trivalent lanthanides (Ln(III)) pose problems during transmutation process because lanthanides act as neutron poisons [45]. Further, Ln(III) do not form solid solutions in metal alloys or in mixed oxide transmutation targets, and as a result they segregate in separate phases with the tendency to grow under thermal treatment [45].

[††] The 'actinide, An' term in mutual separation of lanthanides and actinides refer to minor actinides, Am and Cm

1.10. Mutual separation of lanthanides and actinides

The separation of lanthanides(III) from actinide(III) or vice versa is a challenging task due to the similarity in chemical and extraction behavior of 4f- and 5f- elements [45-47]. The feed solution for lanthanide-actinide (Ln-An) separation is composed of dilute nitric acid solution (0.1 M to 0.001 M) containing minor actinides and lanthanides [40]. Moreover, both minor actinides and lanthanides exist in trivalent oxidation state in the feed solution [40, 48-50]. The methods developed so far [40, 48-59], for the Ln-An separation usually exploits the finer differences in the chemical behavior of lanthanides and actinides towards various ligands. According to HSAB[‡‡] concept, the lanthanides are classified as hard acids as compared to the trivalent actinides [45]. Therefore, the ligands having O-donor atoms preferentially complexes with lanthanides; whereas the ligands with S- or N- donor atoms complexes with trivalent actinides [45, 46]. In addition, the valence 5f- orbitals of actinides are spatially extended more as compared to the 4f-orbitals of lanthnides and thus the trivalent actinides have a greater tendency to form covalent bonding as compared to the lanthanides [45, 46]. Several methods and materials have been reported in literature for lanthanide-actinide separation [48-59]. Kolarik *et al.* [51] studied the selective separation of Am(III) from Eu(III) using triazine based resin, 2,6-ditriazolyl- and 2,6-ditriazinylpyridines, from 1-2 M nitric acid medium. Dithiophosphinic acid (DPAH), commerically available as cyanex 301, and their derivatives are explored for lanthanide-actinide separation [52-53]. Among the various DPAH investigated, orthotrifluoromethylphenyl dithiophosphinic acid, was shown to exhibit a separation factor (americium/europium) of 10^5 from 0.005 M nitric acid medium containing 1 M sodium nitrate. Smith *et al.* [57] employed 4-benzoyl-2,4-dihydro-5-methyl-2-phenyl-3H-pyrazol-3-thione, and trioctylphosphine oxide for separations.

[‡‡] Hard and Soft Acids and Bases (HSAB) theory is a qualitative concept introduced by Ralph Pearson to explain the stability of metal complexes

Among the various methods reported so far [48-59], TALSPEAK (Trivalent Actinide Lanthanide Separation by Phosphorus Extractants Aqueous Komplexes) method has been widely used for the mutual separation of Ln-An [58]. The TALSPEAK process [58] involves the use of bis(2-ethylhexyl)phosphoric acid (HDEHP) as lanthanide selective reagent present in organic phase, and diethylenetriamine-N,N,N',N'',N'''-pentaacetic acid (DTPA) as the actinide selective complexing agent present in aqueous phase.

1.11. Transmuation of minor actinides

The rationale of transmutation of minor actinides is to transform them via fission or spallation[§§] reaction into much shorter-lived or stable FPs [60-62]. This process might involve one or several neutron capture reactions followed by fission or spallation reactions. Two methods proposed for the transmutation of minor actinides: (i) use of fast reactors [60, 61] (ii) use of accelerated driven subcritical systems (ADSs) [62]. In fast reactors, the neutron field required for transmutation is provided by the fission reaction. Fast reactors offer high fission/absorption neutron cross sections as compared to thermal neutron reactors. Therefore, fast reactors are more efficient in transmution of MAs [61]. Such a reactor often employs different mixtures of Pu and MAs.

Recently, accelerator driven subcritical reactors (ADSR or ADS), are also employed for the transmutation of MAs [62]. ADS appear to be a promising way to incinerate MAs. Due to the improved neutron economy of ADS as compared to classical critical reactors, makes them attractive for the purpose of transmutation. Subcritical reactors emerged to be a substitute to fast breeder and fusion reactors.

[§§] Spallation reaction is a process in which a light projectile (proton, neutron, or light nucleus) with the kinetic energy from several hundreds of MeV to several GeV interacts with a heavy nucleus and causes the emission of a large number of mostly neutrons and small fragments.

1.12. Solvent extraction for aqueous reprocessing and waste management

Solvent extraction is considered as the most efficient method for the separation of desired products from a complex mixture, and plays a very important role in various industries such as nuclear, metallurgical, pharmaceutical, food and beverage, chemical, petrochemical, biochemical, catalysis, polymers, etc, [63].

Solvent extraction essentially depends on the distribution of a solute (for example a desired metal ion, M) between two immiscible/partially miscible liquids generally aqueous and organic liquids in contact with each other. The metal ion M, dissolved in one liquid distributes into another immiscible liquid until its chemical potential becomes equal in both the phases. This condition is referred as equilibrium. The distribution of metal ion to the organic phase depends up on the complexing ability of the reagent (also known as extractant) present in organic phase. The distribution ratio of a solute M (D_M) is defined as the ratio of its concentration in the organic phase ($[M]_{org}$) to that in the aqueous phase ($[M]_{aq}$) at equilibrium as shown in equation 1.5.

$$D_M = [M]_{org} / [M]_{aq} \qquad (1.5)$$

The distribution ratio of a solute is constant for a given pair of liquids at constant temperature. In metal recovery operations, the valuable component is a metal ion or a metal complex contained in aqueous solution. This aqueous solution is mixed with an immiscible organic phase containing the extractant. The extractant transfers metal ion from aqueous phase into organic phase by a series of chemical reactions. This process is refered as "extraction". The organic phase loaded with the metal ion is separated from the aqueous phase. The metal ion present in the organic phase is recycled back to aqueous phase by treating with suitable reagent required for the metal recovery. This process is refered as "stripping". The "stripped organic" is called lean organic phase and is recycled and reused subseqeuent extractions and the aqueous phase containing metal now goes to final metal recovery.

1.13. Extractant for the metal ion recovery

Extractants are organic ligands used for the recovery of metal ions from an aqueous phase [63]. The ligand of interest should be selective for the metal ion and it should be immisible in the aqueous phase. In solvent extractions, the extractant is usually dissolved in organic diluents.

Following are the characteristic features of a ligand to be used as extractant.

1. It should have high selectivity for the metal ions.
2. The ligands should be immisible in aqueous phase
3. It should be soluble in the organic diluents for solvent extraction and should have optimum viscocity and surface tension and no third phase formation.
4. High chemical and radiochemical stability.

1.14. Types of extractants

Extraction (also known as metal ion recovery from aqueous phase) involves the transfer of metal ion from aqueous phase to organic phase. The metal ion selective functional group present in the extractant complex with the metal ion and transfers it to organic phase. Metal ion transfer requires the charge neutralization of the metal species and replacement of some or all of its water of hydration by extractants. The metal ion transfer, therefore, depends up on the complexation characteristics of the extractant. Based on the nature of complexation mechanisms involved, the extractant can be classified as (a) cation exchangers (b) anion exchangers (c) neutral extractants and (d) chelating type of extractants.

1.14.1. Cation exchangers

Cation exchangers are those extractants in which the cations or metal ions present in the extractant is used for exchanging with the metal ion to be recovered from aqueous phase [63]. A typical cation exchanger is represented as follows. The metal ion of interest M^{n+} exchanges with the metal present in the ligand, N^+.

$$n\left(\mathrm{RCOO^-N^+}\right)_{org} \quad + \quad \mathrm{M}_{aq}^{n+} \quad \Leftrightarrow \quad \mathrm{M(RCOO)}_{n,org}^{-} \quad + \quad \mathrm{n\,N}_{aq}^{+} \tag{1.1}$$

Acidic extractants or acidic cation exchangers are another class of cation exchangers popularly used in nuclear industry. They generally posses functional groups such as -COOH, >P(O)OH and $-SO_3H$ and they extract metal ions by cation exchange reactions involving metal ion and H^+ present in the extractant. For example, a typical acidic extractant can be represented in equation 1.2.

$$\mathrm{M}^{n+}{}_{(aq)} + \quad n\,\mathrm{HA}_{(org)} \Leftrightarrow \mathrm{M(A)}n_{(org)} + n\,\mathrm{H}^{+}{}_{(aq)} \tag{1.2}$$

Since the extraction takes place with the release of hydrogen ions, usually the extraction of metal ions by acidic extractants takes place at pH ranges and the extracted metal ions can be recovered at higher acidity. Wide varieties of acidic cation exchangers are available in literature. For example, bis(2ethylhexyl)phosphoric acid (HDEHP) is one of the popular extractant used for the separation of trivalent lathanides [58]. Similarly, all the phosphinic acids [64] and phosphonic acids [65] are found use as extractant in variety of applications.

1.14.2. Anion exchangers

In anion exchange based separations, the metal ion is existed as an anionic species and it get exchanged with an anion present in the extractant [63]. A typical anion exchange reaction is showed in equation 1.3. A metal ion, (MY^-), exchange with the anionic site (X^-) of the extractant, $R_3NH^+X^-$.

$$R_3NH^+\,X^-_{(org)} + MY^-_{(aq)} \Leftrightarrow R_3NH^+MY^-_{(org)} + X^-_{(aq)} \quad (1.3)$$

Several quaternary ammonium salts also have been explored for various anion exchange applications. For eg., tri-*n*-octylamine (Alamine 336) [66, 67] and tri-octylmethylammonium chloride (Aliquat 336) [68] are the two important basic extractants used for several applications. Several anion exchangers are reported in literature for variety of applications in reprocessing related applications. Anion exchange procedure is reported for the purification of plutonium from nitric acid medium. It is based on the selective extraction of the anionic plutonium(IV) nitrate species of the type $[Pu(NO_3)_5]^-$ and $[Pu(NO_3)_6]^{2-}$ formed at high concentrations of nitric acid [69] by anion exchange resins. The main advantage of anion exchange method for plutonium purification is due to the fact that plutonium forms anionic species at high nitric acid concentrations, whereas the other interfering elements and fission products do not form such anionic complexes.

1.14.3. Neutral extractants

Neutral extractants are reagents containing donor atoms with lone pair of electrons for the solvation of neutral inorganic species [63]. The metal ion exists as neutral species and it complexes with the extractant.

Extraction of a metal ion (M+) by a neutral extractant (L) can be illustred by equation 1.4.

$$M^+X^- \quad + \quad L \quad \Leftrightarrow \quad (M^+X^-)L \qquad (1.4)$$

The metal ion exists as a neutral species, M^+X^-. Neutral extractants generally posses functional groups such as P=O, C=O, N-H etc as the lone pair electrons donating sites. The lone pair electrons are charge-polarized in acidic medium, donates its electron density to the vacant orbitals of the metal ions. The solvating power depends strongly on the basicity of the reagent. Several neutral extractants such as phosphates, phosphinates, phosphonates, amides, diamides, diglycolamides [13, 36-39] etc. have been reported in literature.

1.14.4. Chelating extractants

The essential feature of chelating extractants is that they show chelation behaviour, the formation of ring structures involving the extractant molecule as a ligand to the metal ion. Reagents such as hydroxyoximes and diketones especially 5,8-diethyl-7-hydroxy-6-dodecanone oxime (LIX 63) [70], 2-hydroxy-5-dodecylbenzophenone oxime (LIX 64) [71], thenoyltrifluoro acetone (TTA) etc., belong to this family of extractants [72].

1.15. Introduction to Solid-phase extractants

Solvent extraction has been widely used in various reprocessing applications. Solid-phase extraction methods have not been explored due to the lack of availability of adsorbents. Separations based on solid phase extractants (SPE) are promising because of the following advantages (a) any ligand can be immobilized into the form of a solid phase extractant (b) no issue of third phase formation[***] (c) less waste generation (d) disposal of the extractant is relatively easier as compared to solvent extraction techniques [73, 74]. Based on the inert support used for immobilizing the extractant, solid phase extractants can be broadly classified as (i) SPE with organic support (ii) SPE with inorganic support.

[***] Third phase: Third phase formation is the splitting of organic phase into two phases with the heavier one, rich in metal–solvate and the lighter phase rich in diluent. Usually it happens due to poor solubility of metal–solvate in non-polar diluent phase at metal loadings beyond a particular value referred as limiting organic concentration (LOC)

If the metal ion separation involved in SPEs is by stoichiometric chemical exchange of metal ions, it can be called as ‘ion exchangers’. The ion exchanger is defined as a solid or liquid, inorganic or organic substance containing ions exchangeable with others of the same charge, present in a solution in which the ion exchanger is considered to be insoluble [75]. In the ion exchanger, the exchangeable ions are called counter ions and the ions of opposite charge to the counter ions are called co-ions. In cation exchange process, redistribution of cations occurs whereas in anion exchange process redistribution of anions occurs between the ion exchanger and a solution. If the metal ion extraction is non-stoichiometric then the metal ion exchange is known as sorption or adsorption.

Initially solvent impregnated solid phase extractants (or solvent impregnated resins, SIRs) were used for the recovery of metal ions [75, 76]. The SIRs offer advantage that any metal ion selective ligand can be immobilized. SIRs are composed of an “inert “polymeric matrix impregnated with readily available extractants [75, 76]. Therefore, SIRs can be easily prepared and they possess the features and advantages exhibited by both liquid-liquid extraction and solid-liquid extraction. Moreover, the dispersion of the extractant over the surface of the polymer is so large, that the distribution coefficients of metal ions achieved with the use of SIRs are usually very high as compared to those achieved by the same extractant in solvent extraction mode. However, the poor chemical stability of SIRs leads to the development of chemically modified solid phase extractants (or also known as anchored resins). These anchored resins posses enhance the selectivity towards metal ions [77]. However, the synthesis of such chelating type ligands on the surface of the polymer is cumbersome and the operations at intense radiation flux and elevated temperatures limit the use of organic resins.

1.15.1. Organic ion exchangers

Organic ion exchanger is a cross-linked polymer matrix, made up of hydrocarbon chains, which carries functional groups [77]. Generally, the polymer matrix of the resins is hydrophobic. The ion exchange resin becomes hydrophilic only after the incorporation of functional (exchangeable) groups. The nature of functional groups can be acidic, basic or chelating. Thus, the synthesis of ion exchange resins involves two steps (i) preparation of polymer matrix, and (ii) incorporation of functional groups. The polymer matrix can be prepared either by condensation or addition polymerization. The first synthesis of organic exchanger was based on polycondensation reaction of phenol and formaldehyde [78]. Addition polymers are chemically more stable than condensation polymers. The addition polymers can be prepared conveniently using suspension polymerization technique. The addition polymer based on styrene and divinylbenzene (DVB) is being widely used in all applications. The degree of cross-linking can be controlled by the ratio of DVB to styrene. Pure DVB is not easily available, and hence commercial DVB consisting of a mixture of isomers, i.e., 55-60% of pure isomer, and 40-45% of ethylstyrene can also be used. The concept of tailoring the metal ion-specific ligands grafted on organic solid supports existed since the very early development of ion exchange resins [78-81]. The advantage of linking the metal ion specific ligands on to the polymer matrix is to avoid the loss of extractant normally encountered in extraction chromatography and solvent extraction procedures. Nevertheless, the employment of these organic solid supports for the treatment of radioactive liquid solutions suffer from a drawback of swelling and the chemical and radiolytic degradation [82, 83]. Also the contaminated spent ion exchange resins require further treatment for final disposal [84].

1.15.2. Inorganic adsorbents for metal ion separation

Inorganic adsorbents are extremely proven candidates for the selective separation of toxic and radiotoxic metal ions [85-90]. Extensive research in this area over few decades have fetched few potential adsorbents, that are also commercially available, for separating long lived fission products such as ^{90}Sr and ^{137}Cs from aqueous wastes [89]. The attraction over this material is further augmented by the surface modification of inorganic matrix with organic complexing moieties. The driving force for this development of organofunctionalized adsorbents (OFS) stems from the fact that it can be tuned to task specific adsorbent by proper selection of complexing moieties. These inorganic materials possess the desirable properties such as high selectivity, chemical and radiation stability for treating radioactive wastes. Moreover, these spent inorganic adsorbents can be immobilized in the form of glass or ceramic for final disposal [91]. Among the various OFS, organo functionalized silica gel based adsorbents have been studied extensively for the separation of metal ions from various feeds. Surface hydroxyl (SOH) groups present on hydrous silicon dioxide are responsible for the surface modification of the adsorbent. Organo modified silica based adsorbents have been explored for wide variety of applications such as removal of uranium from sea water [92], removal of cesium [93], removal of arsenic [94] etc.

1.15.3. Magnetic Solid phase Separation (MSPS).

MSPS is emerging as a promising technique for the separation of toxic and radiotoxic metal ions from various aqueous streams [95-103]. In MSPS technique, the magnetic particles (MPs) are added to the waste solution to extract the target metal ion. The MPs are then separated from the solution by means of an external magnetic force. The separated MPs are then immersed in a stripping solution for recovery of metal ions from the adsorbed surface. The use of MSPS offers several advantages especially for the treatment of nuclear wastes as compared to conventional solid phase extraction. Since this method uses the application of external magnetic field, the particle size of the adsorbent can be lowered to as low as nano-size for efficient and rapid extraction of metal ions from waste solution. In addition, there is no need for packing of MPs in column as it is usually operated in batch mode and the phase separation is quickly achieved by external magnetic field [95, 96]. In this context, Chen *et al.* [101] prepared bentonite-iron oxide composite materials for the removal of cobalt ions from radioactive waste water. Towler *et al.* [102] reported the extraction behavior of radium and polonium from sea water by the use of magnetic adsorbents. Recently, Wu *et al.* [103] has studied the separation behavior of lanthanum by using MSPS technique.

1.16. Scope of the present work

The present work involves the synthesis of various diglycolamic acid based extractants and their evaluation for the mutual separation of lanthanides and actinides. Diglycolamic acid is an acid derivative of diglycolamide. Diglycolamides are the popular reagents for the separation of trivalent lanthanides and actinides from concentrated nitric acid medium (3-4 M nitric acid). A pictorial representation of various extraction methods adopted for the mutual separation Ln(III)-An(III) separation by using diglycolamic acid ligand in the present study is shown in figure 1.5. Conventionally liquid-liquid extraction method is widely used in nuclear industry. A couple of diglycolamic acid based extractants such as bis(2-ethylhexyl)diglycolamic acid (HDEHDGA), bis(2-ethylhexyl)thiodiglycolamic acid (HDEHSDGA) etc. have been developed. The features that make diglycolamic acids unique among the class of extractants used for the mutual separation of lanthanides and actinides are given below.

1. Diglycolamic acids are CHON based.

2. High solubility of diglycolamic acid based extractants in n-dodecane or paraffinic diluents.

Third-phase formation, extractant diluent non-compatibility etc are the major limitations of liquid-liquid extraction. In contrast to the liquid-liquid extraction methods, the studies on the mutual separation of lanthanides and actinides using solid phase extraction methods are very limited. This is essentially due to the lack of availability of adsorbents suitable for lanthanide-actinide separation. Solid phase extraction is a promising technique for the separation of metal ions from aqueous solution owing to its simplicity, robustness, regenerating ability and can be easily engineered into plant scale levels and technologically demonstrated. In fact, solid phase extraction is suitable for the separation of micro-quantities of radionuclides present in a large volume of feed solution, as in the present case. Initially ligand impregnated resins were used for variety of applications. Wide variety of ligands can be impregnated in the form of solid phase extractants (SPE). In connection with this, alkyldiglycolamic acids such as N,N-di butyldiglycolamic acid (HDBDGA), N,N-di hexyldiglycolamic acid (HDHDGA), N,N-di octyldiglycolamic acid (HDODGA) and N,N-didecyldiglycolamic acid (HDDDGA) have been impregnated on resins. These diglycolamic acid impregnated resin offered high extraction of Eu(III) with superior Eu(III)/Am(III) separation. However, due to the poor chemical stability of these impregnated resins, ligand-chemically linked solid phase extractants (SPEs) (or also known as anchored resins) have been used at later stage.

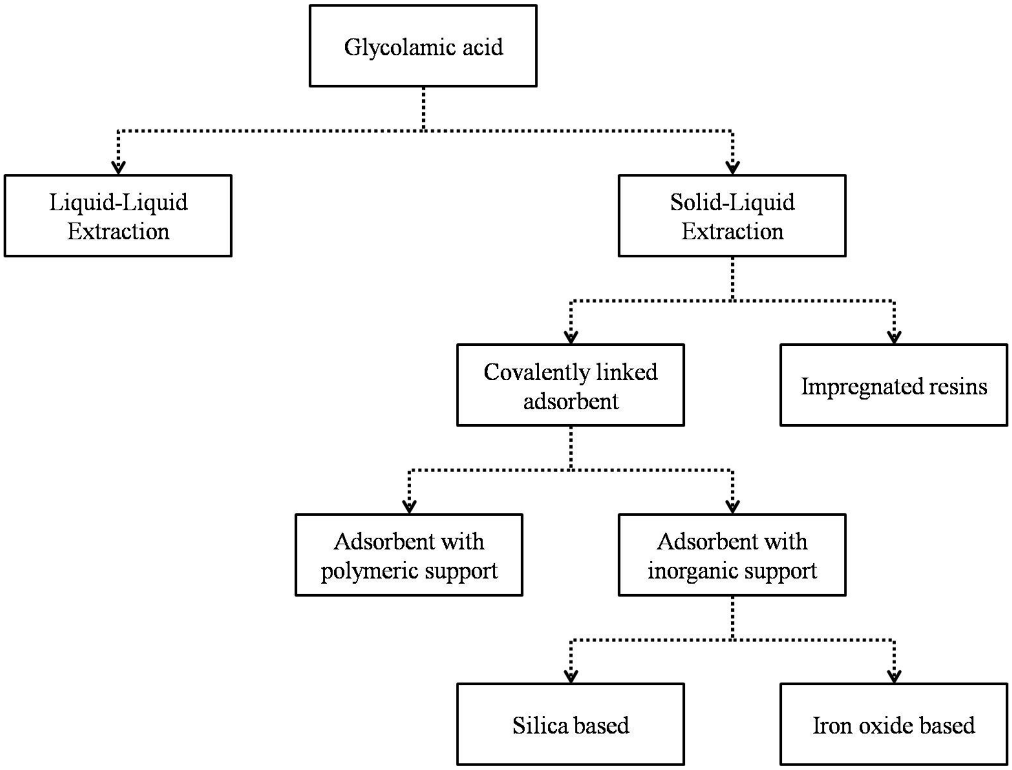

Figure 1.5. Different types of extractants with glycolamic acid

The concept of tailoring the metal ion-specific ligands grafted on organic solid supports existed since the very early development of ion exchange resins. The advantage of linking the metal ion specific ligands on to the polymer matrix is to avoid the loss of extractant normally encountered in extraction chromatography and solvent extraction procedures. The anchored resins have several advantages such as (i) wide variety of functional groups can be incorporated in polymer matrix using organic reactions, (ii) physical properties of polymer matrix can be finely tuned to suit particular applications, and (iii) they can withstand in normal operating conditions. In this context, a polyamine resin modified diglycolamic acid, PA-DGAH was synthesized and used for the mutual separation of lanthanides and actinides. Employment of this organic solid support for the treatment of radioactive liquid solutions suffers from drawbacks of swelling and the chemical and radiolytic degradation. Also the contaminated spent ion exchange resins require further treatment for final disposal. To overcome the problems associated with radiolytic degradation and disposal of spent organic resins, chemically inert inorganic solid supports such as silica grafted with various organic compounds have been studied for the efficient removal of metal ions from waste streams. The advantage of utilizing the inorganic solid support is that it can be vitrified or ceramized to an unleachable solid form for final disposal. In view of this, a silica anchored diglycolamic acid, Si-DGAH was developed for the mutual separation of lanthanides and actinides. However, these functionalized materials also have some drawbacks such as small particle size, choking of the column during engineering-scale operation, etc. These problems can be easily avoided by the use of magnetic solid-phase separation (MSPS) methodology.

MSPS is emerging as a promising technique for the separation of toxic and radiotoxic metal ions from various aqueous streams. In the MSPS technique, the magnetic particles (MPs) are added to the waste solution to extract the target metal ion. The MPs are then separated from the solution by means of an external magnetic force. The separated MPs are then immersed in a stripping solution for recovery of metal ions from the adsorbed surface. The use of MSPS offers several advantages especially for the treatment of nuclear wastes as compared to conventional solid phase extraction. Since this method uses the application of an external magnetic field, the particle size of the adsorbent can be lowered considerably for efficient and rapid extraction of metal ions from waste solution. In addition, there is no need for packing of the MPs in a column, as it is usually operated in batch mode and the phase separation is quickly achieved by the external magnetic field. In this context, an iron oxide (Fe_3O_4) particle functionalized with diglycolamic acid (Fe-DGAH) was developed for the mutual separation of Am(III) and Eu(III).

In nutshell, studies reported in this thesis aimed at the development of diglycolamic acid class of extractants having desirable properties for the mutual separation of trivalent actinides from trivalent lanthanides and vice-versa. Several alkyldiglycolamic acids have been synthesized and studied to examine the feasibility of using them for the mutual separation of trivalent lanthanides and actinides by liquid-liquid extraction as well as solid-liquid extraction route.

1.17. References

1. M.G. Patterson, What is energy efficiency?: Concepts, indicators and methodological issues. Energy policy. 24 (1996) 377-390.
2. S.A. Bhardwaj, Indian nuclear power programme–Past, present and future. Sadhana 38 (2013) 775-794.
3. R.B. Grover, S. Chandra, Scenario for growth of electricity in India. Energy Policy 34 (2006) 2834-2847.
4. M.V. Ramana, The power of promise: Examining nuclear energy in India. Penguin UK; 2012 Dec 15.
5. S. Glasstone, Sourcebook on atomic energy. Krieger Publishing Company, (1979)
6. R.G. Cochran, E.E. Lewis, N. Tsoulfanidis, W.F. Miller, The nuclear fuel cycle: analysis and management. American Nuclear Society (1990).
7. M. Bunn, J.P. Holdren, S. Fetter, B. Van Der Zwaan, The economics of reprocessing versus direct disposal of spent nuclear fuel. Nucl. Technol. 150 (2005) 209-230.
8. J.M. Gras, R.D. Quang, H. Masson, T. Lieven, C. Ferry, C. Poinssot, M. Debes, J.M. Delbecq, Perspectives on the closed fuel cycle–Implications for high-level waste matrices. J. Nucl. Mater. 362 (2007) 383-394.

9. R.K. Sinha, A. Kakodkar, The road map for a future Indian nuclear energy system (No. IAEA-CN--108) (2003)
10. B. Raj, H.S. Kamath, R. Nataraja, P.R. Vasudeva Rao, A perspective on fast reactor fuel cycle in India. Prog. Nucl. Energ. 47 (2005) 369-379.
11. S. Usha, R.R. Ramanarayanan, P. Mohanakrishnan, R.P. Kapoor, Research reactor KAMINI. Nucl. Eng. Des. 236 (2006) 872-880.
12. B. Bhattacharjee, An overview of R and D in fuel cycle activities of AHWR. In: Nuclear fuel cycle technologies: closing the fuel cycle (2003).
13. B.A. Moyer, Ion exchange and solvent extraction: a series of advances (Vol. 19). CRC Press (2009).
14. R. Taylor, Reprocessing and Recycling of Spent Nuclear Fuel, 1st Edition, Woodhead Publishing, pp.9 (2015).
15. D. Westlén. Reducing radiotoxicity in the long run. Prog. Nucl. Energ. 49 (2007) 597-605.
16. A.W. England, N.J. Trask, I.J. Winograd, Geologic disposal of high-level radioactive wastes: Earth-science perspectives. US Department of the Interior, Geological Survey; 1978.
17. http://www.edleaver.com/Archives/2013/06/PandorasBackPages/PandorasBackPages.php
18. M. Salvatores, G. Palmiotti, Radioactive waste partitioning and transmutation within advanced fuel cycles: Achievements and challenges. Prog. Part. Nucl. Phy. 66 (2011) 144-166.
19. T. Inoue, M. Sakata, H. Miyashiro, T. Matsumura, A. Sasahara, N. Yoshiki, Development of partitioning and transmutation technology for long-lived nuclides. Nucl. Technol. 93 (1991) 206-220.

20. K. Raj, K.K. Prasad, N.K. Bansal, Radioactive waste management practices in India. Nucl. Eng. Des. 236 (2006) 914-930.
21. J.P. Ackerman, Chemical basis for pyrochemical reprocessing of nuclear fuel. Ind. Eng. Chem. Res. 30 (1991) 141-145.
22. G.R. Choppin, A. Morgenstern, Radionuclide separations in radioactive waste disposal. J. Radioanal. Nucl. Chem. 243 (2000) 45-51.
23. J.L. Swanson, PUREX Process Flow sheets, In: Science and Technology of Tributyl phosphate (W.W. Schulz, L.L. Burger, J.D. Navratil, K.P. Bender, eds.) Vol III, CRC Press Inc., Boca Raton, p-55 (1984).
24. M. I. Ojovan, W.E. Lee, An introduction to nuclear waste immobilization. Elsevier, London, (2013)
25. W.J. Weber, R.C. Ewing, C.A. Angell, G.W. Arnold, A.N. Cormack, J.M. Delaye, D.L. Griscom, L.W. Hobbs, A. Navrotsky, D.L. Price, A.M. Stoneham, Radiation effects in glasses used for immobilization of high-level waste and plutonium disposition. J. Mater. Res. 12 (1997) 1948-1978.
26. I.W. Donald, B.L. Metcalfe, R.J. Taylor. The immobilization of high level radioactive wastes using ceramics and glasses. J. Mater. Sci. 32 (1997) 5851-5887.
27. K. Nishihara, S. Nakayama, Y. Morita, H. Oigawa, T. Iwasaki, Impact of partitioning and transmutation on LWR high-level waste disposal. J. Nucl. Sci. Technol. 45 (2008) 84-97.
28. E.M. Gonzalez-Romero, Impact of partitioning and transmutation on the high level waste management. Nucl. Eng. Des. 241 (2011) 3436-3444.
29. W.E. Lee, M.I. Ojovan, M.C. Stennett, N.C. Hyatt, Immobilisation of radioactive waste in glasses, glass composite materials and ceramics. Adv. Appl. Cer. amics. 105 (2013) 3-12.

30. A.E. Ringwood, V.M. Oversby, S.E. Kesson, W. Sinclair, N. Ware, W. Hibberson, A. Major, Immobilization of high-level nuclear reactor wastes in SYNROC: a current appraisal. Nucl. Chem. Waste Manag. 2 (1981) 287-305.
31. A.E. Ringwood, Disposal of high-level nuclear wastes: a geological perspective. Mineral. Mag. 49 (1985) 159-163.
32. A. Wilden, C. Schreinemachers, M. Sypula, G. Modolo, Direct Selective Extraction of Actinides (III) from PUREX Raffinate using a Mixture of CyMe4BTBP and TODGA as 1-cycle SANEX Solvent, Solv. Extr. Ion Exch. 29 (2011) 190–212.
33. G.L. Lummetta, A.V. Gelis, G.F., Review: solvent systems combining neutral and acidic extractants for separating trivalent lanthanides from the transuranic elements, Solv. Extr. Ion Exch. 28 (2010) 287–312.
34. G. Modolo, A. Wilden, P. Kaufholz, D. Bosbach, A. Geist, Prog. Nucl. Energ. 72 (2014) 107–114.
35. K. Bell, C. Carpentier, M. Carrott, A. Geist, C. Gregson, X. Hérès, D. Magnusson, R. Malmbeck, F. McLachlan, G. Modolo, U. Müllich, M. Sypula, R. Taylor, A. Wildene, Proc. Chem. 7 (2012) 392–397.
36. Z. Kolarik, E.P. Horwitz, Extraction of metal nitrates with octyl (phenyl)-n, n-diisobutyl-carbamoylmethyl phosphine oxides in alkane diluents at high solvent loading. Solv. Extr. Ion Exch. 6 (1988) 61-91.
37. M. P. Antony, R. Kumaresan, A.S. Suneesh, S. Rajeswari, B. Robertselvan, S. Sukumaran, R. Manivannan, K.V. Syamala, K.A. Venkatesan, T.G. Srinivasan, P.R. Vasudeva Rao, Development of a CMPO based extraction process for partitioning of minor actinides and demonstration with genuine fast reactor fuel solution (155 GWd/Te), Radiochim. Acta 99 (2011) 207–215.

38. J. Ravi, A.S. Suneesh, T. Prathibha, K.A. Venkatesan, M.P. Antony, T.G. Srinivasan, P.R. Vasudeva Rao, Extraction behavior of some actinides and fission products from nitric acid medium by a new unsymmetrical diglycolamide. Solvent Extr. Ion Exch. 29 (2011) 86–105.
39. S.A. Ansari, P. N. Pathak, P.K. Mohapatra, V.K. Manchanda, Aqueous partitioning of minor actinides by different processes. Sep. Pur. Rev. 40 (2011) 43-58.
40. M. Nilsson, K.L. Nash, A review of the development and operational characteristics of the TALSPEAK process, Solvent Extr. Ion Exch. 25 (2007) 665–701.
41. H.H. Dam, D.N. Reinhoudt, W. Verboom, Multicoordinateligands for actinide/lanthanide separations. Chem. Soc. Rev. 36 (2007) 367–385.
42. C. Ekberg, A. Fermvik, T. Retegan, G. Skarnemark, M.R.S Foreman, M.J. Hudson, S. Englund, M. Nilsson, An overview and historical look back at the solvent extraction using nitrogen donor ligands to extract and separate An(III) from Ln(III), Radiochim. Acta. 96 (2008) 225–233.
43. K.L. Nash, Separation chemistry for lanthanides and trivalent actinides. Handbook on the physics and chemistry of rare earths. (1994)
44. H.A. Abderrahim, Contribution of the European Commission to a European Strategy for HLW management through Partitioning & Transmutation. In: Nuclear Back-end and Transmutation Technology for Waste Disposal, pp. 59-71. Springer, Japan. 2015
45. H.C. Aspinall. Chemistry of the f-Block Elements. CRC Press (2001).
46. V. Alexander, Design and synthesis of macrocyclic ligands and their complexes of lanthanides and actinides. Chem. Rev. 95 (1995) 273-342.

47. P.G. Allen, J.J. Bucher, D.K. Shuh, N.M. Edelstein, I. Craig, Coordination chemistry of trivalent lanthanide and actinide ions in dilute and concentrated chloride solutions. Inorg. Chem. 39 (2000) 595-601.
48. C. Leggett, G. Liu, M.P. Jensen, Do aqueous ternary complexes influence the talspeak process, Solvent Extr. Ion Exch. 28 (2010) 313-334.
49. B. Weaver, F.A. Kappelmann, Preferential extraction of lanthanides over trivalent actinides by monoacidic organophosphates from carboxylic acids and from mixtures of carboxylic and aminopolyacetic acids. J. Inorg. Nucl. Chem. 30 (1968) 263-278.
50. A.V. Gelis, G.F. Vandegrift, A. Bakel, D.L. Bowers, A.S. Hebden, C. Pereira, M. Regalbuto, Extraction behaviour of actinides and lanthanides in TALSPEAK., TRUEX and NPEX processes of UREX+. Radiochim. Acta, 97 (2008) 231-245.
51. Z. Kolarik, U. Müllich, F. Gassner, Selective Extraction of Am(III) Over Eu(III) by 2,6-Ditriazolyl- and 2,6-Ditriazinylpyridines, Solvent Extr. Ion Exch. 17(1999) 23-32.
52. T. Suzuki, K. Otake, M. Sato, A. Ikeda, M. Aida, Y. Fujii, M. Hara, T. Mitsugashira, M. Ozawa, Separation of americium and curium by use of tertiary pyridine resin in nitric acid/methanol mixed solvent system, J. Radioanal. Nucl. Chem. 272 (2007) 257-265.
53. D.R. Peterman, M.R. Greenhalgh, R.D. Tillotson, J.R. Klaehn, M.K. Harrup, T.A. Luther, J.D. Law, L.M. Daniels, Separation of minor actinides from lanthanides by dithiophosphinic acid extractants ISEC 2008, INL/CON-07-13474, PREPRINT (2008)
54. G. Modolo, R. Odoj, Method of separating a trivalent actinide from a trivalent lanthanide and or yttrium in aqueous solution, US Patent, No. 6312654 B1 (2001)

55. G. Modolo, R. Odoj, Method of separating a trivalent actinide from a trivalent lanthanides, US Patent, No. 5,966,584 (1999)
56. R. Fitoussi, C. Musikas, H. Ranarivelo, Method for separating actinide from lanthanides in an acidic aqueous solution., US Patent, No.4461747 (1984)
57. B.F. Smith, G.D. Jarvinen, R.R. Ryan, Separation of Lanthanides from actinides, US Patent No. 4867951 (1989)
58. K.L. Nash, The chemistry of TALSPEAK: a review of the science, Solvent Extr. Ion Exch. 33(1) (2015) 1-55.
59. T.S. Grimes, R.D. Tillotson, L. R. Martin. Trivalent lanthanide/actinide separation using aqueous-modified TALSPEAK chemistry, Solvent Extr. Ion Exch. 32 (2014) 378-390.
60. T. Takeda, K.Yokoyama, Study on neutron spectrum for effective transmutation of minor actinides in thermal reactors. Annal. Nucl. Energ. 24 (1997) 705-719.
61. J.P. Grouiller, S. Pillon, C. S. Jean, F. Varaine, L. Leyval, G. Vambenepe, B. Carlier, Minor actinides transmutation scenario studies with PWRs, FRs and moderated targets. J. Nucl. Mater. 320 (2003) 163-169.
62. C.D. Bowman, E.D. Arthur, P.W. Lisowski, G.P. Lawrence, R.J. Jensen, J.L. Anderson JL, Blind B, Cappiello M, Davidson JW, England TR, Engel LN. Nuclear energy generation and waste transmutation using an accelerator-driven intense thermal neutron source. Nucl. Instr. Meth. Phys. Res. 320 (1992) 336-367.
63. J. Rydberg (ed). Solvent extraction principles and practice revised and expanded. CRC Press (2004).
64. K.N. Sabharwal, P.R. Vasudeva Rao, M. Srinivasan, Extraction of actinides by bifunctional phosphinic acid resin. Solvent Extr. Ion Exch. ange. 1994 Oct 1;12(5):1085-101.

65. X. Chunhua, S. Zhengnian, C. Yiyong, Studies on the sorption of macroporous phosphonic acid resin for lanthanum. Ion Exchange and Adsorption. (1997).
66. M. Rovira, L. Hurtado, J.L. Cortina, J. Arnaldos, A.M. Sastre, Recovery of palladium (II) from hydrochloric acid solutions using impregnated resins containing Alamine 336. React. Funct. Polym. 38 (1998) 279-287.
67. J.C. Veselsky, P.C. Kirl, N. Sezginer, The determination of U, Np and Pu in urine by sequential extraction with ALAMINE-336 from hydrochloric acid medium. J. Radioanal. Chem. 21 (1974) 97-106.
68. N. Kabay, M. Arda, B. Saha, M. Streat, Removal of Cr (VI) by solvent impregnated resins (SIR) containing aliquat 336. React. Funct. Polym. 54 (2003) 103-115.
69. R. Kumaresan, K.N. Sabharwal, T.G. Srinivasan, P.R. VasudevaRao, G. Dhekane, Synthesis, characterization, and evaluationof gel-type poly(4-vinylpyridine) resins for plutoniumsorption. Solvent Extr. Ion Exch. 25 (2007) 515–528.
70. P. Zhang, K. Inoue, K. Yoshizuka, H. Tsuyama, Extraction and selective stripping of molybdenum (VI) and vanadium (IV) from sulfuric acid solution containing aluminum (III), cobalt (II), nickel (II) and iron (III) by LIX 63 in Exxsol D80. Hydrometallurgy 41 (1996) 45-53.
71. A.W. Ashbrook, Commercial chelating solvent extraction reagents: I. Purification and isomer separation of 2-hydroxyoximes. J. Chromat. A. 105 (1975)141-150.
72. R.A. Day Jr, R.M.Powers, Extraction of uranyl ion from some aqueous salt solutions with 2-thenoyltrifluoroacetone. J. Am. Chem. Soc. 15 (1954) 3895-3897.
73. N.J. Simpson, Solid-phase extraction: principles, techniques, and applications. CRC Press, (2000).

74. E.M. Thurman, M.S. Mills, Solid-phase extraction: principles and practice. New York: Wiley; (1998).
75. A.A. Zagorodni, Ion exchange materials: properties and applications: properties and applications. Elsevier, (2006).
76. Ion Exchange and Solvent Extraction: A Series of Advances, Volume 8, J. A. Marinsky, Y. Marcus, CRC Press, chapter 3, pp-229, (1981).
77. A. Warshawaky, Chelating Ion Exchangers, in Ion Exchange and Sorption Processes, In: Hydrometallurgy, M. Streat, D. Naden (eds), Critical Reports on Applied Chemistry, Vol. 19, John Wiley & Sons, pp-166 (1987).
78. T. Takemura, Y. Katoh, S. Kurita, S. Sasaki, K. Funabiki, K. Hatano, United States patent US 4,051,098. (1977).
79. R.S.S. Murthy, D.E. Ryan, Preconcentration of copper, cadmium, mercury and lead from sea and tap water samples on a dithiocarbamatecellulose derivative. Anal. Chim. Acta 140 (1982) 163–169.
80. E.P. Horwitz, R. Chiarizia, H. Diamond, R.C. Gatrone, S.D. Alexandratos, A.Q. Trochimczuk, D.W. Crick, Uptake of metal ions by a new chelating ion-exchange resin. Part 1: acid dependencies of actinide ions, Solvent Extr. Ion Exch. 11 (1993) 943–966.
81. K.A. Venkatesan, D.K. Patre, K.N. Sabharwal, T.G. Srinivasan, P.R. Vasudeva Rao, Kinetics of uranium extraction by macroporousbifunctionalphosphinic acid resin. Solvent Extr. Ion Exch. 18 (2000) 551–565.
82. L.R. Van Loon, W. Hummel, Radiolytic and chemical degradation of strong acidic ion-exchange resins: Study of the ligands formed. Nucl. Tech. 128 (1999) 359–371.

83. R. Chiarizia, E.P. Horwitz, Radiolytic stability of some recently developed ion exchange and extraction chromatographic resins containing diphosphonic acid groups. Solvent Extr. Ion Exch. 18 (2000) 109–132.
84. F. Frizon, C. Cau-dit-Coumes, Cementation of ILW ion exchange resins: Impact of sulfate ions released by radiolysis on hydrated matrix. J. Nucl. Mater. 359 (2006) 162–173.
85. A. Clearfield A. Inorganic ion exchange materials. CRC press (1982).
86. K.A. Venkatesan, V. Sukumaran, M.P. Antony, P.R. VasudevaRao, Extraction of uranium by amine, amide and benzamide grafted covalently on silica gel. J. Radioanal. Nucl. Chem. 260 (2004) 443–450.
87. G.E. Fryxell, W. Chouyyok, R.D. Rutledge, Design and synthesis of chelating diamide sorbents for the separation of lanthanides, Inorg. Chem. Commun. 14 (2011) 971–974.
88. A.R. Cestari, C. Airoldi, Chemisorption on thiol–silicas: divalent cations as a function of pH and primary amines on thiol–mercury adsorbed. J. Colloid. Interface Sci. 195 (1997) 338–342.
89. R. Chiarizia, E.P. Horwitz, K.A. D'Arcy, S.D. Alexandratos, A.W. Trochimzuk, Uptake of Actinides and other Ions by Dipiosil. A New Silica based Chelating Ion Exchange Resin In Ion Exchnge Developments and Applications, J.A. Greig (ed). Proceedings of IEX, The Royal Society of Chemistry, UK, pp- 321 (1996).
90. R.A. Bulman, G. Szabo, R.F. Clayton, C.R. Clayton, Investigations of the uptake of transuranicradionuclides by humic and fulvic acids chemically immobilized on silica gel and their competitive release by complexing agents, Waste Manage. 17 (1997) 191–199.

91. W. Lutze, R.C. Ewing, Radioactive waste forms for future, North-Holland, Oxford, 1988.
92. M. Shamsipur, A.R. Ghiasvand, Y. Yamini, Solid-phase extraction of ultratrace uranium (VI) in natural waters using octadecyl silica membrane disks modified by tri-n-octylphosphine oxide and its spectrophotometric determination with dibenzoylmethane. Anal. Chem. 71 (1999) 4892-4895.
93. T. Sangvanich, V. Sukwarotwat, R.J. Wiacek, R.M. Grudzien, G.E. Fryxell, R.S. Addleman, C. Timchalk, W. Yantasee, Selective capture of cesium and thallium from natural waters and simulated wastes with copper ferrocyanide functionalized mesoporous silica. J. Hazard. Mater. 182 (2010) 225-231.
94. D. Mohan, C.U. Pittman, Arsenic removal from water/wastewater using adsorbents—a critical review. J. Hazard. Mater. 142 (2007) 1-53.
95. K. A. Arteaga, J.A. Rodriguez, E. Barrado, Magnetic solids in analytical chemistry. Anal. Chim. Acta 674 (2010) 157–165.
96. G. Giakisikli, A.N. Anthemidis, Magnetic materials as sorbents for metal/metalloid preconcentration and/or separation. A review. Anal. Chim. Acta 789 (2013) 1–16.
97. Y. Liu, M. Chen, H. Yongmei, Study on the adsorption of Cu (II) by EDTA functionalized Fe3O4 magnetic nano-particles. Chem. Eng. J. 218 (2013) 46–54.
98. L.L. Vatta, J. Kramer, K.R. Koch, Diethylenetriamine Functionalized Silica Coated Magnetite Nanoparticles for Selective Palladium Ion Extraction from Aqueous Solutions. Sep. Sci. Technol. 42 (2007) 1985–2002.
99. M.E. Mahmoud, M.S. Abdelwahab, E.M. Fathallah, Design of novel nano-sorbents based on nano-magnetic iron oxide–bound-nano-silicon oxide–immobilized-triethylenetetramine for implementation in water treatment of heavy metals. Chem. Eng. J. 223 (2013) 318–327.

100. A. Afkhami, R. Norooz-Asl, Removal, preconcentration and determination of Mo(VI) from water and wastewater samples using maghemitenanoparticles, Colloids Surf., A 346 (2009) 52–57.

101. L. Chen, Y. Huang, L. Huang, B. Liu, G. Wang, S. Yu, Characterization of Co(II) removal from aqueous solution using bentonite/iron oxide magnetic composites, J. Radioanal. Nucl. Chem. 290 (2011) 675–684.

102. P.H. Towler, J.D. Smith, D.R. Dixon, Magnetic recovery of radium, lead and polonium from seawater samples after preconcentration on a magnetic adsorbent of manganese dioxide coated magnetite. Anal. Chim. Acta 328 (1996) 53–59.

103. D. Wu, Y. Sun, Q. Wang, Adsorption of lanthanum (III) from aqueous solution using 2-ethylhexyl phosphonic acid mono-2-ethylhexyl ester-grafted magnetic silica nanocomposites, J. Hazard. Mater. 260 (2013) 409– 419.

Chapter 2: Experimental

This chapter deals with the synthesis of various extractants used for the mutual separation of Am(III) and Eu(III) from dilute nitric acid solutions. The analytical techniques such as FT-IR, ^{1}H & ^{13}C-NMR, SEM-EDX, XRD, Raman Spectroscopy and TG-DTA etc. used for the characterization of the extractants are presented in this chapter. The experimental methods adopted for the mutual separation of Eu(III) and Am(III) using methods such as liquid-liquid extraction, mixer-settler demonstration, impregnated resin, polymeric ion exchange resin, inorganic adsorbent and magnetic separation etc. are discussed. Methods and materials employed for the analysis of radioactive and non-radioactive samples along with instruments such as NaI(Tl) detector, gamma-spectrometer, inductively coupled plasma-optically emission spectrometry (ICP-OES) etc. employed for the above studies have been explained in detail. Experimental details on the mixer-settler demonstration, column chromatographic demonstration and magnetic separation etc. are also presented in this chapter.

2.1. Chemicals and reagents

All the chemicals and reagents used in this study were of analytical grade and were used as received unless otherwise mentioned.

2.1.1. Radioactive tracers

The radioisotopes $^{(152+154)}$Eu, ^{241}Am were obtained from Bhabha Atomic Research Centre, Mumbai. Approximately 10^{-4} M of these tracers has been used for the experiments involving distribution ratio measurements.

2.1.2. Organic materials and solvents

Diglycolic anhydride

Diglycolic anhydride (97 %), obtained from Alfa Aesar was used.

Dichloromethane

Dichloromethane was obtained from Fischer Inorganics and Aromatics Limited, Chennai, India.

Silica-gel

Silica-gel of mesh 60-120, used for synthesizing the silica functionalized adsorbents, was obtained from Sisco Research Lab Private Limited, Mumbai, India and was dried at 373 K for one hour prior to use.

Dialkylamines

Dibutylamine, dihexylamine, dioctylamine, didecylamine and di-2-ethylhexylamine were procured from Sigma Aldrich Chemie GmbH, Steinheim, Germany. Didodecylamine was obtained from Fluka.

Tetraethoxysilane(TEOS)

TEOS (purity) was procured from Sigma Aldrich Chemie GmbH, Steinheim, Germany.

Triethoxytriaminopropylsilane (APTS)

Triethoxytriaminopropylsilane (97 %) was procured from Sigma Aldrich Chemie GmbH, Steinheim, Germany.

Resins used for the studies

Tulsion ADS 400 resin used for the impregnation of the alkyldiglycolamic acid was procured from M/s. Thermax Pvt. Ltd., Pune, India. Similarly, polyamine resin, Tulsion 10X-MP was also obtained from M/s. Thermax Pvt. Ltd., Pune, India.

2.1.3. Aqueous solutions and complexing agents

Diethylenetriaminepentaaceticacid(DTPA)

Diethylene triaminepentaacetic acid (DTPA) was procured from Acros Organics, Germany. DTPA was poorly soluble in water. Therefore, aqueous solutions of DTPA were prepared in demineralized water with the addition of few drops of concentrated NaOH (2 M). The solution was later adjusted to desired pH by adding few drops of concentrated HNO_3 (5 M).

Acid solutions

The acid solutions (HNO_3, HCl, GR grade, Merck Specialties Private Limited, Mumbai, India) were prepared by the dilution of concentrated acids, and were standardized by standard acid-base titration methods using standard NaOH solution using phenolphthalein as indicator.

Sodium hydroxide solution

Sodium hydroxide (AR grade) was obtained from Ranbaxy Fine Chemicals Limited, New Delhi, India.

Phenolpthalein

Phenolpthalein (Merck Specialities Private Limited, Mumbai, India) solution was prepared by dissolving ~ 500 mg of solid in 100 mL of 1:1 mixture of distilled water and ethanol.

Sodium Nitrate

Sodium Nitrate was obtained from S.D. fine Chemicals, Mumbai, India.

Citric acid

Citric acid, anhydrous was obtained from Otto Chemie, Mumbai, India.

Bis(ethylenediaminetetraacetic acid (EDTA)

Bis(ethylenediaminetetraacetic acid) (EDTA) was obtained from Sigma Aldrich Chemie GmbH, Steinheim, Germany.

Europium nitrate

Europium nitrate hexahydrate was purchased from Sigma Aldrich, India.

2.2. Instrumentation

2.2.1. Sodium Iodide thalium (NaI (Tl) gamma counter

The activity of ^{241}Am, $^{(152+154)}$Eu and other gamma emitting radioisotopes were measured using a gamma counter. The gamma counter constitutes a well type NaI(Tl) detector associate with photomultiplier unit, single channel analyzer and a counter time unit. The NaI(Tl)-photomultiplier integral assembly was procured from M/s. Harshaw, U.S.A and other electronic modules were obtained from M/s. ECIL (Electronic Corporation of India Limited), Hyderabad, India.

For the measurement of radioactivity by NaI (Tl) counter, approximately 10^{-4} M of the tracer spiked aqueous solutions has been used for the equilibration experiments. In $^{(152+154)}$Eu tracer, ^{154}Eu decays predominantly by beta mode with predominant gamma energies (keV) 1274, 1004 and 996 and ^{152}Eu isotop (half life = 13 year and specific activity =180 Ci/g) decays both by beta (28%) and electron capture (72%) modes by predominant gamma energies (keV) 1112, 1085.8 and 1408. ^{241}Am having a half life of 433 years with predominant gamma energy of 60 keV.

2.2.2. High Pure Gamma Spectrometer (HpGe Detector)

The activities of gamma emitting radioisotopes present in simulated and actual high active waste were measured by Gamma Spectrometry. In this technique, a planar high pure germanium (HpGe) crystal semiconductor obtained from OXFORD Instruments, USA was used as the detector.

2.2.3. Rotary evaporator

A rotary evaporator (model R-3000 from M/s. Buchi Laboratory Technique AG, Switzerland) was used for distilling off volatile solvents from the reaction mixture and from fractions collected during the column chromatography.

2.2.4. pH meter

All pH measurements were made with Cyberscan 500 pH, Metrohm. The meter was calibrated at 298 K with standard buffers of pH 4, 7 and 10.

2.2.5. Thermostatted rotary water bath shaker

A JULABO (F33-HE) refrigerated circulator with a temperature controlling accuracy of $\pm$ 0.010 K and a heating immersion circulator with a temperature controlling accuracy of $\pm$ 0.010 K were also used for the experiments.

2.2.6. FT-IR spectrometer

A BOMEM MB-100 FT-IR spectrometer with a range of 4000-650 cm^{-1} with a resolution of 4 cm^{-1} was used for the measurement of IR spectra. The samples to be scanned were sandwiched between two zinc-selenide windows. The sample compartment was purged with nitrogen for a sufficient period prior to scan. For solid sample analysis, a thin pellet of sample was prepared in dry KBr salt and recorded.

2.2.7. Mass spectrometer

A home built reflectron time of flight mass spectrometer was used for the mass analysis. Nicotinic acid was used as a matrix and a fourth harmonic of Nd-YAG laser (266 nm) was used for the desorption/ionization. Fine graphite powder mixed uniformly as the matrix for the mass analysis of organic compounds to enhance the absorption of laser [1].

Some of the mass spectra were also obtained by Thermofisher Scientific make GC-(qudrupole) MS with electron impact ionizer. A 15 m long silica capillary column was used for GC separations during these experiments.

2.2.8. NMR spectrometer

A Brucker Avance III 500 MHz (AV 500) multi nuclei solution nmr spectrometer was used the structure analysis of synthesized diglycolamic acids and diglycolamides. $CDCl_3$ was used as the solvent.

2.2.9. Inductively coupled plasma-optical emission spectrometer

Ultima C spectroanalyser (Jobin Yvon, France) equipped with Inductively Coupled Plasma excitation source was used for several non-radioactive elemental analysis. The spectrometer provides a resolution of 0.015 nm with a polyscan facility of ± 2 nm. RF generator of 40.68 MHz with a maximum output power of 1550 W was used for plasma generation. Samples were injected by the in-built peristaltic pump with the flow rate of 1mL/min. The emission lines chosen for the given metal analysis were the most sensitive lines having no interference from other elements in the group.

2.2.10. SEM-EDX

Field Emission Gun-Scanning Electron Microscopy (FEG-SEM) images were obtained using TESCAN MIRA 3 model at 15 kV. Energy Dispersive X-ray spectral analysis (EDX) image was recorded with an Oxford instrument to examine the surface morphology and elemental composition of the adsorbent.

2.2.11. XRD

The X-ray diffraction pattern of the adsorbent was obtained using a Philips 1011 X-ray diffractometer (operating with 40 KV and 45 mA) with Cu Kα (1.5406 Å) radiation.

2.2.12. Raman

Raman spectra were measured by using a Renishaw Raman imaging microscope, including a spectrometer connected to a CCD detector.

2.2.13. TG-DTA

The TG-DTA pattern was recorded by subjecting the sample at a heating rate of 10 °C/minute for the temperature range of 25-600 °C using a thermogravimetric analyzer, Mettler Toledo (TGA/SDTA 851e).

2.2.14. CHNS

Microelemental CHNS analysis of the samples was carried out by using Elementer Vario-EL.

2.2.15. Particle analyzer

Particle size was measured by Zeta sizer, Malvern Instruments model ZS-90.

2.2.16. Surface area analyzer

The surface area of the magnetic adsorbents were determined by the BET method using Quantachrome Monosorb surface area analyzer.

2.2.17. Electronic single pan balance

A calibrated electronic single pan balance with a sensitivity of 0.01 mg was used to weigh chemicals and solutions.

2.3. Preparation of reagents and their characterization

2.3.1. Synthesis of N,N-dialkyldiglycolamic acids

The synthesis and characterization of dialkyldiglycolamic acids such as N,N-bis(2-ethylhexyl)diglycolamic acid (HDEHDGA), N,N-dibutyldiglycolamic acid (HDBDGA), N,N-dihexyldiglycolamic acid (HDHDGA), N,N-dioctyldiglycolamic acid (HDODGA), N,N-didecyldiglycolamic acid (HDDDGA) were synthesized by condensation reaction between diglycolic anhydride and corresponding N,N-dialkylamines by the method discussed elsewhere [2]. Briefly, the procedure is described below. Diglycolic anhydride (0.03 mol) was mixed with 30 ml of dichloromethane and stirred in a round bottom flask equipped with a $CaCl_2$ guard tube for about 10 minutes. The desired N,N-dialkylamine (0.033 mol) was added drop-wise to the solution of diglycolic anhydride and the reaction mixture was stirred at room temperature for about 6 hours. The crude reaction mixture was washed with 1M hydrochloric acid (20 mL x 5 times). The organic phase was separated out and washed with distilled water (20 mL x 5 times). The separated organic phase was dried in a rotary evaporator at 353 K to remove the solvent. HDEHSDGA was also synthesized by a similar procedure by reacting thiodiglycolic anhydride (0.03 mol) and N,N-bis (2-ethylhexyl)amine (0.03 mol) in presence of dichloromethane as solvent. An illustration of the synthetic scheme is showed in figure 2.1.

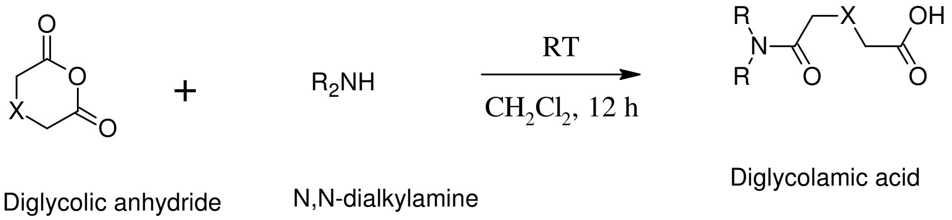

R=butyl, hexyl, octyl, decyl, bis(2-ethylhexyl)
X=O for HDBDGA, HDHDGA, HDODGA, HDDDGA, HDEHDGA and X=S for HDEHSDGA

Figure 2.1. Scheme for the synthesis of alkyldiglycolamic acids

2.3.2. Characterization of N,N-dialkyldiglycolamic acids

The NMR spectra (^1H and ^{13}C) of the samples were characterized using Bruker Avance III 500 MHz (AV500) and FTIR spectra were obtained using Bomem FTIR spectrometer model-103. The results are given below.

HDEHDGA

FTIR ʋ/cm^{-1}: 3454 (COOH), 1739 (-CO in COOH), 1622(-CO in –CON), 1226. ^{1}H NMR ($CDCl_3$, δ/ppm relative to TMS): 10.67 (s, ^{1}H, COOH), 4.32 (s, 2H, $-OCH_2-$), 4.11(s, 2H, $-CH_2O-$), 3.17-3.31 (m, 4H, 2 x CH_2 - N), 2.96-2.98 (m, 2H, 2 x CH), 1.15-1.24 (m, 16H, 8 x CH_2 of alkyl chain), 0.77- 0.84(m, 12H, 4 x CH_3). ^{13}C NMR ($CDCl_3$, δ/ppm relative to TMS): 172.22 (CO), 172.14 (CO), 77.21($-OCH_2$), 71.1($-CH_2O$ -), 49.34 (2 x $-CH_2-N$), 37.16 (2 x CH), 30.35 (2 x $-CH_2$), 28.47(2 x CH_2), 23.58 (2 x CH_2), 22.86 (2 x CH_2), 13.93 (2 x CH_3), 10.47 (2 x CH_3). The Electron ionization mass spectrum shows a peak corresponding to the mass of 356.5. Mass spectrum of HDEHDGA is showed in figure 2.2.

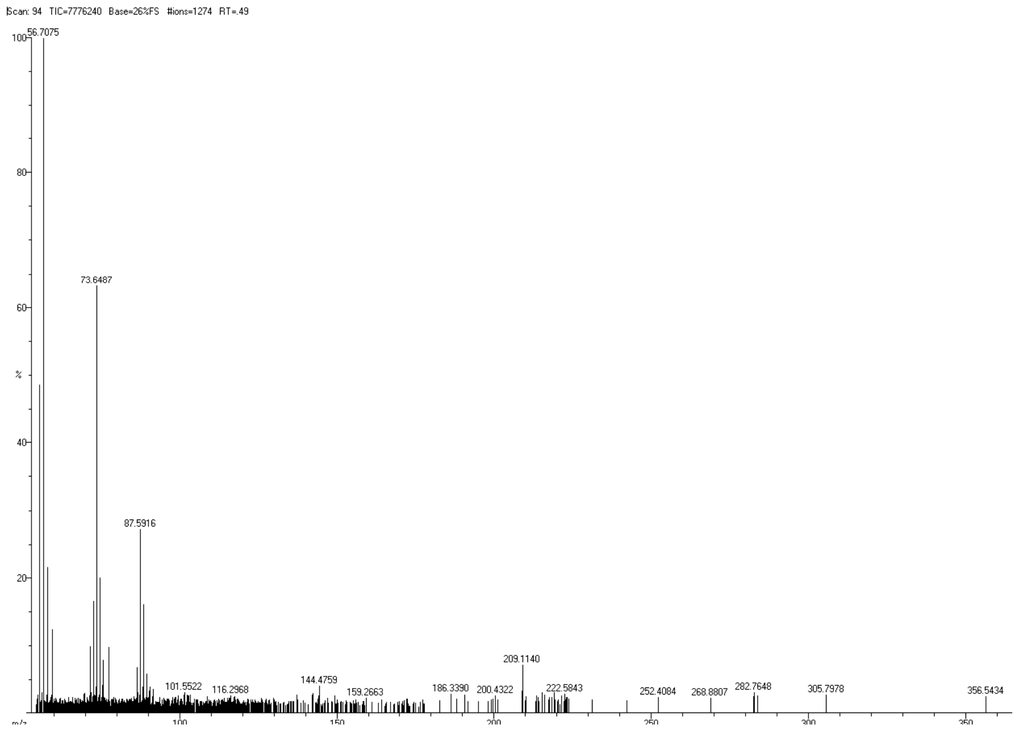

Figure 2.2. Mass spectrum of HDEHDGA recorded using GC-MS

HDEHSDGA

FTIR υ/cm^{-1}: 3637.6 (COOH), 1724(-CO in COOH), 1598 (-CO in –CON), ^{1}H NMR: ($CDCl_3$, δ/ppm relative to TMS: 9.37 (s,1H, COOH), 3.54(s, 2H, -OCH_2-), 3.50(s, 2H, -CH_2O-), 3.38-3.27(m, 4H, 2 x –CH_2-N-), 2.89-2.87(m, 2H, 2 x –CH-),1.74-1.69(m, 4H, 2 x –CH_2),1.62-1.59(m, 4H, 2 x –CH_2),1.40-1.22(m, 8H, alkyl chain), 0.92-0.86(m, 12H, 4 x –CH_3). ^{13}C NMR: ($CDCl_3$, δ/ppm relative to TMS): 171.5 (CO), 170.6(CO), 77.3(-O-CH_2-, 76.8(-CH_2O-), 49.5 (2 x –CH_2-N-), 37.8(2 x CH), 30.5(2 X –CH_2), 28.7(2 x –CH_2-), 23.8 (2 x -CH_2), 22.9 (2 x –CH_2-), 13.9 (2 x CH_3), 10.5(2 x CH_3-). Electron ionization mass spectrum shows the peak at 373.5.

Bis-butyldiglycolamic acid

^{1}H NMR: ($CDCl_3$, δ/ppm relative to TMS): 9.65(s, 1H, COOH), 3.28-3.06 (m, 4H,2 x -CH_2-N), 1.59-1.47 (m, 4H), 1.23(s, 10H). ^{13}C NMR: ($CDCl_3$, δ/ppm relative to TMS):172 (C=O), 169(C=O), 77(-O-CH_2-), 69(-CH_2O-), 47(2 x –CH_2-N-), 31(2 x CH_2-), 26(2 x CH_2), 22(2 x CH_2), 13(2 x CH_3). The FT-IR spectrum showed the transmittance (cm^{-1}) bands at the following frequencies 3389 (O–H stretching), 2901 (–CH_3-stretching), 1701 (C=O-stretching), 1602 (C=O-stretching), 1439 (CH_2-bending), 1400 (–C–N-stretching), 1379 (–CH_3-bending), 1125 (C–O-stretching). The molecular ion peak in the mass spectrum was found at m/z of 245.3.

Bis-hexyldiglycolamic acid

^{1}H NMR: ($CDCl_3$, δ/ppm relative to TMS): 3.36-3.33(d, 4H), 3.14-3.10(m, 3H), 4.36-4.18(s, 2H). ^{13}C NMR: (CDCl3, δ/ppm relative to TMS): 172(C=O), 170(C=O), 77(-O-CH_2-), 70(-CH_2O-), 47(2 x –CH_2-N-), 30(2 x CH_2-), 27(2 x CH_2-), 20(4 x CH_2-), 13(2 x CH_3). The FT-IR spectrum showed the transmittance (cm^{-1}) bands at the following frequencies 3400 (O–H stretching), 2911 (–CH_3-stretching), 1704 (C=O-stretching), 1654

(C=O-stretching), 1436 (CH_2-bending), 1394 (–C–N- stretching), 1388 (–CH_3-bending), 1095 (C–O-stretching). The molecular ion peak in the mass spectrum was found at m/z of 301.4.

Bis-octyldiglycolamic acid

^{1}H NMR: ($CDCl_3$, δ/ppm relative to TMS): 9.34(s, 1H, COOH),3.28-3.06 (m, 4H, 2 x -CH_2-N),1.59-1.47 (m, 4H), 1.23(s, 10H). ^{13}C NMR: ($CDCl_3$, δ/ppm relative to TMS): 172(C=O), 170(C=O), 77(-O-CH_2-), 70(-CH_2O-), 46(2 x –CH_2-N-), 31(2 x CH_2-), 28(2 x CH_2-), 22(8 x CH_2-), 14(2 x CH_3). The FT-IR spectrum showed the transmittance (cm_{-1}) bands at the following frequencies 3413 (O–H stretching), 2926 (–CH_3-stretching), 1713 (C=O-stretching), 1628 (C=O-stretching), 1466 (CH_2-bending), 1400 (–C–N- stretching), 1375 (–CH_3-bending), 1120 (C–O-stretching). The molecular ion peak in the mass spectrum was found at m/z of 357.4.

Bis-decyldiglycolamic acid

^{1}H NMR: ($CDCl_3$, δ/ppm relative to TMS): 9.34(s, 1H, COOH),3.28-3.06 (m, 4H, 2 x -CH_2-N),1.59-1.47 (m, 4H), 1.23(s, 10H). ^{13}C NMR: ($CDCl_3$, δ/ppm relative to TMS): 172(C=O), 170(C=O), 77(-O-CH_2-), 70(-CH_2O-), 47(2 x –CH_2-N-), 30(2 x CH_2-), 27(2 x CH_2-), 20(4 x CH_2-), 13(2 x CH_3). The FT-IR spectrum showed the transmittance (cm_{-1}) bands at the following frequencies 3426 (O–H stretching), 2932 (–CH_3-stretching), 1716 (C=O-stretching), 1614 (C=O-stretching), 1445 (CH_2-bending), 1394 (–C–N- stretching), 1382 (–CH_3-bending), 1106 (C–O-stretching). The molecular ion peak in the mass spectrum was found at m/z of 413.6.

2.3.3. Impregnation of N, N-diglycolamic acids on Tulsion ADS 400 resin

Alkyldiglycolamic acids with straight chain alkyl group such as N,N-dibutyldiglycolamic acid, N,N-dihexyldiglycolamic acid, N,N-dioctyldiglycolamic acid, N,N-didecyldiglycolamic acid etc. were impregnated on to Tulsion ADS 400 resin. Tulsion ADS 400 is an aryclic copolymer having average particle size of 800 µm. The polymer was purified by washing the resin sequentially with water, methanol, and acetone. The washed product was dried at 353 K in a rotary evaporator. The alkyl diglycolamic acids impregnated into Tulsion ADS-400 by contacting the dried resin with a solution of diglycolamic acid in dicholoromethane. The mixture was shaken vigorously for about 8 hours. The dicholormethane was then removed by rotary evaporation at 353 K. The dried resin was used for all studies.

2.3.4. Synthesis and characterization of PA-DGAH

2.3.4.1. Synthesis of PA-DGAH

PA-DGAH was synthesized by the condensation reaction between diglycolic anhydride (10 g) present in chloroform (100 mL) and Tulsion A-10X-MP resin (320 g). The reaction scheme is shown in figure 2.3. The reagents were taken in a round bottom flask equipped with a $CaCl_2$ guard tube. The mixture was refluxed at 440 K for 18 hours. The resin beads were separated by filteration and washed several times with water, isopropanol and acetone. The anchored resin was air-dried and used for equilibration studies.

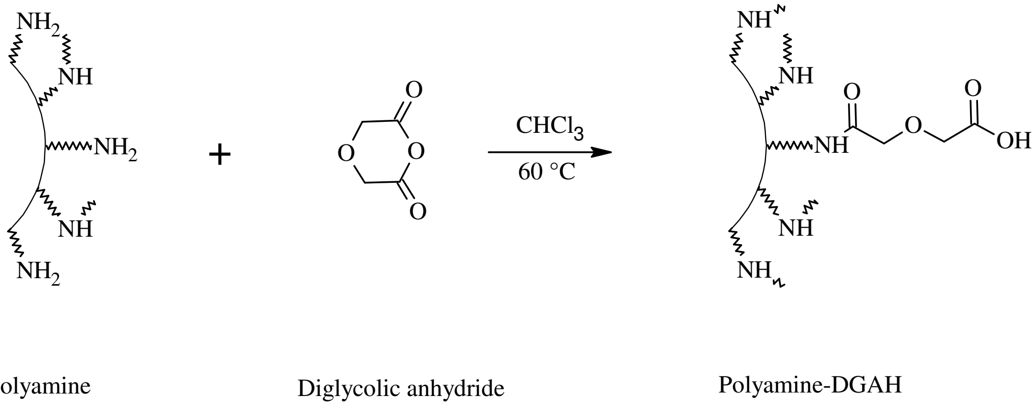

Figure 2.3. Reaction scheme for the preparation of PA-DGAH

2.3.4.2. Characterization of PA-DGAH

The IR spectrum of the product (PA-DGAH) is compared with the polyamine matrix in figure 2.4. It can be seen that PA-DGAH contains the transmittance bands at 1643 cm^{-1} and 1743 cm^{-1}. They are responsible for the C=O stretching of amidic (-NH-C=O) and terminal carboxylic acid (-C=O(OH)) groups respectively. In addition, the PA-DGAH also shows the bands responsible for C-H stretching at 2800 cm^{-1} and C-H bending at 1100 cm^{-1}. The IR pattern obtained in PA-DGAH confirms the anchoring of diglycolamic acid on polyamine resin beads. The amount of diglycolamic acid present in a gram of resin was determined to be 2.5 mmol/g (section 2.6), which is in reasonable agreement with the amount of amine moieties (3 mmol/g), present in polyamine beads.

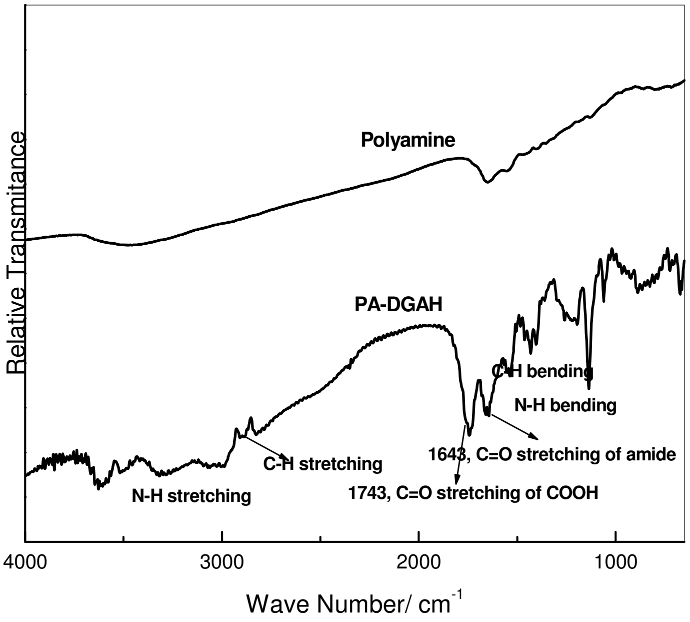

Figure 2.4. FT-IR spectra of PA-DGAH and polyamine resin.

The TG, derivative of TG (DTG) and DTA curves for polyamine resin and PA-DGAH are shown in figure 2.5 and figure 2.6 respectively. The loss of weight occurring below 373 K in both cases is attributed to the loss of water molecules adsorbed on the surface of the adsorbent. A prominent weight loss occurring in the temperature range 373-550 K in PA-DGAH (figure 2.6) could be attributed to the dehydration reaction occurring between the two adjacent carboxylic acid groups, leading to the elimination of water. This reaction essentially occurs in PA-DGAH due to the presence of terminal carboxylic acid. This is also reflected as an endothermic peak at 474 K in DTA curve in figure 2.5. The decomposition of organics occurs in the temperature range 550-1000 K. An exothermic peak occurring in the DTA pattern above 550 K results in a peak at ~990 K is due to combustion of organics present in both polymers.

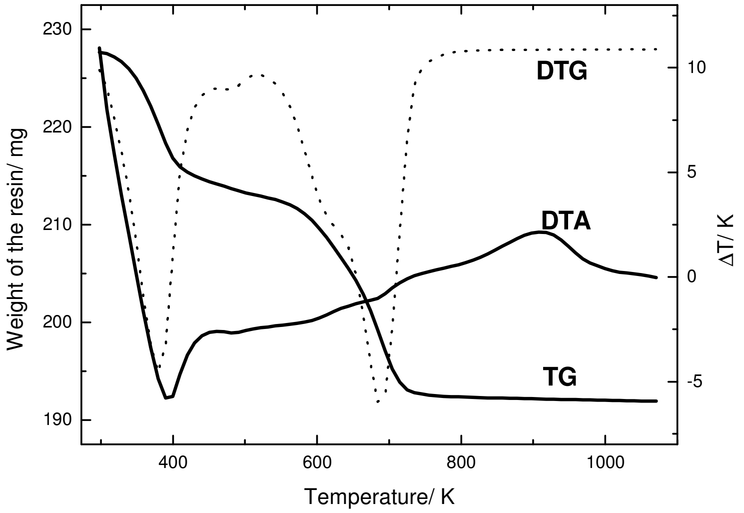

Figure 2.5. TG-DTA pattern obtained for polyamine.

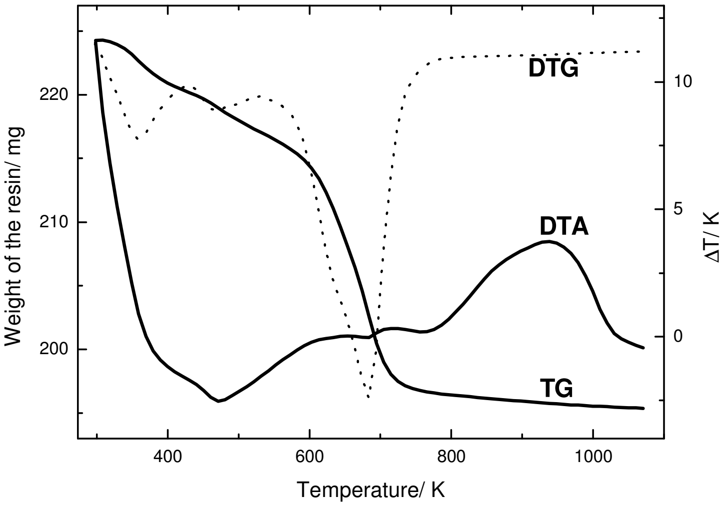

Figure 2.6. TG-DTA pattern obtained for PA-DGAH.

2.3.5. Preparation of silica adsorbent, Si-DGAH

Synthetic scheme involved in the synthesis of the silica-diglycolamic acid, Si-DGAH is shown in figure 2.7. The procedures involved in the synthesis and characterization of Si-DGAH and the intermediate products are described below.

2.3.5.1. Synthesis of silane-diglycolamic acid (Silane-DGAH)

Silane-DGAH was synthesized by the condensation reaction between diglycolic anhydride (0.03 mol.) present in dichloromethane (30 mL) and 3-aminopropyltriethoxysilane (APTS, 0.03 mol.). The diglycolic anhydride was taken in a round bottom flask equipped with a $CaCl_2$ guard tube and APTS was added drop-wise to the solution. The mixture was stirred at room temperature for about 6 hours. The reaction mixture was dried in a rotary evaporator at 353 K to remove the solvent. The product obtained after drying (Silane-DGAH) was characterized by ^{1}H NMR (Bruker Avance III 500 MHz (AV500)). ^{1}H NMR ($CDCl_3$, δ/ppm relative to TMS): 9.65 (s, 1H, COOH), 3.28-3.06 (m, 4H, 2 x $-CH_2-N$), 1.59-1.47 (m, 4H), 1.23(s, 10H).

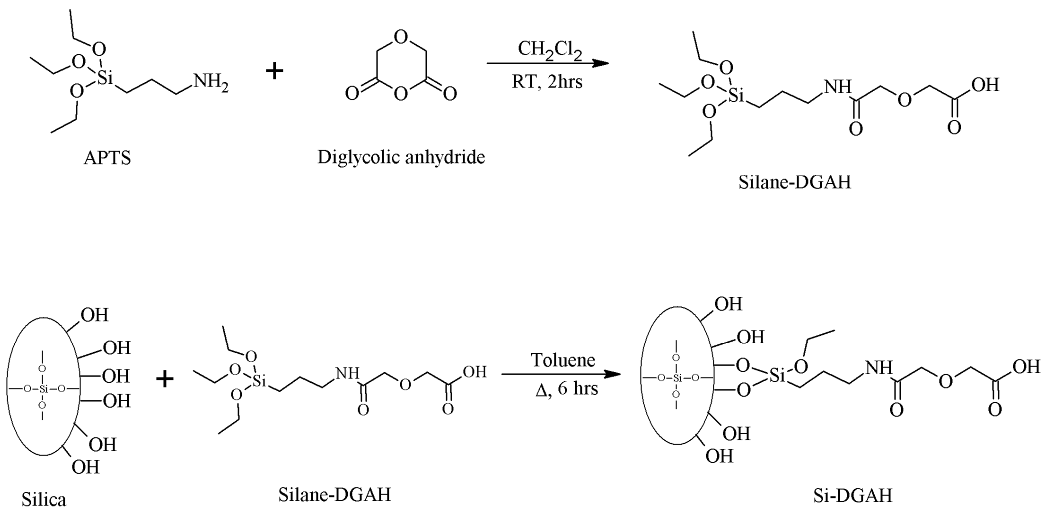

Figure 2.7. Scheme for the synthesis of diglycolamic acid functionalized silica gel

2.3.5.2. Preparation of Si-DGAH

The final product, Si-DGAH, was prepared by refluxing the silica gel and Silane-DGAH in toluene medium for 6 hrs. During this reaction the surface silanol groups present on silica gel reacts with Silane-DGAH to form diglycolamic acid functionalized silica gel, as shown by the reaction scheme in figure 2.7. The functionalized adsorbent was collected and washed several times with toluene, isopropanol, acetone, water and acetone. The product Si-DGAH was dried in air overnight and characterized by FT-IR, ^{29}Si NMR and SEM techniques. FT-IR shows the following peaks (υ/ cm^{-1}) 3451 (O-H in COOH), 1741 (C=O in COOH), 1627 (C=O in –CON).

2.3.6. Characterization of Si-DGAH

The synthesized adsorbent was characterized by elemental analysis, TG-DTA, SEM-EDX and ^{29}Si-NMR studies. The elemental analysis of Si-DGAH shows the presence of 10.2 % carbon and 1.5 % nitrogen. Based on the nitrogen content, the degree of functionalization was determined to be 1.2 mmol/g. The TG, DTG and DTA curves for Si-

DGAH are shown in figure 2.8. The loss of weight occurring below 373 K is attributed to the loss of water molecules adsorbed on the surface of the adsorbent. The weight loss occurring in the temperature range 373–518 K could be attributed to the dehydration reaction occurring between the two adjacent carboxylic acid groups, leading to the formation of anhydrate. The decomposition of organics present in Si-DGAH occurs in the temperature range 523-873 K. An exothermic excursion occurring in the DTA pattern above 523 K leading to a peak at ~873 K is due to the combustion of organics present in Si-DGAH.

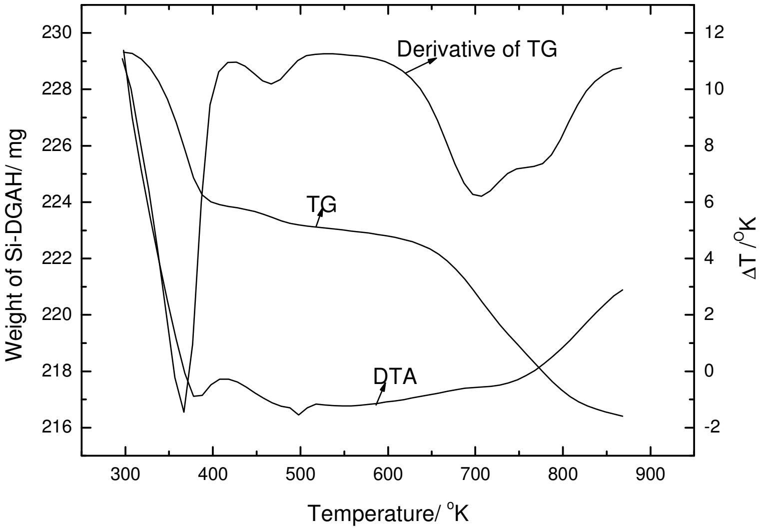

Figure 2.8. TG-DTA pattern obtained for Si-DGAH.

The ^{29}Si NMR (figure 2.9) shows a couple peaks at -99 ppm and -110 ppm, indicating two types of silicon environments are present in the adsorbent, perhaps, due to terminal and cross-linked silicon in silica gel [3,4]. The SEM image of silica gel is shown in figure 2.10. The corresponding EDX pattern shows the presence of silicon and oxygen. However, the surface morphology of final product, Si-DGAH, differs significantly from silica gel, clearly indicating the modification of silica surface by diglycolamic acid. The EDX analysis of Si-DGAH surface shows the presence of carbon in addition to silicon and oxygen. This confirms the functionalization of diglycolamic acid on the surface of silica gel.

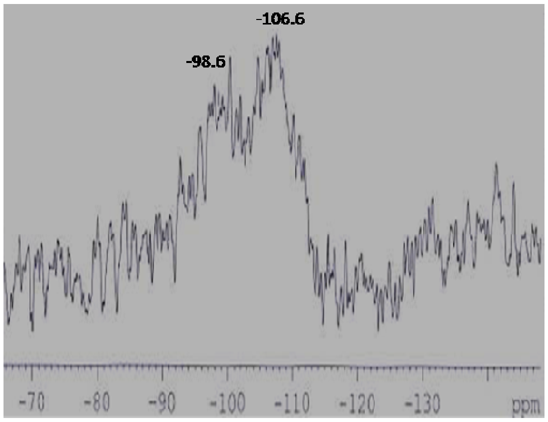

Figure 2.9. ^{29}Si NMR obtained for Si-DGAH.

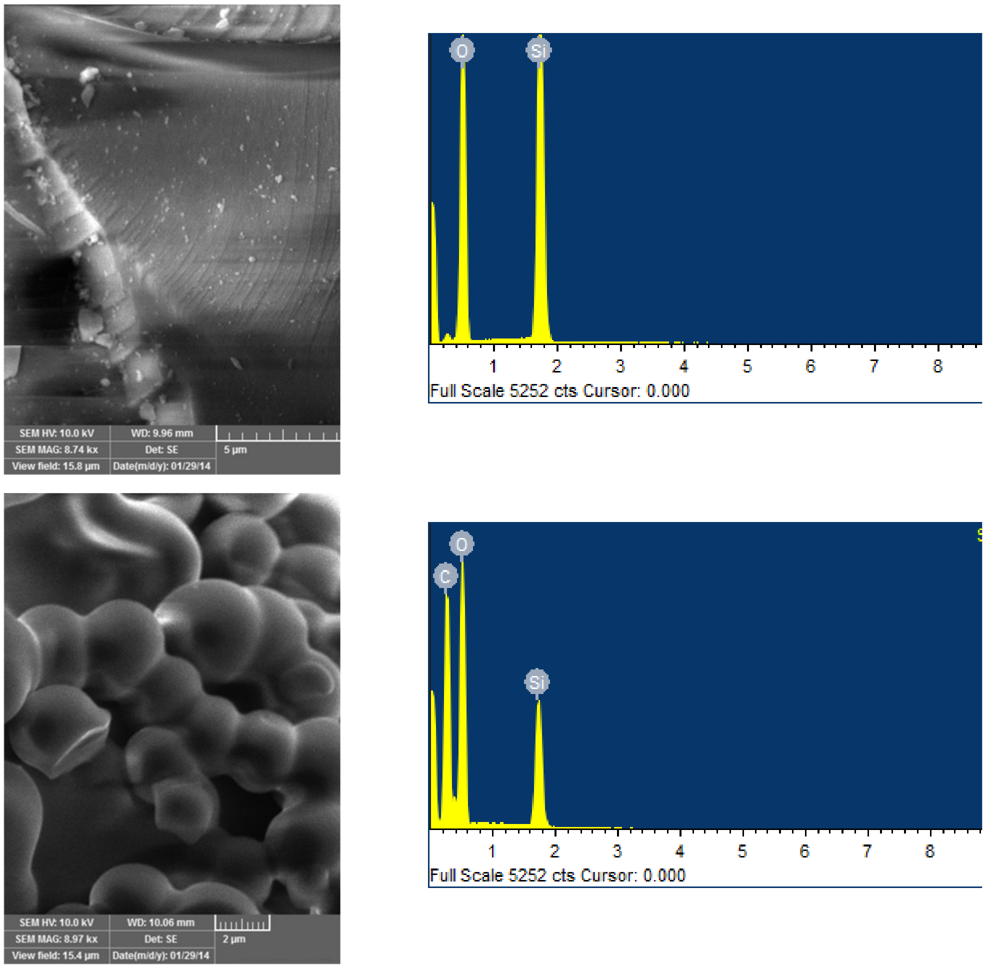

Figure 2.10. SEM and EDX images of silica gel and Si-DGAH

2.3.7. Synthesis of magnetic adsorbents

2.3.7.1. Synthesis of Fe_3O_4

The magnetite (Fe_3O_4) particles were prepared by the co-precipitation method described elsewhere [5-7]. Briefly, it involved hydrolysis of a mixture of $FeCl_3$ (0.8 M) and $FeSO_4$ (0.4 M) present in distilled water (100 mL) with ammonia (1000 mL) solution at 80–90°C under argon atmosphere. The mixture was stirred vigorously for about 2 h, and the Fe_3O_4 particles thus obtained were repeatedly washed with deionized water to remove the residual chloride and sulphate ions. The particles were separated from the aqueous solution by using a permanent magnet and the particles were dried in air, overnight. The reaction scheme is shown in Fig. 2.11.

$$3\ FeCl_3 + 3\ FeSO_4 + 9\ NH_4OH \xrightarrow[\text{353-363 K}]{\text{Distilled water}} 2\ Fe_3O_4 + 3\ NH_4Cl + 3\ (NH_4)_2SO_4 + 9\ H_2O$$

Figure 2.11. Reaction scheme for the preparation of Fe_3O_4

2.3.7.2. Silylation of iron oxide particles (Fe-Si)

Silylation of iron oxide was carried out by the procedure described elsewhere [7-9]. The reaction scheme is shown in Fig. 2.12. The Fe_3O_4 magnetic particles (1 g) were initially dispersed in HCl (5 mL, 2 M). The mixture was subjected to sonication and washed extensively with deionized water. The aqueous phase was removed and the Fe_3O_4 particles were mixed with a solution of ethanol (40 mL) and deionized water (10 mL), which was under stirring in a round bottom flask. The aqueous ammonia solution (1 mL, 28 wt %) was added to this mixture followed by the drop-wise addition of tetraethoxysilane (TEOS, 2 mL). The mixture stirred for about 10 h. During this mixing, the surface hydroxyl groups present on iron oxide react with TEOS to form a coating of siloxane over the surface of iron oxide. The silylated iron oxide (Fe-Si) was collected and washed with ethanol (50 mL x 6 times) and water (50 mL x 6 times). The Fe-Si was separated from the aqueous phase using a permanent magnet, and the particles were dried in air, overnight.

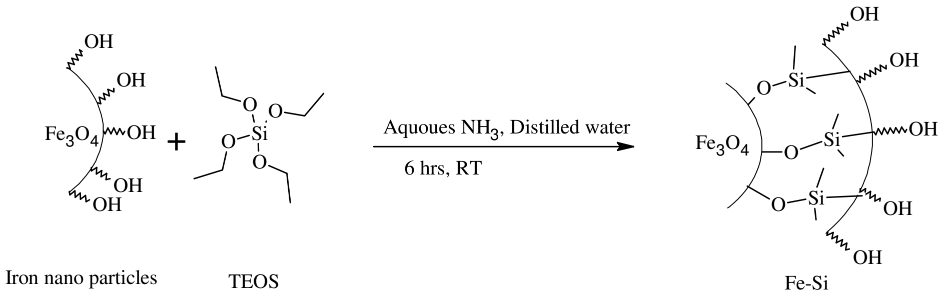

Figure 2.12. Reaction scheme for the preparation of silica coated iron oxide (Fe-Si).

2.3.7.3. Synthesis of silane-thiodiglycolamic acid (Silane-SDGAH)

Si-SDGAH was synthesized by the condensation reaction between thiodiglycolic anhydride (0.03 mol.) present in dichloromethane (30 mL) and 3-aminopropyltriethoxysilane (APTS, 0.03 mol.). The reaction scheme is shown in figure 2.13. The thiodiglycolic anhydride solution was taken in a round bottom flask equipped with a $CaCl_2$ guard tube and APTS was added drop-wise to the solution. The mixture was stirred at room temperature for about 6 hours. The reaction mixture was dried in a rotary evaporator at 353 K to remove the solvent. The product obtained after drying was characterized by ^1H NMR (Bruker Avance III 500 MHz (AV500)). ^1H NMR ($CDCl_3$, δ/ppm relative to TMS): 9.42 (s, 1H, COOH), 3.07-3.02 (m, 4H, 2 x $-CH_2-N$), 1.47-1.39 (m, 4H), 1.20(s, 10H).

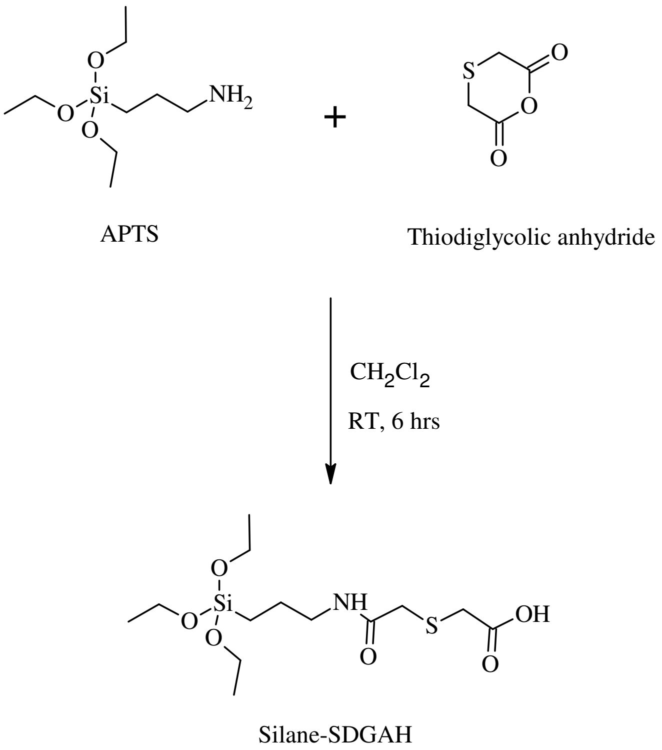

Figure 2.13. Reaction scheme for the synthesis of Silane-SDGAH

2.3.7.4. Preparation of Fe-DGAH

The magnetic adsorbent, Fe-DGAH was prepared by refluxing (80-90°C) the silylated iron oxide (Fe-Si) and Silane-DGAH in toluene medium for 6 h. During this reaction the surface silanol groups present on Fe-Si reacts with Si-DGAH to form diglycolamic acid functionalized iron oxide as shown by the reaction scheme in Fig. 2.14. The functionalized adsorbent was collected using a permanent magnet and washed several times with toluene, isopropanol, acetone, water, and acetone. The product Fe-DGAH was dried in air, overnight and characterized by FT-IR, XRD, and SEM techniques. FT-IR shows the following peaks (υ/cm–1) 3454 (O–H in COOH), 1739 (C=O in COOH), 1622 (C=O in –CON).

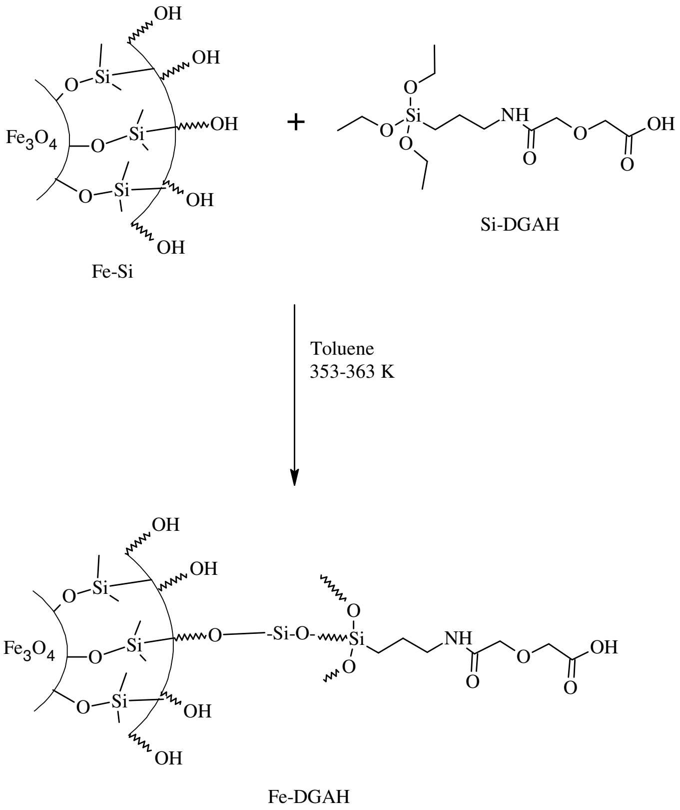

Figure 2.14. Reaction scheme for the synthesis of Fe-DGAH

2.3.7.5. Preparation of Fe-SDGAH

The adsorbent, thioglycolamic acid functionalized iron oxide particles (Fe-SDGAH) was prepared by refluxing (353-363°K) the silylated iron oxide (Fe-Si, 10g) and Si-SDGAH (17 g) in toluene medium for 6 hr. During this reaction the surface silanol groups present on Fe-Si reacts with Si-SDGAH to form thiodiglycolamic acid functionalized iron oxide as shown by the reaction scheme in figure 2.15. The functionalized adsorbent was collected using a permanent magnet and washed several times with toluene, isopropanol, acetone, water and acetone. The product Fe-SDGAH was dried in air, overnight and characterized by TG-DTA, XRD and SEM techniques.

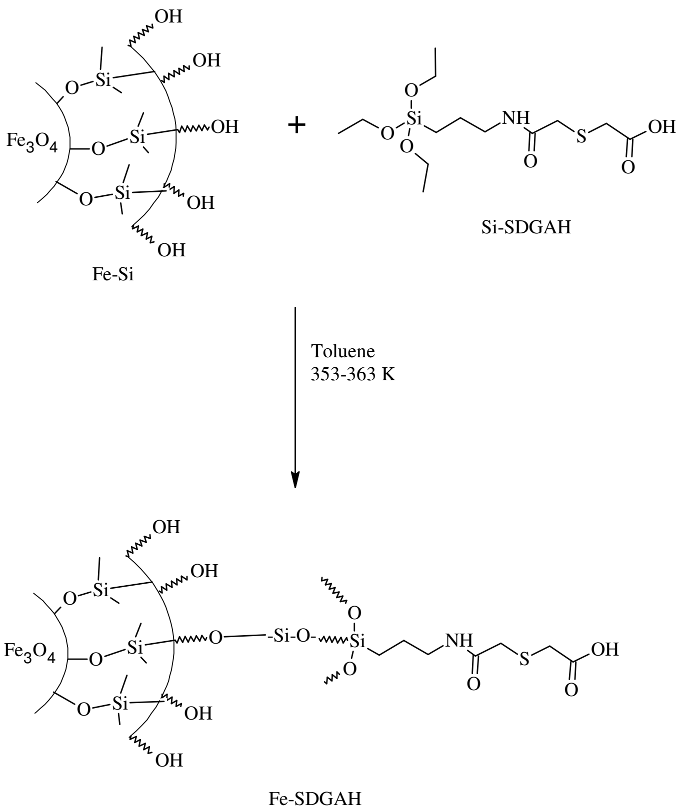

Figure 2.15. Reaction scheme for the synthesis of Fe-SDGAH

2.3.8. XRD patterns of Fe-DGAH and Fe-SDGAH.

The X-ray diffraction pattern of the adsorbent was obtained using a Philips 1011 X-ray diffractometer (operating with 40 KV and 45 mA) with Cu Kα (1.5406 Å) radiation. X-ray diffraction patterns of Fe_3O_4, Fe-Si, Fe-DGAH are shown in Fig.2.16. The XRD pattern compares well with the pattern of standard Fe_3O_4 (JCPDS No. 65-3107). The characteristic peaks at (2θ) 30.17°, 35.46°, 43.38°, 53.69°, 57.23°, and 62.77° correspond to (220), (311), (400), (422), (511), and (440) planes of Fe_3O_4 structure. The crystallite size of iron oxide was determined using Sherrer's relation, shown in equation 2.1. The error in the measurement of crystalline size using Sherrer's equation was ~10 %.

$$D = \frac{k\lambda}{\beta \cos\theta} \qquad (2.1)$$

where λ is the wavelength of CuKα radiation (1.54 Å), *k* is the shape factor which can be assigned a value of 0.89 for unknown shapes, θ is the Bragg angle, and β is the full width at half maximum in radians. The peak at 2θ = 35.46° was chosen to determine the crystallite size. Using equation 2.1, the average crystallite size of iron oxide particles is determined to be 20.6 nm for Fe_3O_4, 21.2 nm for Fe-Si, and 24.6 nm for Fe-DGAH, 23.2 for Fe-SDGAH. Similar values of crystalline size were obtained by considering 2θ = 57.23°, and 62.77°.

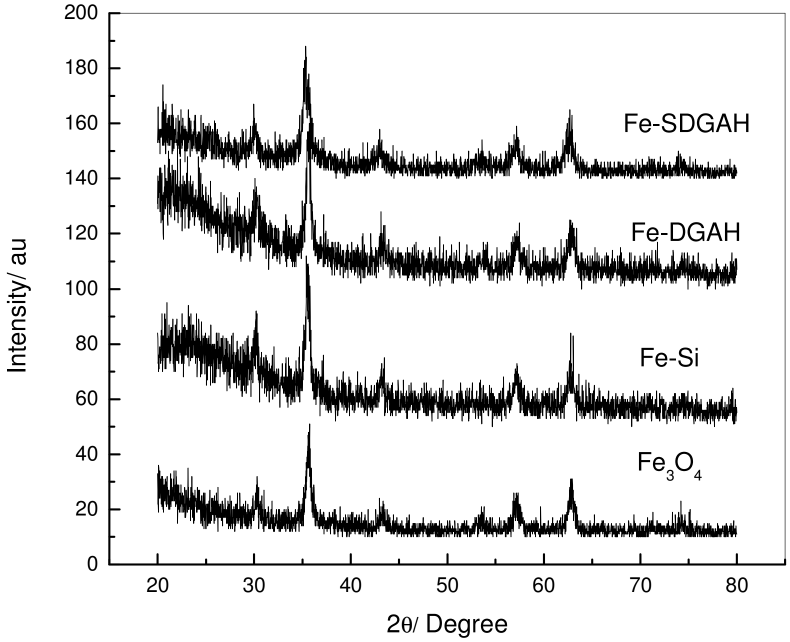

Figure 2.16. Powder X-ray diffraction pattern of Fe_3O_4, Fe-Si, Fe-DGAH and Fe-SDGAH

2.3.9. Surface morphology of Fe-DGAH and Fe-SDGAH

The SEM-EDX images of Fe_3O_4 and Fe-Si are showed in figure 2.17 and that of Fe-DGAH and Fe-SDGAH are showed in figure 2.18. It is observed that the particles are very fine and dense. The EDX pattern shows the presence of iron and oxygen. In contrast to this, the images of silica coated iron oxide (Fe-Si) and diglycolamic acid functionalized iron oxide (Fe-SDGAH) differs significantly from Fe_3O_4 due to bonding of siloxane and diglycolamic acid on the surface of iron oxide particles. The EDX analysis of Fe-Si surface shows the presence of carbon and silicon in addition to iron and oxygen. Similarly, EDX analysis of Fe-SDGAH surface shows the presence of carbon, silicon, nitrogen, iron and oxygen and EDX analysis of Fe-SDGAH shows the presence of sulfur in addition to carbon, silicon, iron and oxygen. All these observation indicate the functionalization of diglycolamic acid on the surface of iron oxide. A gradual change in the surface morphology is observed in the SEM images of Fe_3O_4, Fe-Si and Fe-DGAH. A similar morphological change is observed for the formation of Fe-SDGAH. EDX images of the Fe_3O_4, Fe-Si and the adsorbents Fe-DGAH and Fe-SDGAH shows the presence of the constituent elements [11].

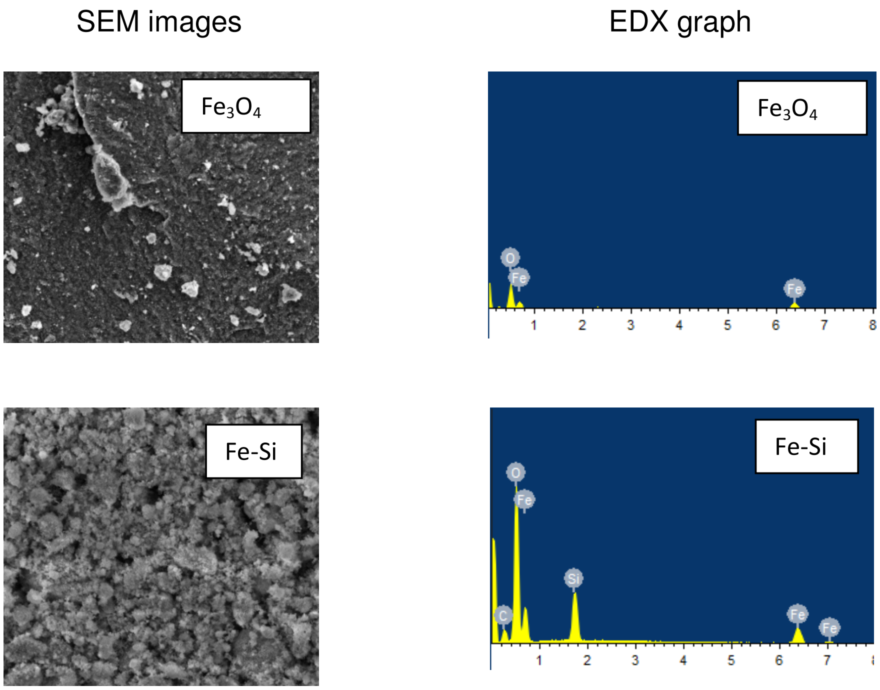

Figure 2.17. SEM and EDX images of Fe_3O_4 and Fe-Si.

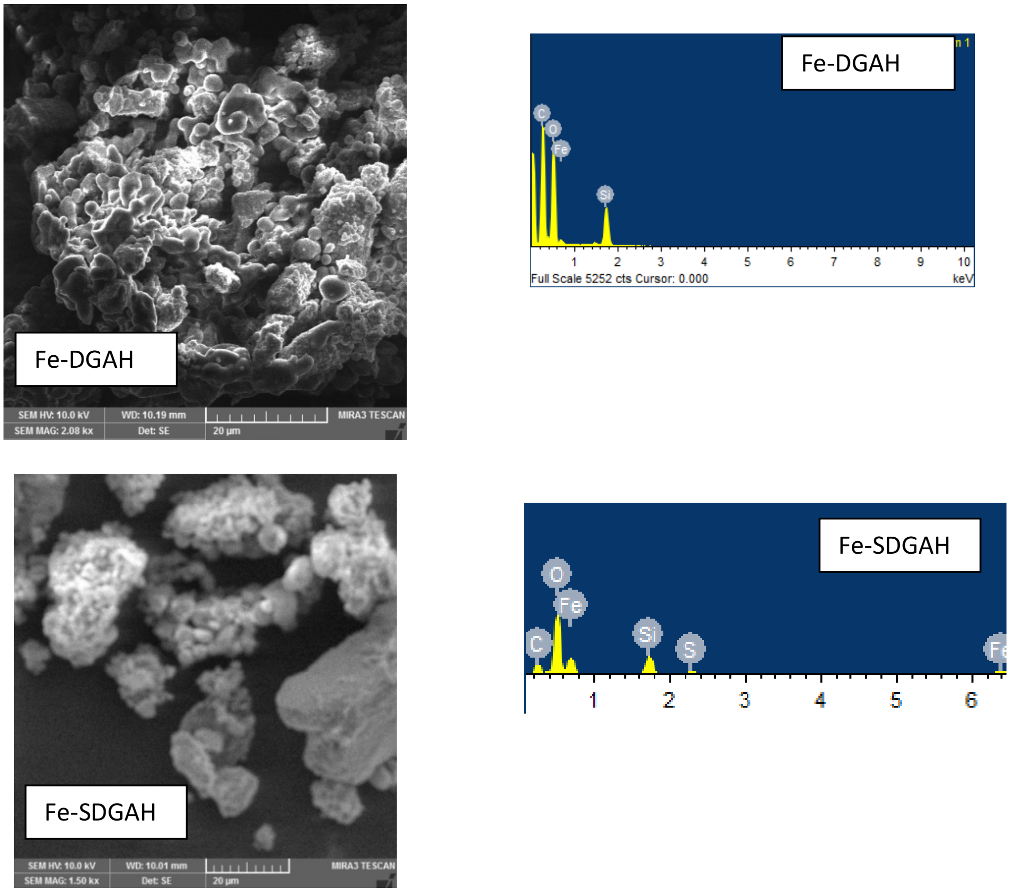

Figure 2.18. SEM and EDX images of Fe-DGAH and Fe-SDGAH

2.3.10. TG-DTA patterns of Fe-DGAH and Fe-SDGAH

The TG-DTA curves for Fe-DGAH are shown in Fig. 2.19. The loss of weight occurring below 373 K is attributed to the loss of water molecules adsorbed on the surface of the adsorbent. The decomposition of organics present in Fe-DGAH occurs in the temperature range 523-873 K. An exothermic excursion occurring in the DTA pattern above 523 K leading to the peak at ~873 K is due to the combustion of organics present in Fe-DGAH. A similar pattern was observed for Fe-SDGAH also, as seen in figure 2.20.

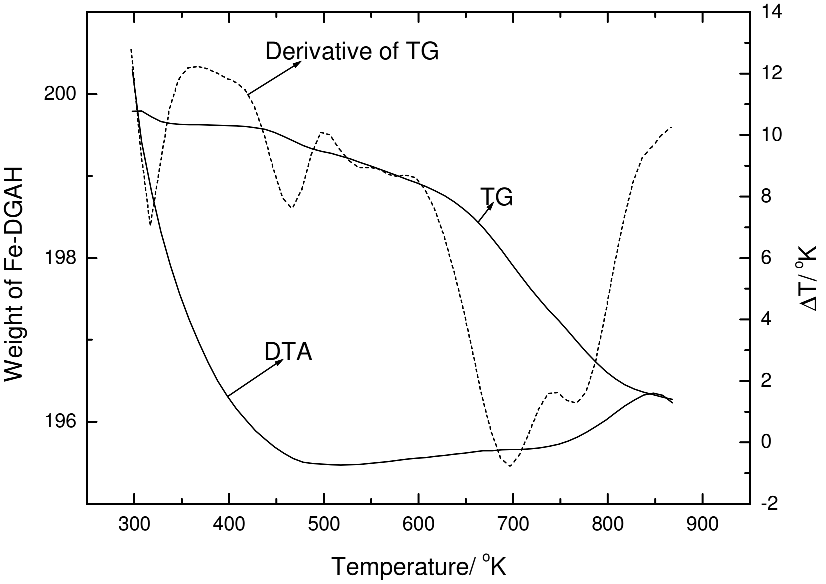

Figure 2.19. TG-DTA patterns of Fe-DGAH

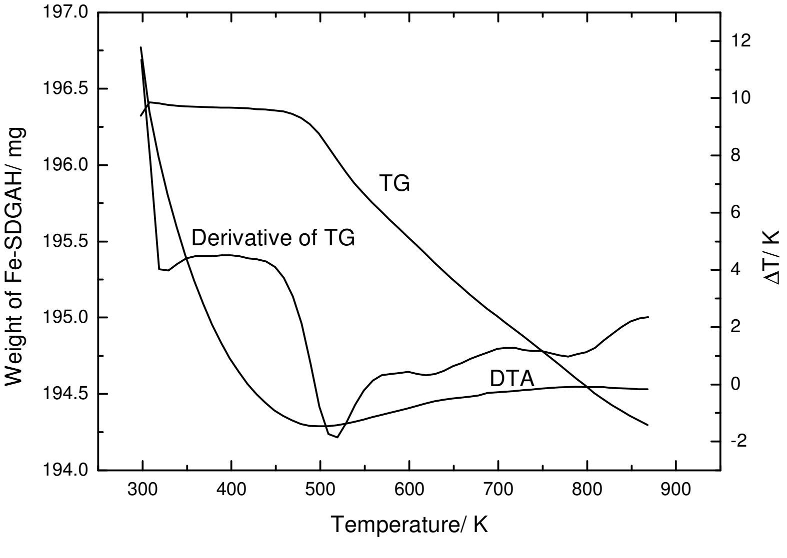

Figure 2.20. TG-DTA patterns of Fe-SDGAH

2.3.11. Particle size and Surface area of Fe-DGAH

The average particle size determined (by using Zeta-sizer) to be ~50 µm for both Fe-DGAH and Fe-SDGAH respectively. The BET surface area was found to be ~120 m^2/g for Fe-DGAH and ~110 m^2/g for Fe-SDGAH.

2.3.12. Raman spectroscopy of Fe-DGAH

The iron oxide and Fe-DGAH were characterized by Raman spectroscopy, shown in figure 2.21. The various phases of iron oxide can be easily distinguished by the characteristic traces in Raman spectrum. It can be seen from trace A (as prepared sample) that a very small peak observed at 670 cm^{-1} at the laser power of 2.5 mW, is due to the characteristic magnetite (Fe_3O_4). The XRD-pattern of the as prepared iron oxide also confirmed the presence of magnetite phase. Upon increasing the duration exposure the pattern changes to that shown in traces B, C and D. These are significantly different from trace A. The characteristic bands observed at 704, 499 and 360cm^{-1} in traces B, C and D are due to maghemite (γ-Fe_2O_3). Trace E is obtained only when the power of the laser and exposure time are increased to 25mW and 10 minutes respectively. The peaks observed at 604, 487, 398, 283, 240 and 219cm^{-1} are characteristic to hematite (α-Fe_2O_3). The study thus shows that laser irradiation could cause the transformation of magnetite into maghemite and then to hematite at higher powers. In contrast, the Raman spectrum of Fe-DGAH recorded at the higher power of 25 mW, and exposure for 10 minutes (trace E) is comparable with trace A obtained for magnetite. The observed trace E is in contrast to the expected pattern of hematite, at this laser power. This indicates that the organic moiety present on the surface seems to prevent the conversion of the core Fe_3O_4 into hematite [11].

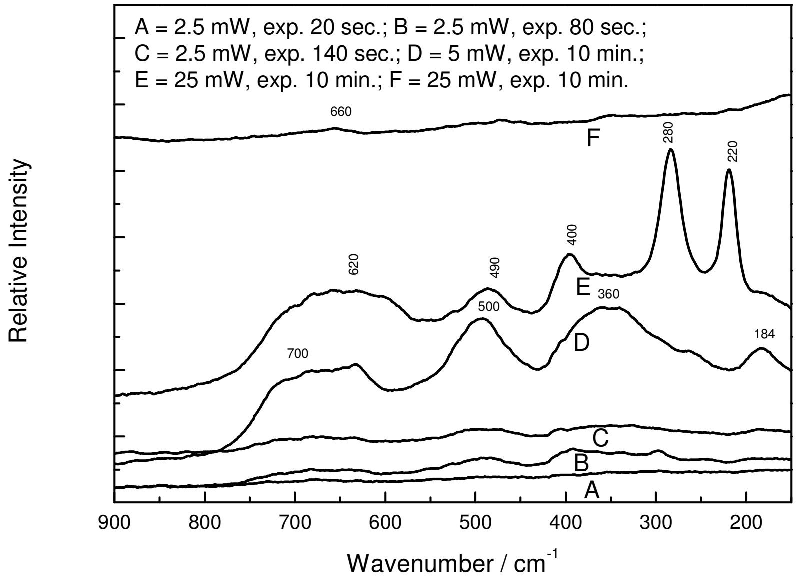

Figure 2.21. Raman spectrum of iron oxide and Fe-DGAH at various powers and exposure time.

2.4. Methods

2.4.1. For the solvent extraction experiments involving HDEHDGA and HDEHSDGA

2.4.1.1. Measurement of distribution ratio

All equilibration experiments were conducted in duplicate at 298 K using an aqueous to organic phase ratio of 1:1. The experiments involved equilibration of aqueous and organic phases (1 mL each) in a 10 mL capacity test tube immersed in a constant temperature water bath and rotated in up-side-down manner for about an hour. The concentration of HDEHDGA (or HDEHSDGA) was varied from 0.05 M to 0.5 M. The organic phase was pre-equilibrated with desired concentration of nitric acid. Extraction of americium(III) and europium(III) as a function of nitric acid was studied by equilibrating the organic phase with nitric acid solution spiked with ^{241}Am(III) (or $^{(152+154)}$Eu(III)) tracer (20 mg/L in all experiments). The pH of the aqueous solution was varied from pH 1 to 3.5.

After one hour of equilibration, the radioactivity of ^{241}Am(III) and $^{(152+154)}$Eu(III) in the organic and aqueous phases was measured using a well-type NaI(Tl) scintillation detector. The pH of the aqueous phase at equilibrium was measured. The distribution ratio (D_M) of metal ion was determined using equation 2.2. The separation factor was computed using equation 2.3.

$$D_M = \frac{[\mathrm{M}]_{\mathrm{org}}}{[\mathrm{M}]_{\mathrm{aq}}}, \ \mathrm{M} = {}^{241}\mathrm{Am(III)} \quad \text{or} \quad {}^{(152+154)}\mathrm{Eu(III)} \tag{2.2}$$

$$\mathrm{SF} = \frac{D_{\mathrm{Eu(III)}}}{D_{\mathrm{Am(III)}}} \ \text{for HDEHDGA and} \ \mathrm{SF} = \frac{D_{\mathrm{Am(III)}}}{D_{\mathrm{Eu(III)}}} \ \text{for HDESHDGA} \tag{2.3}$$

The effect of [DTPA] and [NO_3^-] in aqueous phase on the distribution ratio (D_M) was studied by varying their concentration from 0.005 M to 0.1 M. Similarly, the effect of [HDEHDGA], [HDEHSDGA] and [TPEN] in organic phase was studied by varying their concentration from 0.01 M to 0.3 M.

2.4.1.2. Demonstration of mutual separation of Eu(III) and Am(III) by HDEHDGA

2.4.1.2.1. Extraction studies

Batch equilibration was performed to obtain the number of contacts needed for the quantitative extraction of Am(III) and Eu(III). The organic phase was a solution of 0.1 M HDEHDGA in n-DD and the aqueous phase was 0.1 M CA and 0.1 M HNO_3 spiked with $^{(152+154)}$Eu(III) or ^{241}Am(III) tracer. The pH of aqueous phase was adjusted to 3. The organic phase was pre-equilibrated with aqueous phase adjusted to pH 3. The extraction experiments involved mixing of equal volumes of organic and aqueous phases for about 10 minutes. From the radioactivity measurements, the amount of Eu(III) and Am(III) extracted into organic phase was determined. The organic phase was discarded and aqueous phase was contacted again with equal volume of fresh organic phase for subsequent extraction. The percentage extraction was determined in each contact from the radioactivity measurements. This procedure was repeated until the aqueous phase radioactivity was negligible.

2.4.1.2.2. Stripping studies

Similarly, the number of contacts needed for the recovery of Am(III) and Eu(III) from the loaded organic phase was studied by contacting equal volumes of the loaded organic phase with aqueous solution containing 0.01 M DTPA and 0.025 M CA adjusted to pH 1.5. The radioactivity present in organic and aqueous phases was measured and the amount of Eu(III) or Am(III) back-extracted into aqueous phase was determined. The aqueous phase was removed and the organic phase was contacted again with equal volume of fresh aqueous phase for subsequent back-extraction. The percentage recovery was determined as described above.

2.4.1.2.3. Mixer-settler studies

For the mixer-settler studies, the organic phase was a solution of 0.1 M HDEHDGA in n-DD and the aqueous phase was 0.1 M CA and 0.1 M HNO_3 spiked with $^{(152+154)}$Eu(III) or ^{241}Am(III) tracer. The pH of aqueous phase was adjusted to 3. The extraction of Am(III) and Eu(III) was performed in a counter current mode using a 20-stage ejector mixer settler. Mixing of the organic and aqueous phases was achieved by air pulsing in the column by applying vacuum and pressure alternatively with the help of a solenoid valve operated by a cyclic timer. The aqueous and organic solutions (2 L each) were fed to the mixer settler at a constant flow rate of 3 mL per minute by means of metering pumps equipped with precise flow control. The system was operated for ~6 hrs. Steady state was attained in four hours. The stage samples of organic and aqueous phase were collected for analysis. The loaded organic and raffinate were collected separately in a

2 L container. The Am(III) was back extracted from the loaded organic phase in a counter current mode using the same mixer settler in a separate run. The stripping formulation was composed of 0.01 M DTPA and 0.025 M CA at pH 1.5. Extraction and stripping of Eu(III) and Am(III) was monitored by the radioactivity of $^{(152+154)}$Eu(III) and ^{241}Am(III) in various streams by using HPGe detector coupled with a multichannel analyzer. The experimental conditions adopted for the mixer-settler run is illustrated in figure 2.22. An image of the mixer-settler facility used for the demonstration for the mutual separation of lanthanides and actinides is showed in figure 2.23.

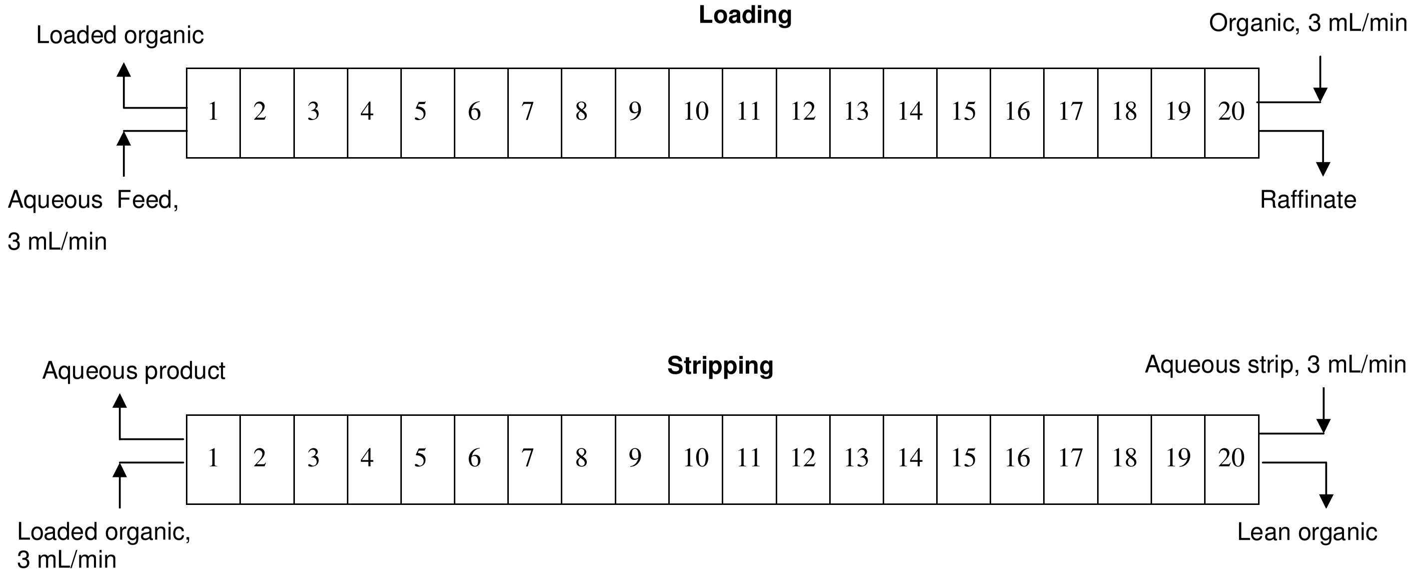

Aqueous feed: 0.1 M CA+ 0.1 M HNO_3 spiked with $^{(152+154)}$Eu(III) and ^{241}Am(III) tracers and was adjusted to pH 3
Organic: 0.1 M HDEHDGA/n-DD
Loaded organic: 0.1 M HDEHDGA/n-DD containing Eu(III) and Am(III)
Aqueous Strip: 0.01 M DTPA + 0.025 M CA adjusted to pH 1.5

Figure 2.22. Illustration of a 20- stage mixer-settler and the conditions employed for extraction and stripping.

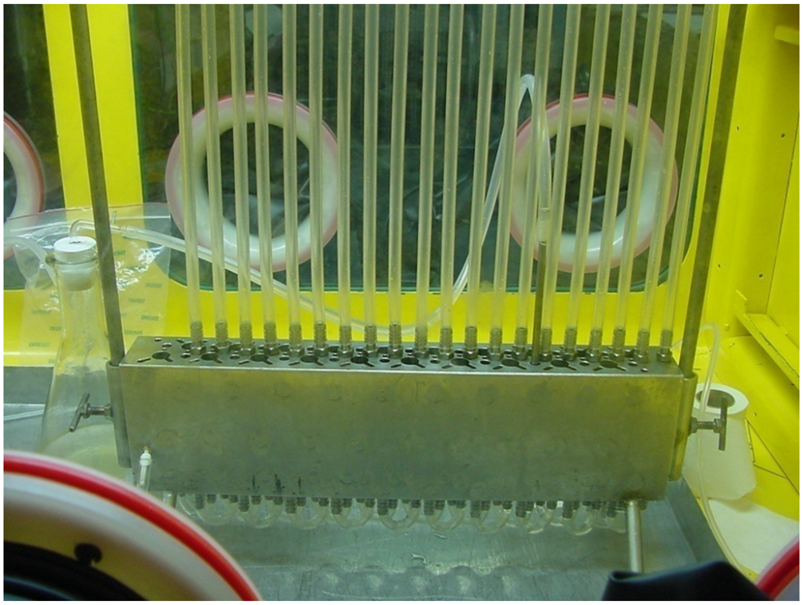

Figure 2.23. Mixer-settler facility used for the demonstration for the mutual separation of Eu(III) and Am(III)

2.4.2. For experiments involving solid-phase reagents

2.4.2.1. Measurement of distribution coefficient

Distribution coefficients of the metal ions Eu(III) or Am(III) were determined by equilibration experiments. The method involved equilibration of 0.05 g of the adsorbent with 10 mL of the aqueous phase (nitric acid at concentration varied from 0.001 M to 0.5 M) spiked with the corresponding radiotracers (~10^{-4} M ^{241}Am tracer was used for Am(III) and $^{(152+154)}$Eu tracer was used for Eu(III)) in 20 mL stoppered test-tubes. The test-tubes were rotated with a constant speed of 50 rpm for a specified period of time. The system was maintained at constant temperature thermostat (298 K). After equilibration, the radioactivities of the radiotracers were determined by radiation counting techniques by using NaI(Tl)-Single Channel analyser. The distribution coefficient (K_d) was computed from the radioactivity measurement of aqueous phase using equation 2.4. The separation factor (SF) was determined using equation 2.5.

$$K_d\ (mL.g^{-1}) = \left(\frac{A_0 - A_f}{A_f}\right) \times \left(\frac{V}{m}\right) \qquad \ldots\ldots\ldots \quad (2.4)$$

$$SF = \frac{K_d \text{ of } Eu(III)}{K_d \text{ of } Am(III)} \qquad \text{………(2.5)}$$

where A_0 and A_f are the initial and final radioactivity of aqueous phase. V is the volume of aqueous phase, and m is the mass of the adsorbent taken for equilibration. To understand the extraction behavior of metal ions in the walls of the test-tube (for blank correction), experiments were conducted by equilibrating 10 mL of the 0.01 M nitric acid solution (or 0.001 M) spiked with $^{(152+154)}$Eu(III) (or ^{241}Am) tracer for about 4-6 hours (depending up on the adsorbent). After four hours (some times six hours depending up on the type of adsorbent) of equilibration, the radioactivity of the aqueous solution was measured. The results indicated that the changes in the radioactivities before and after equilibration were negligible. This indicates that there was no sorption of Eu(III) and Am(III) by the equilibration tube.

2.4.2.2. Kinetics of adsorption

Rate of uptake of Am(III) (or Eu(III)) were studied by equilibrating 0.05 g of adsorbent with 10 mL of nitric acid (0.001 M to 0.001 M), spiked with ^{241}Am(III) tracer (or $^{(152+154)}$Eu(III) in the case of Eu(III) study). Separate experiments were performed for 5 minutes to 360 minutes. Aliquots were drawn from the aqueous phase before and after equilibration. From the initial activity and the activity measured at various intervals of time the percentage of Am(III) (or Eu(III) extracted was calculated.

The rate of extraction of the metal ion in the resin phase (mmol/g) is directly proportional to the concentration of “free” sites, q_{free}, available for extraction.

$$\frac{dq_t}{dt} = k_1\, q_{free} \qquad (2.6)$$

or

$$\frac{dq_t}{dt} = k_2\, q_{free}^2 \qquad (2.7)$$

where q_t is the amount of metal ion extracted at time t (in mmol.g^{-1}), q_{free} is the "free sites" available for extraction (in mmol.g^{-1}) and k_1 and k_2 are the pseudo-first order and pseudo-second order rate constants. The q_{free} can be tacitly related to the amount of metal ions extracted at equilibrium by equation 2.8.

$$q_{free} = q_e - q_t \tag{2.8}$$

where q_e is the amount of metal ion extracted at equilibrium (in mmol/g). Substituting equation 2.8 in equation 2.6 results in equation 2.9.

$$\frac{dq_t}{dt} = k_1 \left(q_e - q_t\right) \tag{2.9}$$

Integrating the equation 2.6 between the limits $t = 0$ to t and $q_t = 0$ to q_t results in the Lagregren equation of the form shown in equation 2.10.

$$q_t = q_e\left(1 - e^{-k_1 t}\right) \tag{2.10}$$

Similarly, substituting q_{free} in equation 2.7 and upon integration results in the pseudo-second order equation of the form shown in equation 2.11.

$$q_t = \frac{q_e^{2}\, k_2\, t}{1 + q_e\, k_2\, t} \tag{2.11}$$

In the present study, q_t, the amount of metal ion extracted at time t, is taken as percentage extraction of either Eu(III) or Am(III) at a time t. The rate constants, k_1 and k_2 were obtained by non-linear regressional analysis of the plot of q_t versus t. Based on the of fitting parameters, χ^2 and R^2, the kinetics of metal ion extraction was approximated to either first order or second order kinetic models. Detailed discussion on non-linear regressional analysis with explannations of χ^2 and R^2 can be seen in section 2.4.2.7.

2.4.2.3. Capacity of the resin by sorption isotherm

Batch experiments were conducted at 298 K by equilibrating 0.05 g of the adsorbent with 10 mL of nitric acid solution containing various quantities of europium nitrate spiked with $^{(152+154)}$Eu(III) tracer. The experiments were carried out for two hours. Aliquots were collected from the aqueous phase before and after extraction. The amount of Eu(III) sorbed was measured from the initial and final activity values. The amount of Eu(III) sorbed was plotted against amount of Eu(III) present in the aqueous phase. These values were fitted with Langmuir adsorption model (and Freaundlich adsorption model in some experiments). Sorption capacity was obtained from the Langmuir adsorption isotherm.

2.4.2.4. Ion exchange capacity measurements by column method

Total ion exchange capacity of the adsorbent under dynamic condition was measured by column chromatography. About 1 g of the adsorbent was initially immersed in water and loaded into a glass column of radius 0.5 cm. The resin was conditioned by using 0.1 M of nitric acid (50 mL). An experimental feed solution composed of 0.1 M NaOH (100 mL) was passed through the resin and the effluent was collected in a 250 mL standard flask. This was followed by passing water through the resin bed and the effluent was collected in the same standard flask up to the mark. The flow rate of the effluent was maintained at a flow rate of 2 mL/min. Ion exchange capacity of the resin was measured from the total amount of sodium exchanged with the resin, which was measured by titrating the feed against potassium hydrogen phthalate.

2.4.2.5. Desorption studies

Loading of Am(III) in Fe-SDGAH was carried out equilibrating 0.05 g of the adsorbent with 10 ml of nitric acid solution at pH 3 spiked with ^{241}Am(III) tracer at 298 K for 2 hours. After equilibration, the aqueous phase was removed quantitatively. From the measurement of radioactivity of ^{241}Am(III) present in aqueous phase, the amount of Am(III) loaded in the adsorbent was determined. The adsorbent was then contacted with

10 mL of 0.5 M nitric acid. The equilibration was carried out for 30 minutes. An aliquot was taken from aqueous phase and radioactivity of Am(III) present in aqueous phase was determined. The aqueous phase was then removed and contacted again with the fresh aqueous phase of 0.5 M nitric acid (10 mL). This procedure was repeated until the Am(III) was recovered quantitatively. A similar experiment was performed for Eu(III) recovery.

2.4.2.6. Adsorbent recycling

Recycling study was carried out by equilibration procedure. During extraction 0.05 g of the adsorbent was equilibrated with 10 ml of nitric acid solution at pH 3 spiked with ^{241}Am(III) tracer at 298 K for 2 hours. After the extraction the aqueous phase was separated and the distribution coefficient of ^{241}Am(III) was determined as described above. The recovery of Am(III) from the loaded adsorbent phase was studied by equilibrating the loaded adsorbent with 10 mL of 0.5 M nitric acid for 30 minutes. After equilibration an aliquot was taken from aqueous phase and the distribution coefficient of ^{241}Am(III) during stripping was determined. After stripping, the adsorbent was again subjected to extraction and stripping. This procedure was repeated for 5 cycles. After each equilibration, the distribution coefficient of Am(III) during extraction and stripping was measured.

2.4.2.7. Non-linear regressional analysis

Non-linear regressional analysis inovoles the fitting of pseudo-first order or pseudo-second order kinetic equation to the experimental data points. Non-linear regressional analysis finds the curve that minimizes the scatter of points around the curve. In the non-linear regressional analysis, the scattering of experimental data from the hypothetical fitted equation is expressed as chi-square value, χ^2. If this chi-square value is high, then the scatter around the curve is larger than the expected value, which infer that fitting is poor. This test is also known as chi-squre fit for goodness of fit [12, 13]. Chi-square, χ^2, is defined by equation 2.12.

$$\chi^2 = \frac{\sum_{i=1}^{i=n} (Y_i - Y_{curve})^2}{SD^2} \tag{2.12}$$

where SD is the standard deviation and Y_i are the experimental values and Y_{curve} are the hypothetical fitting curve.

Statistic parameters, R^2, measures how successful the fit is in explaining the variation of the data [13]. R-square (R^2) is the square of the correlation between the response values and the predicted response values. It is also called the square of the multiple correlation coefficient and the coefficient of multiple determination. R^2 is defined as the ratio of the sum of squares of the regression (SSR) and the total sum of squares (SST). SSR is defined by equation 2.13.

$$SSR = \sum_{i=1}^{n} W_i \left(\hat{y}_i - \overline{y}\right)^2 \tag{2.13}$$

where W_i is the weighting applied to each data point, usually wi = 1.

R-square can also be expressed as

$$R^2 = \frac{SSR}{SST} = 1 - \frac{SSE}{SST}$$

Value of R^2 lies between 0 and 1. Value of R^2 closer closer to 1 indicates the closeness of the experimental data with fitted equation. SST is the sum of squares about the mean, and is defined as

$$SST = \sum_{i=1}^{n} W_i \left(y_i - \overline{y}\right)^2$$

where SST = SSR + SSE. SSE is the sum of squares due to error, which is also defined by an expression similar to 2.13. A value of SSE closer to 0 indicates that the model has a smaller random error component.

2.5. **References**

1. P. Manoravi, M. Joseph, N. Sivakumar, R. Balasubramanian, Determination of isotopic ratio of boron in boric acid using laser mass spectrometry. Analytical Sci. 21 (2005) 1453-1455.
2. K. Shimojo, H. Naganawa, J. Noro, F. Kubota, M. Goto, Extraction behavior and separation of lanthanides with a diglycol amic acid derivative and a nitrogen-donor ligand, Anal. Sciences. 23 (2007) 1427-1435
3. K.A. Venkatesan, T.G. Srinivasan, P.R. Vasudeva Rao, Removal of complexed mercury from aqueous solutions using dithiocarbamate grafted on silica gel, Sep. Sci. Technol. 37 (2002) 1417-1429.
4. K.A. Venkatesan, T.G. Srinivasan, P.R. Vasudeva Rao, Cobalt-extraction studies on dithiocarbamate grafted on silica gel surface, Colloid. Surf. A 180 (2001) 277–284.
5. D. Wu, Y. Sun, Q. Wang, Adsorption of lanthanum (III) from aqueous solution using 2-ethylhexyl phosphonic acid mono-2-ethylhexyl ester-grafted magnetic silica nanocomposites, J. Hazard. Mater. 260 (2013) 409– 419.
6. Y. Cheng, R. Tan, W. Wang, Y. Guo, P. Cui, W. Song, Controllable synthesis and magnetic properties of Fe_3O_4, and Fe_3O_4@SiO_2 microspheres, J. Mater. Sci. 45 (2010) 5347–5352.
7. X.D. Wang, Z.X. Shen, T. Sang, X.B. Cheng, M.F. Li , L.Y. Chen, Z.S. Wanga, Preparation of spherical silica particles by Stöber process with high concentration of tetra-ethyl-orthosilicate, J. Colloid Interface Sci. 341 (2010) 23–29.
8. A. Afkhami, R. Norooz-Asl, Removal, preconcentration and determination of Mo(VI) from water and wastewater samples using maghemite nanoparticles, Colloids Surf. 346 (2009) 52–57.

9. L. Chen, Y. Huang, L. Huang, B. Liu, G. Wang, S. Yu, Characterization of Co(II) removal from aqueous solution using bentonite/iron oxide magnetic composites, J. Radioanal. Nucl. Chem. 290 (2011) 675-684.
10. P.H. Towler, J.D. Smith, D.R. Dixon, Magnetic recovery of radium, lead and polonium from seawater samples after preconcentration on a magnetic adsorbent of manganese dioxide coated magnetite, Anal. Chim. Acta 328 (1996) 53–59.
11. Surface Characterization of Novel Diglycolamic Acid Functionalized Iron Oxide Particles by Raman Spectroscopy and Scanning Electron Microscopy, A.S. Suneesh, R. Kumaresan, K.A. Venkatesan, M.P.Antony, P. R. Vasudeva Rao, In: DAE-BRNS, 5th Interdisciplinary Symposium on Materials Chemistry, (ISMC-2014), December 9 – 13, 2014, Bhabha Atomic Research Centre, Mumbai – 400085, INDIA (p-153)
12. H. Motulsky, A. Christopoulos, Fitting models to biological data using linear and nonlinear regression: a practical guide to curve fitting. Oxford University Press (2004).
13. R.D. Evans, The Atomic Nucleus, McGraw-Hill (1969).

Chapter 3: Development of materials for Ln(III)-An(III) separation by liquid-liquid extraction

This chapter deals with the development of two extractants, bis(2-ethylhexyl)diglycolamic acid (HDEHDGA) and bis(2-ethylhexyl)thiodiglycolamic acid (HDEHDSDGA) for Eu(III)-Am(III) separation. This chapter is divided into two parts. Part 1 deals with the synthesis and evaluation of HDEHDGA and HDESDGA for the mutual separation of Eu(III) and Am(III) and part 2 deals with the demonstration of HDEHDGA for the mutual separation of lanthanides and actinides by using simulated and actual feed solutions.

3.1. Introduction

Ln-An separation is a challenging task, since both actinides and lanthanides exist in trivalent oxidation state in the feed solution. The methods developed so far, for the Ln-An separation usually exploits the finer differences in the chemical behavior of lanthanides and actinides towards various ligands [1-10]. According to HSAB concept, the lanthanides are classified as hard acids as compared to the trivalent actinides. Therefore, the ligands having O-donor atoms preferentially complexes with lanthanides; whereas the ligands with S- or N- donor atoms complexes with trivalent actinides [1, 2]. In addition, the valence 5f- orbitals of actinides are spatially extended more compared to the 4f- orbitals of lanthnides and thus the trivalent actinides have a greater tendency to form covalent bonding as compared to the lanthanides [1, 2].

Several methods have been proposed for lanthanide-actinide separations by liquid-liquid extraction mode, by exploiting the presence of spatially extended 5f- orbitals in actinides [1-10] for mutual separation of actinides from lanthanides. Among the various process reported till-date, the TALSPEAK (Trivalent Actinide Lanthanide Separation by Phosphorus Extractants Aqueous Komplexes) process, is regarded as a promising technique for the mutual separation [4-8]. Basically, the TALSPEAK process exploits the differential complexing abilities of bis(2-ethylhexyl)phosphoric acid (HDEHP), present in organic phase and diethylenetriamine-N,N,N',N'',N'''pentaacetic acid (DTPA) present in aqueous phase towards lanthanides and actinides. TALSPEAK process requires an aromatic diluent for the dissolution of HDEHP or it requires an additional phase modifier. Sulfur based ligands such as dithiophosphinic acid (DPAH), commercially available as cyanex 301, and their derivatives are explored for lanthanide-actinide separation [9, 10]. Again, the sulfur based extractants are also not advisable to use as it is more vulnerable to chemical and radiation degradtion.

In the recent past, pyridine and bipyridine based N- donor ligands are being studied for lanthanide –actinide separations. In this connection, Ekberg *et al.* [11] reviewed the use of nitrogen based ligands for such purpose. The authors discussed the studies on ligands such as Terpy (2,2',6',2"-terpyridine), TPTZ (2,4,6-tripyridyl-1,3,5-triazine), BTP (2,6-bis-(1,2,4-triazine-3-yl)pyridines), BTBPs (6,6'-bis(5,6-dialkyl- [1,2,4]-triazin-3-yl)-2,2'-bipyridines, etc. Kolarik *et al.* [12] proposed 2,6-ditriazolyl- and 2,6-ditriazinylpyridines for Am(III)-Eu(III) separation from 1-2 M nitric acid medium. However, these extractants suffers the disadvantage that they are not completely soluble in commonly used reprocessing compatible diluents such as kerosene, paraffine, n-dodecane etc, require the use of an additional phase modifiers.

Alkyl diglycolamides (DGA) are emerging as superior candidates for the separation of Ln(III) & An(III), from high-level liquid waste [13-22]. Introduction of an etheric oxygen between the two-amide groups, as in DGAs, increases the extraction of trivalents due to enhanced tridentate complex formation with them. The acid derivative of this family, namely the alkylglycolamic acid is also expected to be an attractive candidate for the separation of lanthanides and actinides from aqueous medium. Shimojo *et al.* [18]

studied the extraction behaviour of lanthanides using N,N-dioctyldiglycolamic acid (HDODGA) and reported the mutual separation of lighter, middle and heavier lanthanides using HDODGA and tetrakis(2-pyridylmethyl)ethylenediamine (TPEN). However, the mutual separation of lanthanides and actinides using diglycolamic acid has not been reported so far.

In this context, we synthesized two alkyl diglycolamic acids- bis(2-ethylhexyl)diglycolamic acid (HDEHDGA) and the thio-derivative of diglycolamic acid, bis(2-ethylhexyl)thiodiglycolamic acid (HDEHSDGA), and studied the extraction behaviour of $^{(152+154)}$Eu(III) and ^{241}Am(III) from nitric acid medium. The structures of HDEHDGA and HDEHSDGA are shown in figure 3.1. Due to the presence of –COOH group and –C=O (hard donating sites) groups present, HDEHDGA is expected to exhibit selectivity towards lanthanides (hard acidic) and due to the presence of sulfur atom (soft donating sites), HDESDGA is expected to exhibit selectivity towards actinides (soft acidic). Details of the synthesis and characterization of HDEHDGA and HDEHSDGA are discussed in section 2.3.1 and 2.3.2 of chapter 2.

HDEHDGA

HDEHSDGA

Figure 3.1. Structure of HDEHDGA an HDESDGA

Part 1. Evaluation of HDEHDGA and HDEHSDGA for the mutual separation of Am(III) and Eu(III).

3.2. pKa of the extractants

Both HDEHDGA and HDEHSDGA are expected to be weak acids. pKa of the extractants were determined by pH titrations. The pH titrations were carried out by the procedure described elsewhere [19]. It involved the titration of 0.05 M of HDEHDGA in ethanol (50mL) with standard 0.1 M NaOH. The pH of the solution was recorded after every addition of sodium hydroxide (approximately 100 μL) and the pH of the solution was plotted against volume of NaOH. The pH titration curves for HDEHDGA and HDEHSDGA are shown in figure 3.2. From the pH titration curves, the pKa of HDEHDGA and HDEHSDGA were determined to be 5.08 and 5.83, respectively [23].

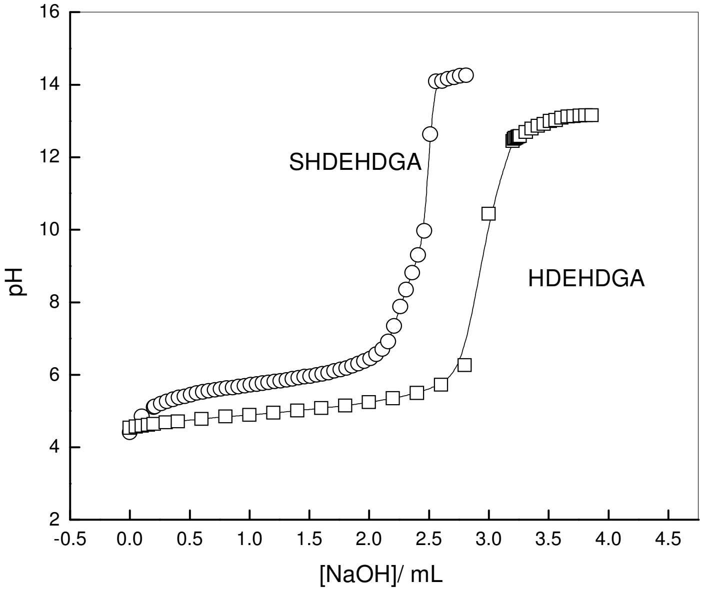

Figure 3.2. Titration curves of HDEHDGA and HDEHSDGA in ethanol at 298 K. Titrant: 50 mL of 0.05 M HDEHDGA or HDEHSDGA/ethanol Titrate: 0.1 M standard NaOH

3.3. Effect of diluents

Traditionally, n-dodecane (n-DD), NPH or kerosene etc have been used extensively as the diluent in nuclear fuel reprocessing applications. However, aromatic diluents, fluorinated hydrocarbons, etc., have also been employed in some studies due to the compatibility of the extractant with them and to facilitate higher separation. For instance, TALSPEAK process employs 1,4-diisopropylbenzene (1,4-DIPB) as the diluent [4, 5]. Therefore identification of a compatible diluent is essential for solvent extraction applications. In addition, most of the Ln(III)-An(III) mutual separation process reported sofar suffers from the limitation that they are not completely soluble in nuclear diluents such as n-dodecane or NPH etc. Table 3.1 shows the distribution ratios (please see section 2.4.1.1 of chapter 2) of Eu(III) and Am(III) as a function of the nature of diluent. Among the various diluents investigated, n-dodecane exhibits maximum distribution ratio for Eu(III) and Am(III). Since n-DD is the preferred diluent in industrial scale solvent extraction processes, and since the extractants, HDEHDGA and HDEHSDGA, are easily soluble, in n-dodecane, it was used for all the subsequent studies. Since, the extractant is completely soluble in n-dodecane, phase modifiers may not be required.

Table 3.1. Variation in the distribution ratio of Eu(III) and Am(III) in HDEHDGA or HDEHSDGA in various diluents at pH=3, 298 K. Organic: Aq. phase ratio is 1:1. For HDEHDGA, Organic phase: 0.1 M HDEHDGA/n-DD, Aq. Phase: [HNO_3]. For HDEHSDGA, Organic phase: 0.3 M HDEHSDGA/n-DD, Aq. Phase: [HNO_3].

Diluent	D in 0.1 M HDEHDGA		D in 0.3 M HDEHSDGA	
	D_{Eu}	D_{Am}	D_{Am}	D_{Eu}
Dodecane	439	68	1.7	1.2×10^{-2}
1,4-DIPB	124	27	0.3	4.4×10^{-3}
Xylene	0	0	0.01	7×10^{-4}

3.4. Effect of pH

The distribution ratios of europium (III) and americium (III) in 0.01 M HDEHDGA and 0.3 M HDEHSDGA, as a function of pH_{eq}, are compared in figure 3.3. It is observed that the distribution ratio of Eu(III) and Am(III) increase with increase of pH_{eq} in both the cases. The distribution values are much higher in HDEHDGA as compared to HDEHSDGA. However, the separation factor (D_{Am}/D_{Eu}) remains at < 5 in HDEHDGA/n-DD, due to the similarity in the distribution ratio of Eu(III) and Am(III). In contrast to this, the distribution ratio of americium(III) is much higher than europium(III) in HDEHSDGA. This could, perhaps, be attributed to the presence of sulfur in the extractant moiety, which is a soft base donor. The trivalent lanthanide and actinide ions are classified as hard acids according to hard-soft acid base concept. However, the trivalent actinides are regarded as relatively soft as compared to the corresponding lanthanide ions. Thus, the higher selectivity of Am(III) over Eu(III) observed in the case of HDEHSDGA could be attributed to the efficient interaction between the soft donor and americium(III). It is interesting to observe that the separation factor increases from the value of unity at pH 1 to ~500 at pH 3.5 in this case. Moreover, the distribution ratio of Am(III) at pH $\geq$ 3 (~10) is also significantly higher compared to that of europium(III) ($D_{Eu(III)}$ ~10^{-2}), which is indeed desirable for lanthanide-actinide separations [23-25].

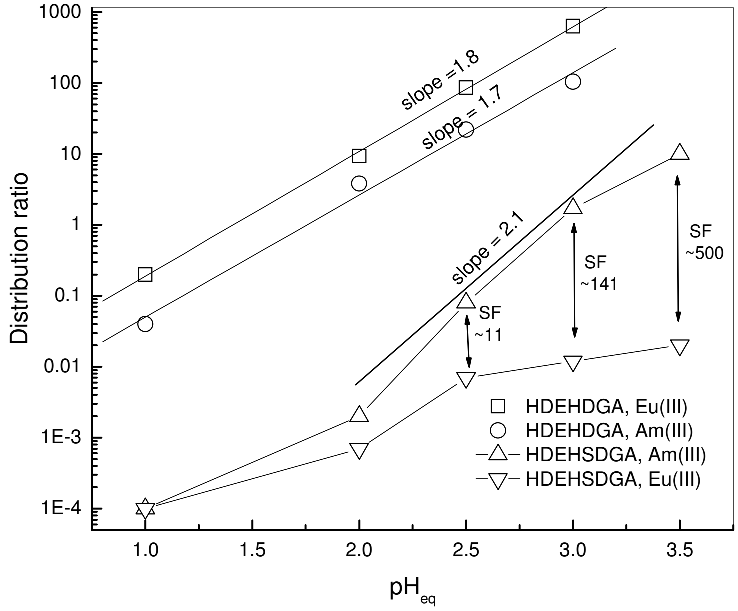

Figure 3.3. Variation in the distribution ratio of Eu(III) and Am(III) in HDEHDGA or HDEHSDGA in n-dodecane as a function of pH, at 298 K. Organic: Aq. phase ratio is 1:1. For HDEHDGA, Organic phase: 0.01 M HDEHDGA/n-DD, Aq. Phase: [HNO_3], For HDEHSDGA, Organic phase: 0.3 M HDEHSDGA/n-DD, Aq. Phase: [HNO_3].

3.5. Mechanism of extraction

Figure 3.4 shows the variation in the distribution ratio of Eu(III) and Am(III) as a function of extractant concentration in organic phase at pH ~3. It is observed that the distribution ratios of Eu(III) and Am(III) increased with increase in the concentration of extractants in both the cases. The extraction trend observed in figure 3.4 as well as that observed in figure 3.3 indicates the involvement of cation exchange mechanism, shown in equation 2.1, for the extraction of trivalents (M^{3+}) by these acidic extractants (HA).

$$M^{3+}_{aq} + x\,HA_{org} \Leftrightarrow \{MA_x\}_{org} + x\,H_{aq}^{+} \qquad (3.1)$$

where HA is HDEHDGA or HDEHSDGA and A is the proton dissociated form of glycolamic acids. The equilibrium constant for the above reaction is given by

$$K = \frac{[MA_x]_{org}\,[H^+]^x_{aq}}{[M^{3+}]_{aq}\,[HA]^x_{org}} \tag{3.2}$$

$$K = \frac{D_M\;[H^+]^x_{aq}}{[HA]^x_{org}} \tag{3.3}$$

where D_M is defined as

$$D_M = \frac{[MA_x]_{org}}{[M^{3+}]_{aq}}$$

At a constant pH, the variation of D_M with HDEHDGA is given by equation 2.4.

$$\log D_M = \log K_1 + x \log [HA]_{org} \tag{3.4}$$

where K_1 (= $K / [H^+]^3_{aq}$) is a constant. Thus, a plot of log D_M against log $[HA]_{org}$ should result in a straight line with slope of 3. At constant pH, the logarithmic variation of D_M against $[HA]_{org}$ is shown in figure 3.4. Linear regression of the distribution data yields a slope of ~2 for both the extractants, indicating the involvement of two molecules of HDEHDGA or HDEHSDGA for extraction. The involvement of two molecules of HDEHDGA or HDEHSDGA is also supported by slope value of two obtained in the plot shown in figure 3.3.

However, the extraction of trivalent cation by a monobasic acid extractant requires one more anion for charge neutralization. This could be compensated by the extraction of NO_3^- from aqueous phase. Therefore the extraction mechanism of trivalents by HA could be represented as

$$M^{3+}_{aq} + 2HA_{org} + NO^-_{3\,aq} \Leftrightarrow \{MA_2(NO_3)\}_{org} + 2H^+_{aq} \tag{3.5}$$

The equilibrium constant for the above reaction is given by equation 2.6.

$$K_2 = \frac{[MA_2(NO_3)]_{org}\,[H^+]^2{}_{aq}}{[M^{3+}]_{aq}\,[(NO_3)^-]_{aq}[HA]^2{}_{org}} \tag{3.6}$$

$$K_2 = \frac{D_M\,[H^+]^2_{aq}}{[(NO_3)^-]_{aq}[HA]^2_{org}} \tag{3.7}$$

At a fixed concentration of extractant and pH, the variation of D_M with $[NO_3^-]$ is be given by equation 2.8,

$$\log D_M = K_3 + \log[NO_3^-]_{aq} \tag{3.8}$$

where K_3 ($=K_2.[HA]^2_{org}/[H^+]^2_{aq}$) is a constant. At constant pH and concentration of extractant, the variation of D_M with $[NO_3^-]$ is shown in figure 3.5. Linear regression of distribution data yielded a slope of 1 indicating one molecule of NO_3^- is involved in the extraction step as shown in equation 2.5 [23]. Turanov *et al.* [20] also reported a similar mechanism for the extraction of trivalents by a monobasic phosphorous acid, in which NO_3^- ion was reported to be involved in the extraction step.

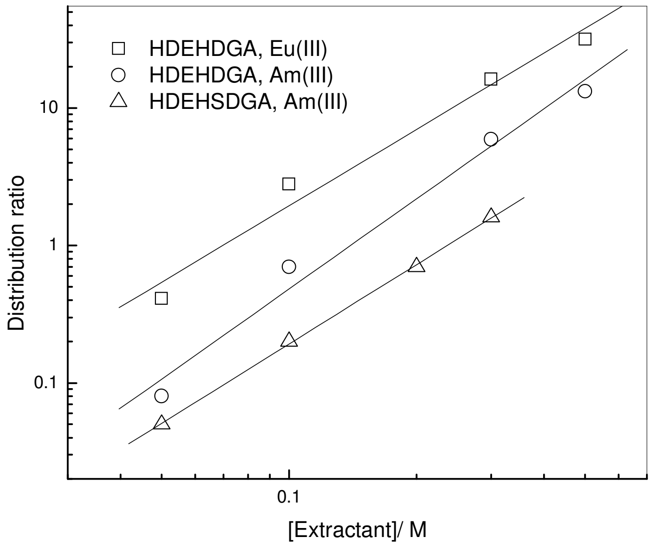

Figure 3.4. Variation in the distribution ratio of Eu(III) and Am(III) as a function of [HDEHDGA] or [HDEHSDGA] in n-DD at 298 K. Organic: Aq. phase ratio is 1:1. For HDEHDGA, Organic phase: HDEHDGA/n-DD, Aq. Phase: [HNO₃)], pH=1. For HDEHSDGA, Organic phase: HDEHSDGA/n-DD, Aq. Phase: [HNO₃], pH=3

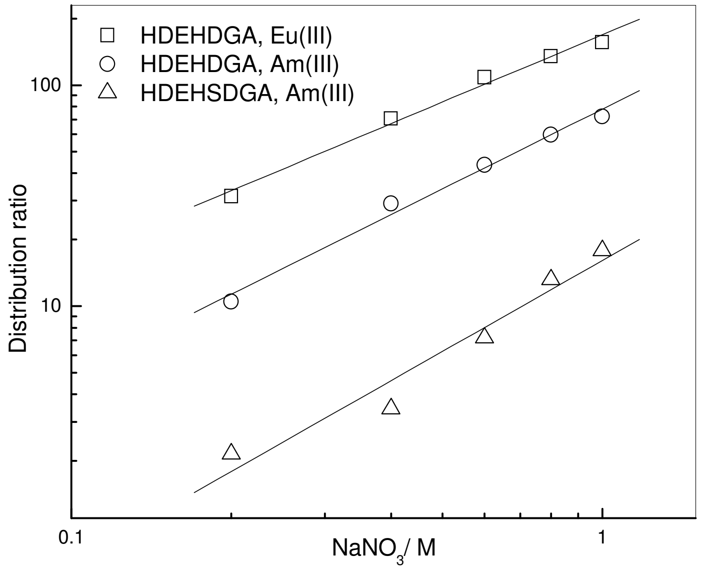

Figure 3.5. Variation in the of distribution ratio of Eu(III) and Am(III) as a function of concentration of NO_3^- in aqueous phase at 298 K. Organic: Aq. phase ratio is 1:1. For HDEHDGA, Organic phase: 0.1 M HDEHDGA/n-DD, Aq. phase: [$NaNO_3$] at pH=1, For HDEHSDGA, Organic phase: 0.3 M HDEHSDGA/n-DD, Aq. phase: [$NaNO_3$] at pH=3

3.6. Effect of additives

Co-extractants and aqueous soluble reagents are usually added to organic and aqueous phases respectively to augment the separation factor. The aqueous soluble organopolycarboxylic acid, such as diethylenetriamine-N,N,N',N'',N'''-pentaacetic acid (DTPA) [2,6] and the organic soluble, N, N, N',N'-tetrakis(2-methylpyridyl)ethylenediamine (TPEN) [18] have been reported as potential candidates for the retention of americium(III) the respective phases. Structures of DTPA and TPEN are showed in figure 3.6. In HDEHDGA system, it is desirable to retain the less extractable americium(III) in the aqueous phase by the addition of aqueous phase modifiers and facilitate the extraction of americium(III) in HDEHSDGA system by the use of organic phase coextractants. Table 3.2 shows the distribution ratio of Am(III) and Eu(III) in HDEHDGA/n-DD as a function of DTPA concentration in aqueous phase. As expected the distribution values of both the metal ions decrease with increase in the concentration of DTPA. It is interesting to observe that a maximum separation factor ~150 is observed when the concentration of DTPA is 10^{-5} M. Further increase in the concentration of DTPA lowers the extraction of Eu(III) and Am(III) and decreases the separation factor thereafter [23, 26].

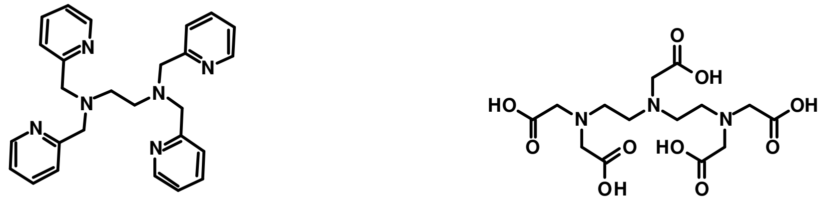

TPEN

DTPA

Figure 3.6. Structures of TPEN and DTPA

Table 3.2 also shows the distribution ratio of Am(III) and Eu(III) in 0.3 M HDEHSDGA/n-DD as a function of TPEN concentration. Interestingly it is observed that the distribution ratio of Am(III) increases with the increase of TPEN concentration, whereas the distribution ratio of Eu(III) remain constant at 10^{-3}. Therefore the SF increases remarkably with increase of TPEN concentrtion. At 0.1 M TPEN, the SF of about 2600 is observed, which is indeed promising for the separation of Am(III) from Eu(III) [26].

Table 3.2: Variation in the distribution ratio of Eu(III) and Am(III) in HDEHDGA or HDEHSDGA in n-DD as a function of additives at 298 K. Organic: Aq. phase ratio is 1:1. For HDEHDGA, Organic phase: 0.1 M HDEHDGA/n-DD, Aq. Phase: [DTPA], pH=3. For HDESHDGA, Organic phase 0.3 M HDEHSDGA+[TPEN]/n-DD, Aq. Phase: [HNO_3], pH=3.

HDEHDGA				HDEHSDGA			
[DTPA]/ M	D_{Eu}	D_{Am}	SF	[TPEN]/ M	D_{Am}	D_{Eu}	SF
10^{-5}	27.6	0.19	145	0.005	0.7	4.6×10^{-3}	152
10^{-4}	4.9	6.5×10^{-2}	75	0.01	1.0	2.3×10^{-3}	440
0.001	0.8	1.7×10^{-2}	45	0.1	9.8	3.7×10^{-3}	2648
0.005	0.2	2.5×10^{-2}	10	-	-	-	-

3.7. Effect of co-extractants

Table 3.3 shows the distribution ratio of Eu(III) and Am(III) in glycolamic acid (HDEHP) and thioglycolamic acid (HDEHSDGA) as a function of nature of extractant (CMPO, TBP and TOPO). The extraction of Eu(III) and Am(III) in both HDEDGA and HDEHSDGA increases in the presence of these extractants. However the separation factor decreases in the presence of extractants in glycolamic acid/n-DD [23].

Table 3.3: Variation in the distribution ratios of Eu(III) and Am(III) in the presence of various co-extractants at 298 K. Organic: Aq. phase ratio is 1:1. For HDEHDGA, Organic phase: [HDEHDGA] + synergic extractants /n-DD, Aq. Phase: 10^{-3}M [DTPA], pH=3. For HDEHSDGA, Organic phase: [HDEHSDGA] + co-extractants /n-DD, Aq. Phase: [HNO_3], pH=3

Co-extractant	D in 0.1 M HDEHDGA			D in 0.3 M HDEHSDGA		
	D_{Eu}	D_{Am}	SF	D_{Eu}	D_{Am}	SF
---	0.8	0.017	47	1.6	0.012	133
0.005 M CMPO	67.4	12.5	5.4	2.9	1.6	1.8
0.005 M TBP	64	18.5	3.5	3.7	1.8	2
0.005 M TOPO	27	14.5	1.9	3.2	1.5	2.1

The study showed that the extractants, HDEHDGA and HDEHSDGA are promising candidates for the mutual separation of lanthanides and actinides. Both HDEHDGA and HDEHSDGA can be conveniently dissolved in a traditional diluent, n-dodecane, for achieving efficient separations. HDEHDGA showed selectivity for europium (III) in the presence of DTPA in aqueous phase, whereas, the thio-derivative showed superior selectivity for americium(III) in the presence of TPEN in organic phase. Based on the slope analysis of extraction data, two molecules of HDEHDGA or HDEHSDGA were involved in the extraction of trivalents, with the other charge on the cation compensated by nitrate. Among these extractants, HDEHSDGA shows the potential of separating actinides from lanthanides in a single contact with a separation factor of ~2600 at pH 3.

Part 2. Demonstration of Ln(III)-An(III) separation by using HDEHDGA.

3.8. Optimization of pH for extraction conditions

Though, HDEHSDGA offered high separation factors of the order of ~2600, HDEHDGA was chosen for the mixer-settler demonstration run owing to the fact that sulfur containing extractants are less stable towards high nitric acid and radiation background. In order to develop a Ln(III)-An(III) separation by using HDEHDGA, various batch studies were performed to optimize the conditions required for mixer-settler operation. Experimental details involved in this study are discussed in section 2.4.1.2 of chapter 2. Figure 3.7 shows the variation in the extraction behavior of Am(III) and Eu(III) in a solution of 0.1 M HDEHDGA/n-DD as a function of pH. The aqueous phase contained 0.1 M citric acid[†††] spiked with ^{241}Am(III) or $^{(152+154)}$Eu(III) tracer at a particular pH. It is observed that the distribution ratio of Eu(III) and Am(III) increases with increase of pH, reaches a maximum value at pH 2, followed by decrease in distribution values. The extraction of Eu(III) is always higher than Am(III) at all pH values, which is characteristic to the diglycolamides and diglycolamic acid extractants [14, 16, 18]. Since the extractant is a monobasic acid, the initial increase in the distribution ratio with pH could be attributed to the enhanced dissociation of HDEHDGA, as seen in equation 2.5. However, the decrease in distribution ratio observed above pH 2 could be due to the complexation of metal ions by citric acid present in aqueous phase [27, 28].

[†††] Citric acid was added as a pH buffer to maintain constant pH the aqueous phase in experiments involving mixer-settler.

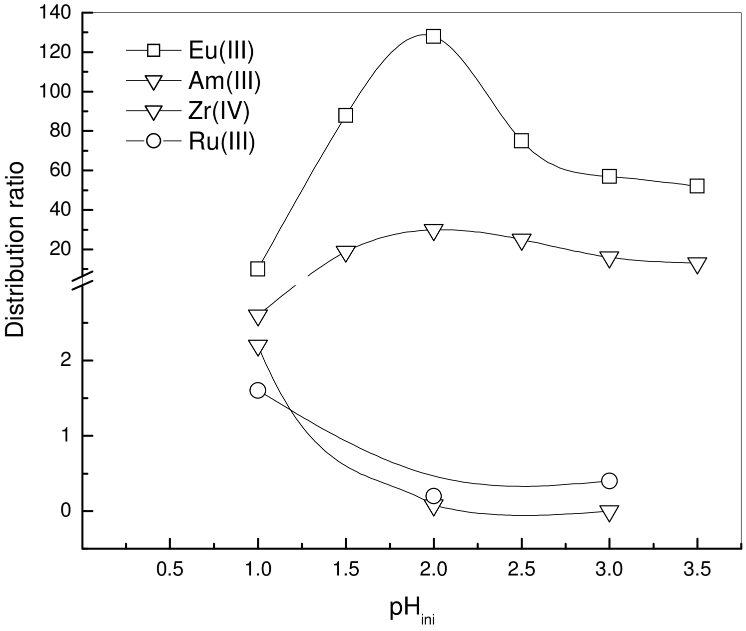

Figure 3.7. Variation in the distribution ratio of different metal ions as a function of pH. Organic phase: 0.1 M HDEHDGA/n-DD. Aqueous phase: 0.1 M HNO_3+0.1 M CA adjusted to various pH values spiked with the corresponding radioactive tracer.

It is also observed from figure 3.7 that the distribution ratio of Am(III) and Eu(III) reaches a maximum value at pH 2. Therefore, it is desirable to fix the pH of the feed solution to 2 for the separation process. However, the real feed solution also contains other fission products such as ^{106}Ru(III), ^{95}Zr(IV) *etc.* in 0.1 M nitric acid medium [21]. It is essential to retain these fission products in aqueous phase as much as possible during the extraction of Am(III) and Eu(III) for minimizing the contamination. In view of this, the variation in the distribution ratios of ^{106}Ru(III) and ^{95}Zr(IV) as a function of pH was studied and the results are also shown in figure 3.7. It is observed that the distribution ratio of ^{106}Ru(III) and ^{95}Zr(IV) are quite low and they decrease with increase of pH. This indicates that, it is advantageous to fix the pH of feed solution to higher value during extraction. However, above pH 4, it is likely that Am(III) and Eu(III) may undergo hydrolysis and complicate the separation process. Therefore, it was decided to maintain the pH of the feed solution to the optimum value of 3 for mixer-settler studies [27, 28].

3.9. Stripping studies of Am(III)

The cumulative extraction of Am(III) and Eu(III) in 0.1 M HDEHDGA/n-DD from 0.1 M citric acid medium at pH 3 is shown in figure 3.8. It is observed that more than 90% of Am(III) and Eu(III) is extracted in one contact and quantitative extraction is achieved in 3-4 contacts. The Am(III) and Eu(III) present together in organic phase, need to be separated from each other during stripping. The TALSPEAK process developed for the mutual separation of lanthanides and actinides exploited the differential complexing ability of DTPA present in aqueous phase and bis(2-ethylhexyl)phosphoric acid (HDEHP) present in organic phase. The process employed a solution of DTPA or a solution of DTPA in citric acid or lactic acid for selective stripping of Am(IIII) from the loaded organic phase. Therefore, in the present study also, the DTPA solution was attempted for back extraction of Am(III). However, when 0.01 M DTPA at pH 2-3 was used, the time required for phase disengagement was more than 3 minutes, which is undesirable for counter-current liquid-liquid extraction. This indicates that the aqueous phase requires phase modifier for the efficient phase disengagement. Del Cul *et al.* [22] developed a citric acid based TALSPEAK process for the mutual separation of lanthanides form actinides. The citric acid was added to DTPA in this process to enhance the phase disengagement and separation factor of Am(III) from Eu(III). Therefore, citric acid could be combined with DTPA in the present case also, to study the Am(III)-Eu(III) separation from the loaded organic phase [27, 28].

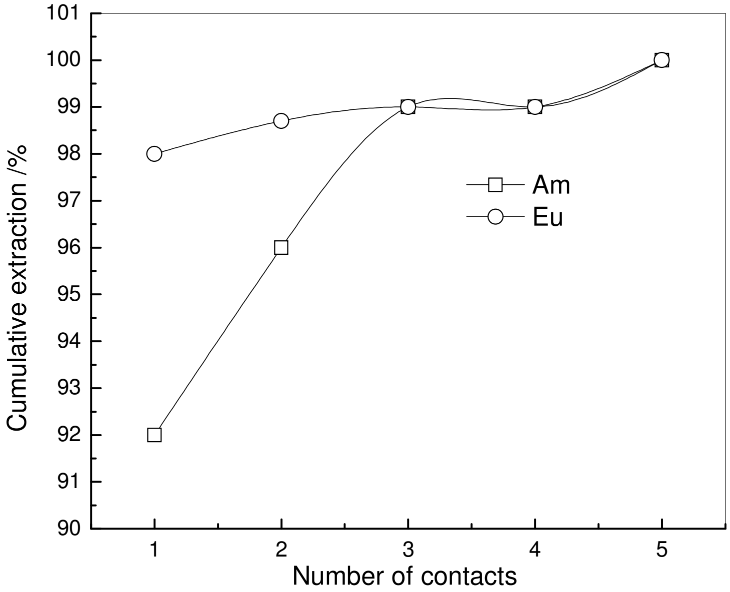

Figure 3.8. Cumulative extraction of Eu(III) and Am(III) from CA medium at pH 3. Organic phase: 0.1 M HDEHDGA/n-DD. Aqueous phase: 0.1 M CA+ 0.1 M HNO_3 spiked with $^{(152+154)}$Eu(III) or ^{241}Am(III) tracer adjusted to pH 3. Phase ratio: 1:1, 298 K.

3.10. Effect of CA on the stripping of Am(III) and Eu(III).

The effect of citric acid concentration in aqueous phase on stripping of Eu(III) and Am(III) from the loaded 0.1 M HDEHDGA/n-DD phase is shown in table 3.4. In this experiment, the loaded organic was contacted with a fresh aqueous solution of 0.01 M DTPA-citric acid at pH 3 each time. This procedure was repeated until Am(III) was completely stripped to aqueous phase. For detailed experimental procedure please refer to section 2.4.1.2 of chapter 2. It is observed from table 3.4 that Am(III) and Eu(III) could be stripped in 3 and 8 contacts respectively, when the concentration of citric acid in aqueous phase is 0.5 M. For mutual separation, it is essential to retain Eu(III) in organic phase as much as possible during stripping. Therefore, the concentration of citric acid in aqueous phase was decreased and the experiment was repeated. It is observed that the number of contacts required for stripping of metal ion increases with decrease in the concentration of citric acid. At 0.025 M citric acid, Am(III) could be recovered quantitatively in seven contacts. However, Eu(III) stripping was only 63% at the eighth contact. When the concentration of citric acid was further reduced to 0.01 M, the time needed for phase disengagement was quite high. In view of this, the concentration of citric acid needed for stripping of Am(III) was fixed to 0.025 M [28].

Table 3.4. Cumulative stripping (%) of Am(III) and Eu(III) from the loaded organic phase. Loaded organic phase: 0.1 M HDEHDGA/n-DD containing Eu(III) and Am(III). Stripping agent: 0.01 M DTPA + CA adjusted to pH 3, Phase ratio: 1:1, 298 K

Number of contacts	Cumulative (%) stripping at							
	0.5 M CA		0.1 M CA		0.05 M CA		0.025 M CA	
	Am(III)	Eu(III)	Am(III)	Eu(III)	Am(III)	Eu(III)	Am(III)	Eu(III)
1	90	29	85	29	48	20	45	14
2	98	50	98	51	76	41	71	29
3	100	67	100	68	89	53	86	38
4	-	79	-	78	96	65	93	44
5	-	87	-	85	99	71	97	51
6	-	93	-	89	100	80	99	58
7	-	96	-	92	-	87	100	63
8	-	99	-	94	-	90	-	68

Table 3.5. Cumulative stripping (%) of Am(III) and Eu(III) from the loaded organic phase. Loaded organic phase: 0.1 M HDEHDGA/n-DD containing Eu(III) and Am(III), Stripping agent: 0.01 M DTPA + 0.025 M CA adjusted to various pH values, Phase ratio: 1:1, 298 K

Number of contacts	Cumulative stripping(%) at					
	pH 3		pH 2		pH 1.5	
	Am(III)	Eu(III)	Am(III)	Eu(III)	Am(III)	Eu(III)
1	45	14	47	10	20	2
2	71	29	71	19	36	5
3	86	38	85	28	49	7
4	93	44	93	35	59	10
5	97	51	97	41	68	12
6	99	58	99	47	74	15
7	100	63	-	54	81	17
8	-	68	-	60	88	19

Table 3.5 shows the comparison in stripping behavior of Am(III) and Eu(III) as a function of pH. The aqueous phase contained 0.025 M citric acid and 0.01 M DTPA at different pH values. It is observed from table 3.5 that stripping of Eu(III) and Am(III) decreases with decrease of pH. The batch studies shown in table 3.5 thus suggests that Am(III) could be back extracted quantitatively using a solution of 0.01 M DTPA-0.025 M citric acid at pH 1.5. The co-stripping of Eu(III) is less using this formulation. Moreover, in a counter-current run, the stripped solution goes for contacting with the organic phase in the next stage (figure 2.22 of chapter 2). Since Eu(III) exhibits higher distribution ratio than Am(III), it is quite likely that the stripped Eu(III) could be extracted by organic phase subsequently. Therefore, it is possible to achieve the mutual separation of Am(III) and Eu(III) using this stripping formulation in a mixer-settler [27].

3.11. Mixer-settler studies

Based on the optimized conditions indicated above for extraction and stripping, the counter-current run was performed using a 20- stage ejector mixer-settler. The schematic illustration of the mixer-settler run and the conditions employed for the extraction and stripping are shown in figure 2.22 of chapter 2. For experimental details please refer to section 2.4.1.2.3 of chapter 2.

The stage-wise extraction profile of Am(III) and Eu(III) obtained in a mixer-settler run is shown in figure 3.9. The Eu(III) exhibiting a higher distribution ratio than Am(III), is extracted quantitatively in two stages. Complete extraction of Am(III) is achieved in ~3-4 stages, which is in good agreement with batch studies shown figure 3.8. The radioactivity remaining in the raffinate was determined to be negligible. The loaded organic phase was collected and stripping of Am(III) from the organic phase was performed by using 0.01 M DTPA-0.025 M citric acid at pH 1.5. The stripping profile in a 20-stage mixer-settler is shown in figure 3.10. It is observed that the quantity of Am(III) remaining in organic phase decreases with increase in number of stages. About 70% of the Am(III) remains in organic phase in the first stage. This indicates that 30% of Am(III) is back extracted in to aqueous phase. The stripping of Am(III) then increases with number of stages. After 20 stages of stripping in a mixer-settler, only 4% of Am(III) is retained by the organic phase, indicating that the recovery of Am(III) into aqueous phase is 96%. It is worthwhile to note that more than 98% of Eu(III) is retained in the organic phase in all stages of a mixer-settler and only ~2% of Eu(III) is stripped to aqueous phase after 20-stages. The measurement of radioactivity of Am(III) and Eu(III) in lean organic and aqueous product also confirmed that the contamination of Eu(III) in Am(III) product was less than 2%, whereas the contamination of Am(III) in the organic phase was ~4% [27, 28].

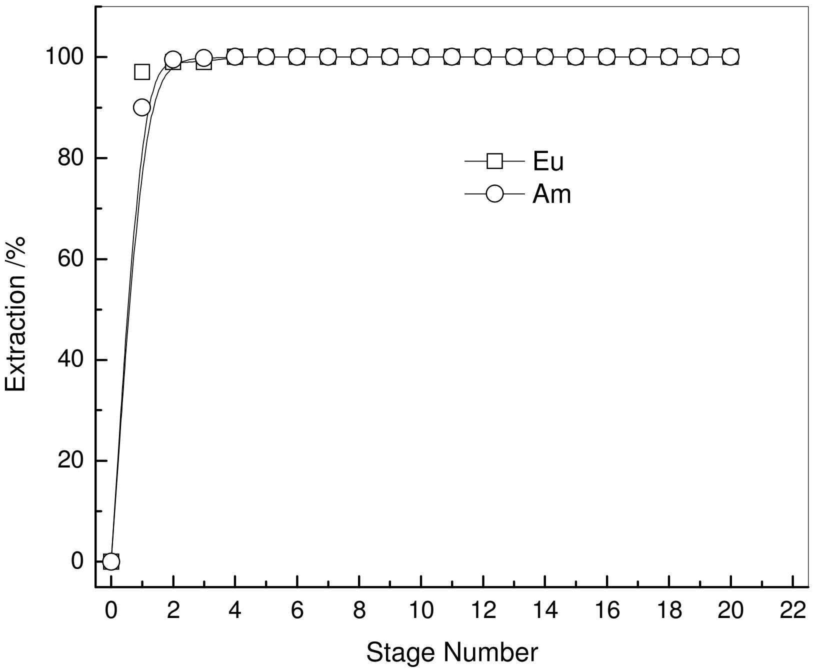

Figure 3.9. Extraction profile of Am(III) and Eu(III) in a 20 stage mixer-settler. Organic phase: 0. 1 M HDEHDGA/n-DD. Aqueous phase: 0.1 M CA+ 0.1 M HNO_3 spiked with $^{(152+154)}$Eu(III) or ^{241}Am(III) tracer, adjusted to pH 3. Flow rate: Organic 3 mL/min, aqueous 3 mL/min.

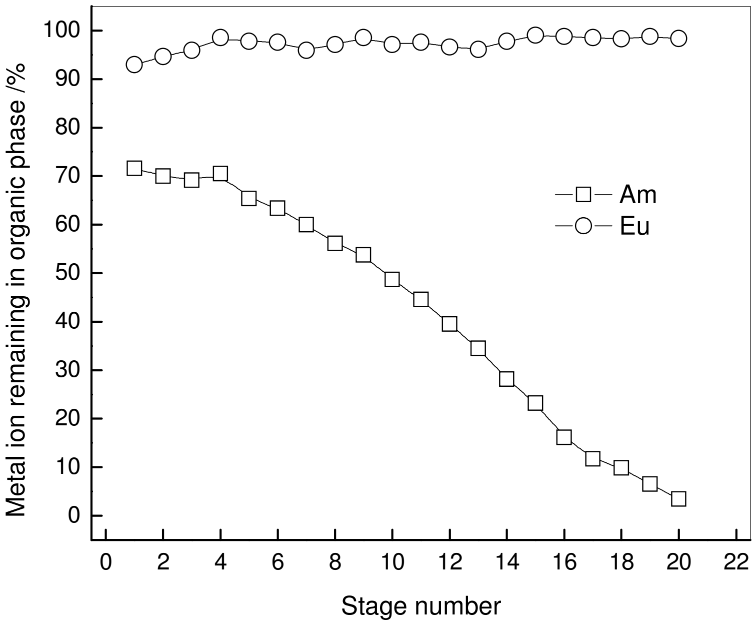

Figure 3.10. Back extraction profile of Am(III) and Eu(III) in a 20 stage mixer-settler. Loaded organic phase: 0. 1 M HDEHDGA/n-DD containing Eu(III) and Am(III), stripping aqueous phase: 0.01 M DTPA + 0.025 M CA, adjusted to pH 1.5. Flow rate: Loaded organic 3 mL/min, stripping aqueous phase 3 mL/min.

3.12. Conclusion

The extractants, HDEHDGA and HDEHSDGA are promising candidates for the mutual separation of lanthanides and actinides. HDEHDGA showed selectivity for europium (III) in the presence of DTPA in aqueous phase, whereas, the thio-derivative showed superior selectivity for americium(III) in the presence of TPEN in organic phase. Based on the slope analysis of extraction data, two molecules of HDEHDGA or HDEHSDGA were involved in the extraction of trivalents, with the other charge on the cation compensated by nitrate. Among these extractants, HDEHSDGA shows the potential of separating actinides from lanthanides in a single contact with a separation factor of ~2600 at pH 3. Though, HDEHSDGA offered high separation factors of the order of ~2600, HDEHDGA was chosen for the mixer-settler demonstration run owing to the fact that sulfur containing extractants are less stable towards high nitric acid and radiation background. Though, HDEHSDGA offered high separation factors of the order of ~2600, HDEHDGA was chosen for the mixer-settler demonstration run owing to the fact that sulfur containing extractants are less stable towards high nitric acid and radiation background

A method was also developed for the mutual separation of Am(III) and Eu(III) from 0.1 M nitric acid medium by using a solution of 0.1 M HDEHDGA/n-DD. Unlike the other lanthanide-actinide separating extractants in use, HDEHDGA is made up of CHON-atoms and compatible with a nuclear diluent, n-dodecane. Quantitative extraction of Am(III) and Eu(III) from dilute nitric acid medium was achieved in 2-3 contacts with the use of 0.1 M HDEHDGA/n-DD, at pH 3. Under this condition, the co-extraction of unwanted metal ions such as Zr(IV) and Ru(III) was negligible. The conditions needed for the selective recovery of Am(III) from the loaded organic phase was optimized. By using 0.01 M DTPA-0.025 M CA at pH 1.5, more than 96% of Am(III) could be recovered from the loaded organic phase after 20-stages in a mixer-settler. However, the stripping of Eu(III) was only 2%. The results, therefore, confirmed the feasibility of using HDEHDGA/n-DD for the mutual separation of Eu(III) and Am(III) from nitric acid medium.

3.13. References

1. G.L. Lumetta, A.V. Gelisb, G.F. Vandegrift, Solvent systems combining neutral and acidic extractants for separating trivalent lanthanides from the transuranic elements, Solvent Extr. Ion Exch. 28 (2010) 287-295.
2. M. Nilsson, K.L. Nash, A Review of the development and operational characteristics of the TALSPEAK process, Solvent Extr. Ion Exch. 25 (2007) 665-668.

3. C. Leggett, G. Liu, M.P. Jensen, Do aqueous ternary complexes influence the talspeak process?, Solvent Extr. Ion Exch. 28 (2010) 313-334.
4. B. Weaver, F.A. Kappelmann, Preferential extraction of lanthanides over trivalent actinides by monoacidic organophosphates from carboxylic acids and from mixtures of carboxylic and aminopolyacetic acids, J. Inorg. Nucl. Chem. 30 (1968) 263-281.
5. A.V. Gelis, G.F. Vandegrift, A. Bakel, D.L. Bowers, A.S. Hebden, C. Pereira, M. Regalbuto, Extraction behaviour of actinides and lanthanides in TALSPEAK., TRUEX and NPEX processes of UREX+, Radiochim. Acta 97 (2008) 231-245.
6. M. Nilsson, K.L. Nash, Trans-Lanthanide extraction studies in the TALSPEAK system: investigating the effect of acidity and temperature. Solv. Extr. Ion Exch. 27 (2009) 354-367.
7. T. Guoxin, Z. Yongjun, X. Jingming, Extraction of Am(III) and Ln(III) by dialkyldithiophosphinic acid with different alkyl groups, Solv. Extr. Ion Exch. 19 (2001) 993-1002.
8. K.C. Sole, J.B. Hiskey, Solvent extraction characteristics of thiosubstituted organophosphinic acid extractants, Hydrometallurgy 30 (1992) 345-359.
9. C. Ekberg, A. Fermvik, T. Retegan, G. Skarnemark, M.R.S. Foreman, M.J. Hudson, S. Englund, M. Nilsson, An overview and historical look back at the solvent extraction using nitrogen donor ligands to extract and separate An(III) from Ln(III), Radiochim. Acta 96 (2008) 225-233.
10. Z. Kolarik, U. Müllich, F. Gassner, Selective extraction of Am(III) Over Eu(III) by 2,6-ditriazolyl- and 2,6-ditriazinylpyridines, Solvent Extr. Ion Exch. 17 (1999) 23-32.

11. K.L. Nash, A Review of the basic chemistry and recent developments in trivalent f-elements separations. Solvent Extr. Ion Exch. 11 (1993) 729 (1993).
12. H.H. Dam, Reinhoudt, D N., Verboom, W.: Multicoordinate ligands for actinide/lanthanide separations, Chem. Soc. Rev. 36 (2007) 367-375.
13. S.A. Ansari, P.N. Pathak, P.K. Mohapatra, V.K. Manchanda, Aqueous partitioning of minor actinides by different processes, Sep. Pur. Rev. 40 (2011) 43-53.
14. J. Ravi, K.A. Venkatesan, M.P. Antony, T.G. Srinivasan, P.R. Vasudeva Rao, Tuning the diglycolamides for modifier-free minor actinide partitioning, J. Radioanal. Nucl. Chem. 295 (2013) 1283-1292.
15. D. Magnusson, B. Christiansen, J.P. Glatz, R. Malmbeck, G. Modolo, D.S. Purroy, C. Sorel, Demonstration of a TODGA based extraction process for the partitioning of minor actinides from a PUREX raffinate Part III: Centrifugal contactor run using genuine fuel solution, Solv. Extr. Ion Exch. 27 (2009) 26-35.
16. J. Ravi, K.A. Venkatesan, M.P. Antony, T.G. Srinivasan, P.R. Vasudeva Rao, Unsymmetrical diglycolamide for the safe management of nuclear waste. J. Environ. Chem. Eng. 1 (2013) 690-695.
17. Y. Sasaki, G.R. Choppin, Solvent extraction of Eu, Th, U, Np and Am with N, N' –dimethyl-N,N' di-hexyl-3-oxapentanediamide and its analogous compounds, Anal. Sci. 12 (1996) 225-230.
18. K. Shimojo, H. Naganawa, J. Noro, F. Kubota, M. Goto, Extraction behavior and separation of lanthanides with a diglycol amic acid derivative and a nitrogen-donor ligand, Anal. Sci. 23 (2007) 1427-1435.
19. P.R. Zalupski, M.P. Jensen, R. Chiarizia, M.P. Chiarelli, A.W. Herlinger, Acid-base and organic-water distribution equilibria for symmetrically-substituted P,P'-Dialkyl Alkylenebisphosphonic Acids, Solv. Extr. Ion Exch. 24 (2006) 177-185.

20. A.N. Turanov, V.K. Karandashev, V.E. Baulin, Extraction of lanthanides(III) from nitric acid solutions by selected polyfunctional monoacidic organophosphorus compounds, Solv. Extr. Ion Exch. 25 (2007) 165-176.
21. M.P. Antony, R. Kumaresan, A.S. Suneesh, R. Rajeswari, B. Robertselvan, V. Sukumaran, R. Manivannan, K.V. Syamala, K.A. Venkatesan, T.G. Srinivasan, P.R. Vasudeva Rao, Development of a CMPO based extraction process for partitioning of minor actinides and demonstration with genuine fast reactor fuel solution (155 GWd/Te). Radiochim. Acta 99 (2011) 207-215.
22. G.D. Del Cul, W.D. Bond, L.M. Toth, G.D. Davis, S. Dai, D.H. Metcalf, Citrate based "TALSPEAK" Lanthanide-Actinide separation process, ORNL Document, ORNL/TM-12785 (1994)
23. A.S. Suneesh, K.A. Venkatesan, K.V. Syamala, M.P. Antony, P.R. Vasudeva Rao, Mutual separation of americium (III) and europium (III) using glycolamic acid and thioglycolamic acid, Radiochim. Acta 100 (2012) 425-30.
24. A.S. Suneesh, K.V. Syamala, K.A. Venkatesan, M.P. Antony, P.R. Vasudeva Rao, Bis(2-ethylhexyl)diglycolamic acid for the mutual separation of europium(III) and americium(III) from citric acid- nitric acid medium, In: Symposium of emerging trends on separation science and technology (SESTEC). SVKM Mithibhai College, Mumbai, India, P.N. Pathak, R.M. Sawant, P.K. Mohapatra, A. Goswami, K.L. Ramakumar (eds), (2012) p-87
25. A.S. Suneesh, K. A. Venkatesan, K. V. Syamala, M. P. Antony, P. R. Vasudeva Rao, Glycolamic acids for lanthanide-actinide separation, In: International conference on vistas in chemistry (ICVC): IGCAR Kalpakkam, India, V. Ganesan, S. Antonysamy, Kitheri Joseph (eds) (2011), p-161.

26. A.S. Suneesh, K. V. Syamala, K. A. Venkatesan, M. P. Antony, P. R. Vasudeva Rao, Effect of additives on the mutual separation of lanthanides and actinides usnig glycolamic acids, In: International conference on vistas in chemistry (ICVC): IGCAR Kalpakkam, India, V. Ganesan, S. Antonysamy, Kitheri Joseph (eds) (2011), p-198.
27. A.S. Suneesh, R. Kumaresan,S. Rajeswari, P.K. Nayak, K.V. Syamala, K.A. Venkatesan, M.P. Antony, P.R. Vasudeva Rao, Development and demonstration of americium (III)-europium (III) separation using diglycolamic acid, Sep. Sci. Technol. 48 (2013) 1998-2006.
28. A. S. Suneesh, R. Kumaresan, S. Rajeswari, P. K. Nayak, K. V. Syamala, K. A. Venkatesan, M. P. Antony, P. R. Vasudeva Rao, Demonstration of Eu(III)-Am(III) separation in a 20-stage mixer-settler using diglycolamic acid, In: Nuclear and Radiochemistry Symposium (NUCAR)-2013, Govt. Model Science College, Jabalpur, India, R. Tripathy, G.A. Rama Rao, B.S. Tomar, K.L. Ramakumar (eds), (2013), p 193.

Chapter 4: Develpment of diglycolamic acid-impregnated resins for the mutual separation of Eu(III) and Am(III)

This chapter deals with the indigenous development of a macroporous polyacrylic resin impregnated with diglycolamic acid for the mutual separation of lanthanides and actinides. This chapter is divided in to two parts. Part 1 discusses about the evaluation of various alkyldiglycolamic acid impregnated resins for the mutual separation of Am(III) and Eu(III). Part 2 discusses about the demonstration of Eu(III)-Am(III) separation by using N,N-dioctyldiglycolamic acid (HDODGA) in column chromatographic mode.

4.1. Introduction.

The ion exchange technology is a simple and robust method for the separation of toxic and radiotoxic metal ions from wide variety of wastes [1]. Conventional organic polymer based ion exchange materials are in general suitable for the separation of alkali and alkaline earth metal ions from simple waste streams [2-6]. To enhance the selectivity, the polymeric material is modified with chelating type organic ligands [7-9]. However, the synthesis of such chelating type ligands on the surface of the polymer is difficult, cumbersome and uneconomical. Moreover, such chelates would not exhibit the desired selectivity from a complex feed solution, as the conformation required for efficient complex formation with the metal ion is generally lost during linking of chelating ligands on the surface of the polymer,

In contrast, the solvent impregnated resin (SIRs) is considered as an alternative to covalent linking of chelating ligands on a polymeric matrix [10-15]. SIRs are composed of an “inert “polymeric matrix impregnated with readily available extractants [10, 17]. Therefore, unlike covalent linking of ligands, SIRs can be easily prepared and they possess the features and advantages exhibited by both liquid-liquid extraction and solid-liquid extraction. Moreover, the dispersion of the extractant over the surface of the polymer is so large, that the distribution coefficients of metal ions achieved with the use of SIRs are usually very high as compared to those achieved by the same extractant in solvent extraction mode. A number of studies have been reported in literature on SIRs. In this context, excellent review by Warshawshy *et al.* [16] describes the preparation and potential application of SIRs for the separation of metal ions from wide variety of feeds. More recently, Kabay *et al.* [10] reported a review on the development of SIRs and their applications for the separation of metal ions and organic compounds.

In view of this, diglycolamic acid derivates (alkyl = butyl to decyl) synthesised and were impregnated in Tulsion ADS 400 resin. These impregnated resins were studied for the mutual separation of Eu(III) and Am(III). The synthetic procedures for the synthesis of alkyldiglycolamic acid and their impregnation procedure are discussed in section 2.3.2. of chapter 2. Structure of alkyldiglycolamic acid is showed in figure 4.1.

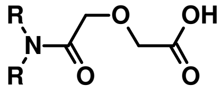

Diglycolamic acid
R is Butyl, hexyl, octyl, decyl

Figure 4.1. Structures of diglycolamic acid.

Part 1. Evaluation of various alkyldiglycolamic acids for the mutual separation of Am(III) and Eu(III)

4.2. Optimization of the extent of impregnation.

In order to optimize the amount of diglycolamic acid required for impregnation, resins having various compositions of diglycolamic acid was synthesized and the extraction behaviour of Am(III) and Eu(III) was determined. Figure 4.2 shows the variation in the distribution coefficient of Am(III) and Eu(III) as a function of percentage impregnation of diglycolamic acid at a fixed pH of 3. The loading of extractant (N,N-bis-octyl diglycolamic acid) in the resin was varied from 10 wt% to 30 wt%. It is observed that the distribution coefficient of both Am(III) and Eu(III) increases with increase in loading of extractant in the resin. The K_d of Eu(III) is twice that of Am(III) leading to the separation factor (ratio of distribution coefficients) of about 2 in all cases. For efficient extraction of trivalents, it is desirable to choose the resin containing a minimum of 30 wt% loading, where the distribution coefficient of more than 5000 mL/g is obtained for both the metal ions. Therefore, for all subsequent studies, the resin with 30 wt% extractant loading was employed.

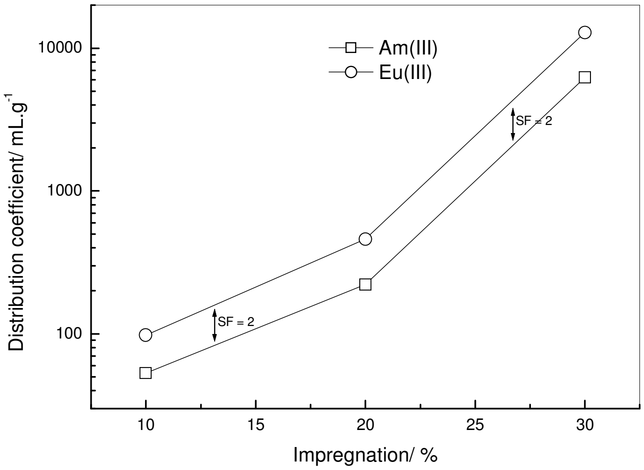

Figure 4.2. Variation in the distribution coefficient of Am(III) and Eu(III) as a function of percentage of impregnation of N,N-bis-octyl diglycolamic acid in Tulsion ADS 400, at 298 K. Resin phase: N,N-bis-octyl diglycolamic acid (30 wt %) impregnated in Tulsion ADS 400 (0.05 g). Aqueous phase: 0.001 M HNO_3 spiked with ^{241}Am(III) or $^{(152+154)}$Eu(III) tracer (10 mL).

4.3. Effect of pH.

Extraction behaviour of Am(III) and Eu(III) by Im-DGAH was studied by equilibrating 0.05 g of resin with 10 mL of aquous phase spiked with $^{(152+154)}$Eu or ^{241}Am tracer at 298 K. The variation in the distribution coefficient of Am(III) and Eu(III) as a function of pH for various alkyl diglycolamic acids is shown in figure 4.3. It can be seen that the distribution coefficient of these metal ions increases with increase in pH of aqueous phase. This is due to the acidic nature of diglycolamic acids. It is important to note that the distribution ratio is dependent on the nature of alkyl group attached to amidic nitrogen atom. Increasing the chain length of alkyl group increases the distribution ratio of metal ions. The reason for such behavior is not clear at present. It is observed that the separation factor varies from 1 to 2 in most cases (see table 4.1), which is unsuitable for the mutual separation of Eu(III) and Am(III). At pH 1, the SF of ~ 5 is obtained. However, the distribution coefficient of both Am(III) and Eu(III) is quite low under this condition, which is also unsuitable for efficient extraction.

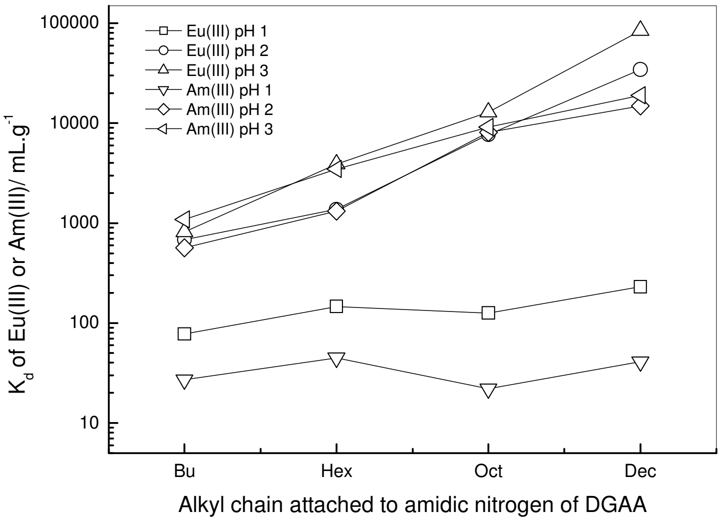

Figure 4.3. Variation in the distribution coefficient of Am(III) and Eu(III) in the resin phase as a function of pH at 298 K. Resin phase: N,N-Bis-octyl diglycolamic acid (30 wt %) impregnated in Tulsion ADS 400 (0.05 g). Aqueous phase: Aqueous solutions at different pH adjusted with dilute HNO_3 spiked with ^{241}Am or $^{(152+154)}$Eu tracer (10 mL).

Table 4.1. Separation factor of Eu(III) over Am(III) achieved in N,N-bis-octyl diglycolamic acid impregnated resin as a function of pH. Resin phase: N,N-Bis-octyl diglycolamic acid (30 wt %) impregnated in Tulsion ADS 400 (0.05 g). Aqueous phase: Aqueous solution at different pH adjusted with dilute HNO_3 spiked with ^{241}Am or $^{(152+154)}$Eu tracer (10 mL).

	Separation factors achieved in alkyl DGAA's with alkyl group			
pH	Butyl	Hexyl	Octyl	Decyl
1	3	3.2	5.7	5.5
2	1.2	1.2	1	2.3
3	0.75	1.1	1.4	4.7

4.4. Effect of DTPA.

To enhance the separation factor and facilitate mutual separation, co-extractants or aqueous soluble reagents are usually added to organic and aqueous phases respectively. In the present system, it is desirable to retain less extractable Am(III) in aqueous phase by adding aqueous phase modifiers. As discussed in chapter 3, DTPA was employed for the selective retention of Am(III) in aqueous phase as compared to Eu(III). Therefore, the distribution coefficient of Eu(III) and Am(III) in the resin phase was measured in the presence of DTPA at pH 3 and the results are shown in figure 4.4. It is observed that the distribution coefficient of both metal ions decrease in the presence of DTPA (compare with figure 4.3). At very low concentration of DTPA (10^{-4} M) the distribution coefficient of Eu(III) and Am(III) increases marginally with increase in chain length of alkyl group attached to DGAA. However, at DTPA concentration more than 0.005 M, the K_d decreases with increase in alkyl chain length of DGAA. This differences observed at various concentrations of DTPA could be perhaps due to the competition between the DTPA and alkyl DGAA for extraction of Eu(III) and Am(III). It appears that at very low concentration (10^{-4} M) the DTPA seems to be ineffective or insufficient for retaining the metal ions in aqueous phase. Therefore, the distribution trend of Am(III) and Eu(III) observed at 10^{-4} M DTPA concentration is similar to that observed in the absence of DTPA (shown in figure 4.3).

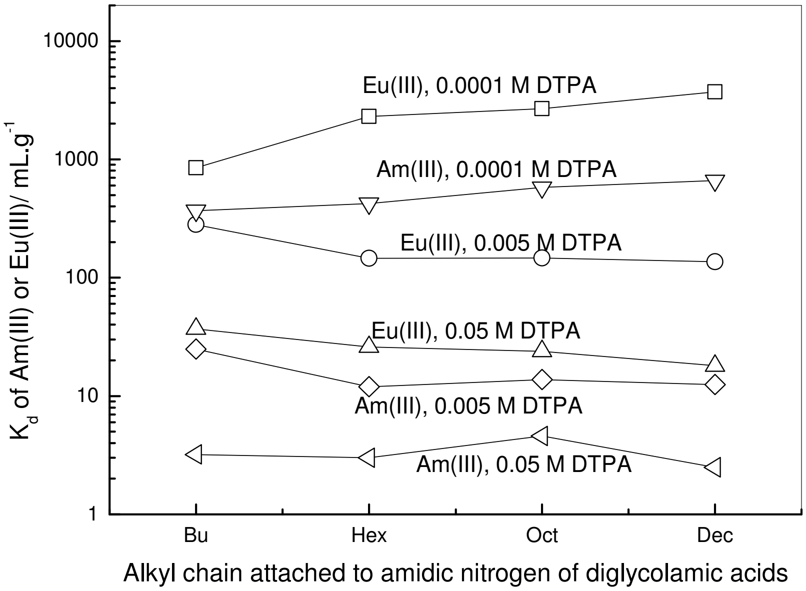

Figure 4.4. Variation in the distribution coefficient of Am(III) and Eu(III) in the resin phase as a function of DTPA concentration at 298 K. Resin phase: N,N-Bis-octyl diglycolamic acid (30 wt %) impregnated in Tulsion ADS 400 (0.05 g). Aqueous phase: Aqueous solutions at different concentrations of DTPA adjusted to pH 3 spiked with ^{241}Am or $^{(152+154)}$Eu tracer (10 mL).

Table 4.2. Separation factors of Eu(III) over Am(III) achieved in N,N-bis-octyl diglycolamic acid impregnated resin as a function of DTPA at pH 3. Resin phase: N,N-Bis-octyl diglycolamic acid (30 wt %) impregnated in Tulsion ADS 400 (0.05 g). Aqueous phase: Aqueous solution at various concentrations of DTPA spiked with ^{241}Am or $^{(152+154)}$Eu tracer (10 mL).

DTPA	Separation factors achieved in alkyl DGAA's with alkyl group			
	Butyl	Hexyl	Octyl	Decyl
0.0001	4	2.2	4.4	2.3
0.001	16	4.8	8.9	4.9
0.005	10	10.5	15.7	4.2
0.05	0.5	3.3	12.1	3.8

Table 4.2 shows the separation factor of Eu(III) over Am(III) achieved in various diglycolamic acids as a function of DTPA concentration in aqueous phase at pH 3. It is observed that the separation factor remains at values of 2 to 4, at 10^{-4} M DTPA concentration. The separation factor increases with increase in the concentration of DTPA in all resins, reaches a maximum separation factor at a DTPA concentration of 0.001-0.005 M followed by decrease in separation factors. Since DTPA forms a preferential complex with Am(III) as compared to Eu(III), the separation factor increases initially with increase in the concentration of DTPA. Above 0.005M DTPA, it appears that both Am(III) and Eu(III) are retained in aqueous phase to a similar extent. Therefore, the separation factor falls at high concentration of DTPA. From the above study, it is obvious that octyl substituted DGAA, namely N,N-dioctyldiglycolamic acid, offering a separation factor of ~16 when the DTPA concentration is 0.005 M, is a promising candidate for mutual separation of Eu(III) and Am(III) by extraction chromatography. Therefore, the performance of the HDODGA impregnated resin was taken for evaluation in the column study.

<u>Part 2. Demonstration of the mutual separation of Am(III) and Eu(III) by HDODGA with extraction chromatography.</u>

4.5. Column studies

4.5.1. Column breakthrough

The performance of the resin under dynamic condition was assessed by column breakthrough experiments. About 1 g of the resin was initially immersed in water and loaded into a glass column of radius 0.5 cm. The resin bed was conditioned with 50 ml of 0.01 M nitric acid. The experimental feed solution was composed of nitric acid solution adjusted to the desired pH, spiked with ^{241}Am(III) or $^{(152+154)}$Eu(III) tracer. The solution was passed at a flow rate of 2 mL/min. The effluent was collected at various intervals of time and analyzed for $^{(152+154)}$Eu(III) and ^{241}Am(III) by gamma spectrometry. The ratio of the radioactivity of $^{(152+154)}$Eu(III) (or ^{241}Am(III)) in the effluent (A_f) to that of feed (A_0) was plotted against the volume of the solution passed through the bed to obtain a breakthrough curve. The breakthrough was followed up to A_f/A_0= 0.25. Elution of the metal ions was carried out by using 0.005 M DTPA solution adjusted to pH 2.5.

The breakthrough curve for the extraction of Am(III) from pH 2 solution is shown in figure 4.5. It also shows a breakthrough curve for Eu(III) carried out under similar conditions in a separate study. Since the distribution coefficient of Eu(III) is higher than that observed for Am(III), under this condition, the breakthrough of Am(III) occurs early after passing ~100 mL of feed solution. The effluent radioactivity of Am(III) increases with increase in the volume of feed solutions. 20 % breakthrough is achieved after passing 1000 mL. However the radioactivity of Eu(III) is negligible in the effluent even after passing 1000 mL of feed solution. The breakthrough study thus shows the feasibility of separating Am(III) and Eu(III) from nitric acid medium. The elution of Am(III) was performed by passing a solution of 0.005 M DTPA solution at pH 2.5. The elution profile of Am(III) is shown in figure 4.6. In the first 50 mL fraction, the eluent contains more than 90 % of Am(III). The elution was quantitative after passing 150 mL. A similar elution experiment was also performed from the Eu(III) loaded column. The cumulative elution of Eu(III) increases with increase in the volume of eluent passed as shown in figure 4.6. Based on this elution profile, it is obvious that the Am(III) fraction (ie. in the first 100 mL) contains about 35 % of Eu(III) loaded in the resin. After passing 150 mL of the solution, eluent contains only Eu(III). Quantitative elution of Eu(III) is achieved after passing 700 mL of eluate.

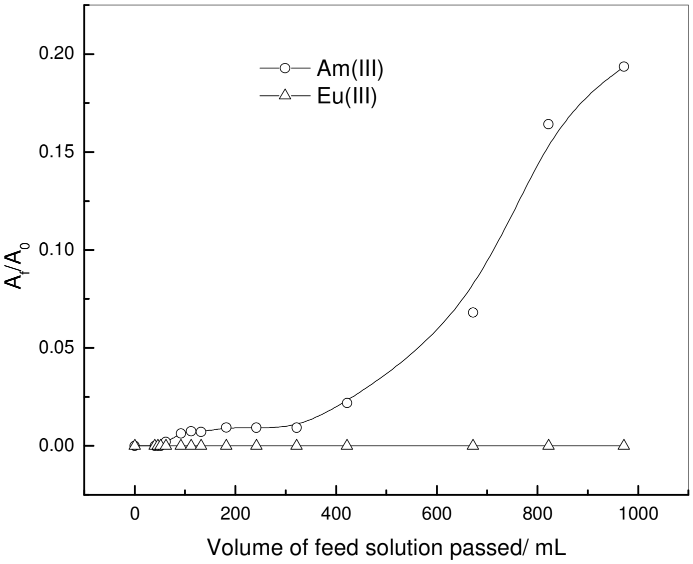

Figure 4.5. Breakthrough curve for loading of Am(III) and Eu(III) from nitric acid medium. Feed solution: 0.01 M HNO_3 spiked with ^{241}Am(III) or $^{(152+154)}$Eu(III). Resin phase: N,N-Bis-octyl diglycolamic acid (30 wt %) impregnated in Tulsion ADS 400 (1 g). Flow rate: 2 mL/min.

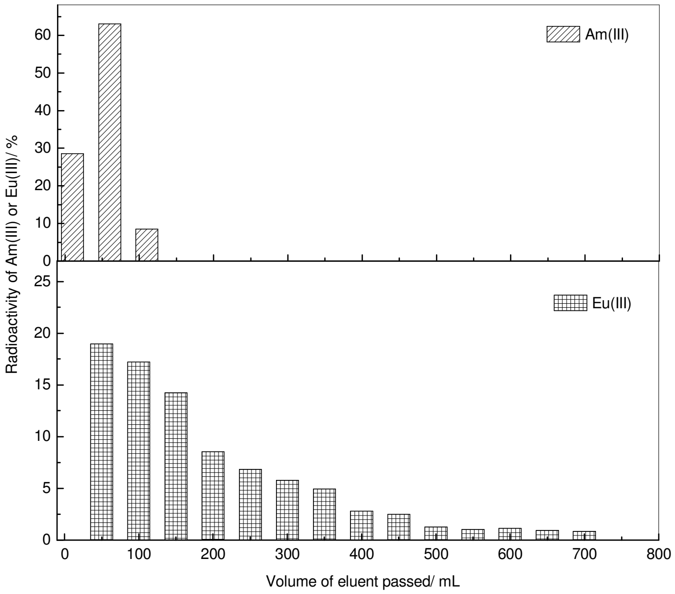

Figure 4.6. Elution profile of Eu(III) and Am(III). Eluate: 0.005 M DTPA at pH 2.5. Resin phase: N,N-Bis-octyl diglycolamic acid (30 wt %) impregnated in Tulsion ADS 400 (1 g) loaded with ^{241}Am or $^{(152+154)}$Eu. Flow rate: 2 mL/min.

4.5.2. Mutual separation of Am(III) and Eu(III) in column chromatography

To confirm the mutual separation of Eu(III) and Am(III) by extraction chromatography, about 100 mL of the nitric acid solution containing both Am(III) and Eu(III) adjusted to pH 1.5 was passed in to the column containing octyl-DGAA (HDODGA) impregnated resin (1 g). The γ-spectrum of the feed is shown in the figure 4.7, which indicates that the feed contains both Am(III) and Eu(III). The effluent activity after passing 100 mL of the solution was negligible. This ensures both Am(III) and Eu(III) present in the feed are quantitatively extracted into resin phase. The elution of Am(III) from the column was performed by passing 0.001 M DTPA solution at pH 2.5. The concentration of DTPA was reduced in this case as compared to the previous study to minimize the contamination of Eu(III) in the Am(III) product. The elution profile is shown in the figure 4.8. It is observed that elution of Am(III) alone increases with increase in the volume of eluate passed, reaches a maximum followed by a long tailing in elution. The γ-spectrum (figure 4.7) of the eluate obtained after passing 80 mL of the eluent shows that there is no contamination of Eu(III) in the Am(III) product. Quantitative elution of Am(III) was achieved after passing ~100 mL of the eluate with out any contamination of europium. The Eu(III) present in the column was then easily eluted by increasing the concentration of DTPA to 0.01 M at pH 1.5. The recovery in this case was quantitative in 20 mL of eluate. The γ-spectrum of the Eu(III) fraction (figure 4.7) is devoid of any Am(III) contribution confirms that the Eu(III) fraction is free from any contamination of Am(III). Therefore, the study demonstrates the feasibility of separating Am(III) from Eu(III) by extraction chromatography using HDODGA [18, 19].

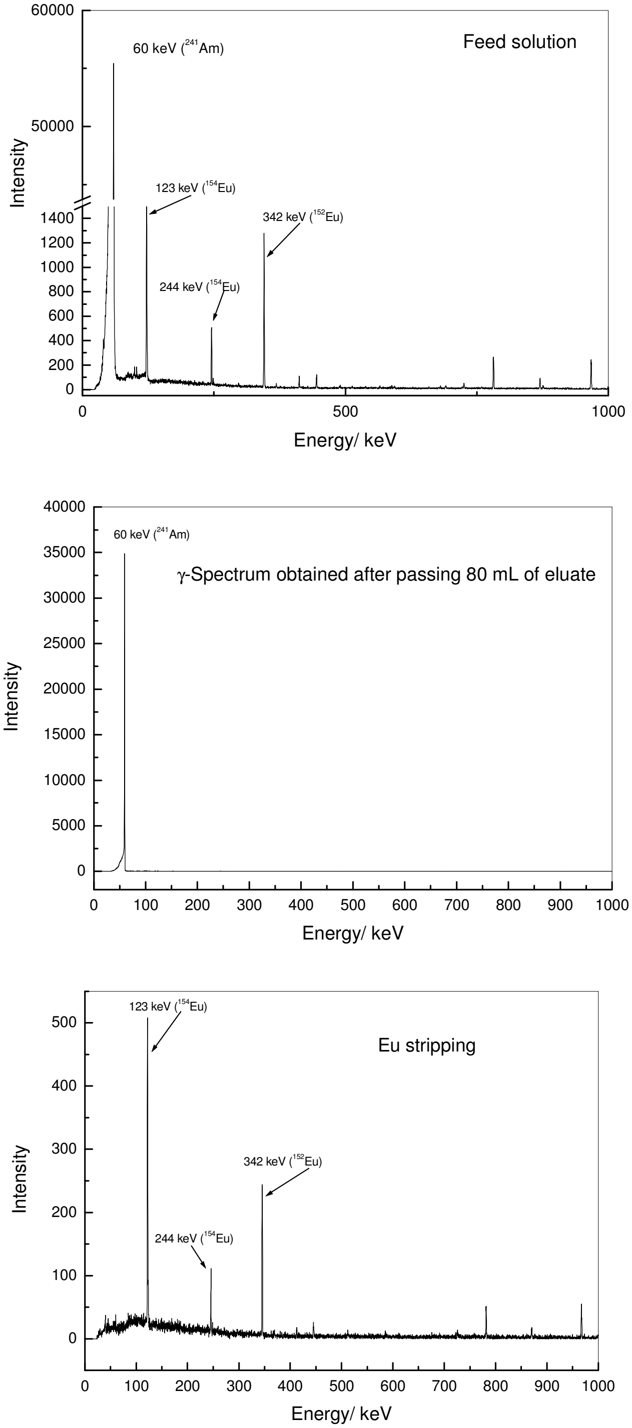

Figure 4.7. The γ-spectrum of the feed, Am(III) fraction and Eu(III) fraction.

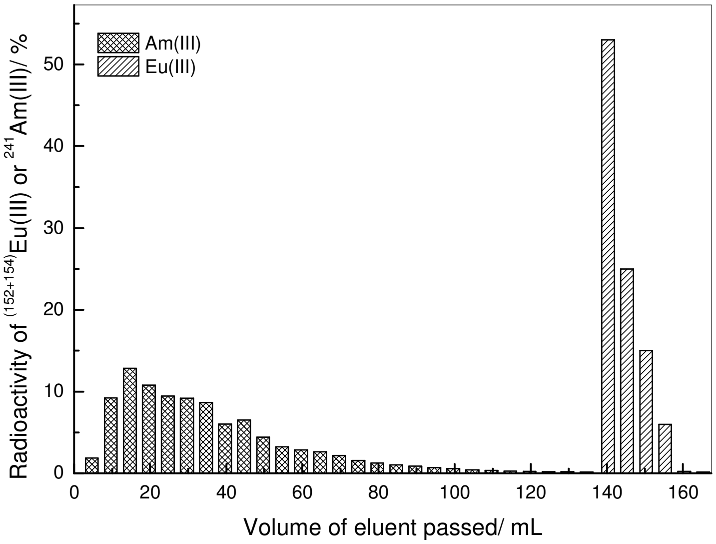

Figure 4.8. Elution profile of Am(III) and Eu(III). Resin phase: N,N-Bis-octyl diglycolamic acid (30 wt %) impregnated in Tulsion ADS 400 (1 g). Conditions for loading: HNO_3 feel solution spiked with $^{(152+154)}$Eu(III) and ^{241}Am(III) adjusted to pH 1.5. Flow-rate: 2 mL/min. Conditions for elution: 0.001 M DTPA adjusted to pH 2.5 for Am(III) elution followed by 0.01 M DTPA adjusted to pH 1.5 for Eu(III) elution. Flow-rate: 2 mL/min.

4.6. Conclusions

The alkyl derivatives of diglycolamic acid with alkyl group varied from butyl to decyl group were prepared and studied for the mutual separation of Am(III) and Eu(III) by extraction chromatography. The glycolamic acids were impregnated in Tulsion ADS 400 and the extraction behavior of Eu(III) and Am(III) in the impregnated resin was studied as a function of various parameters. While the separation factor of Eu(III) over Am(III) remained at ~2 in the absence of DTPA, the separation factor increased to ~15 when 0.005 M DTPA was present in aqueous phase. Based on the optimized conditions, the column study was performed for chromatographic separation. The study confirmed that quantitative and mutual separation of Eu(III) and Am(III) was feasible by extraction chromatography with the use of octyl DGAA (HDODGA) impregnated resin.

4.7. References

1. F.G. Helfferich, Ion Exchange, Dover Publications Inc. New York (1962)
2. M.V. Sivaiah, K.A. Venkatesan, R.M. Krishna, P. Sasidhar, G.S. Murthy, Ion exchange properties of strontium on in situ precipitated polyantimonic acid in amberlite XAD-7, Sep. Purif. Technol. 44 (2005) 1-9.
3. D.G. Kinniburgh, M.L. Jackson, J.K. Syers, Adsorption of alkaline earth, transition, and heavy metal cations by hydrous oxide gels of iron and aluminum. Soil Sci. Soc. Am. J. 40 (1976) 796-9.
4. K.A. Venkatesan, V. Sukumaran, M.P. Anton, T.G. Srinivasan,) Studies on the feasibility of using crystalline silicotitanates for the separation of cesium-137 from fast reactor high-level liquid waste, J. Radioanal. Nucl. Chem. 280 (2009) 129-136.
5. M.V. Sivaiah, K.A. Venkatesan, P.M. Krishna, P. Sasidhar, G.S. Murthy, Ion exchange and chromatographic separation of cesium, strontium and europium from acidic streams using uranium antimonite,Radiochim. Acta, 92 (2004) 507-512.
6. K.A. Venkatesan, G.P. Selvam, P.R. Vasudeva Rao, Sorption of strontium on hydrous zirconium oxide. Sep. Sci. Technol. 35 (2000) 2343-2357.
7. F. Fu, Q. Wang, Removal of heavy metal ions from wastewaters: a review, J. Environ. Manag. 92 (2011) 407-418.
8. R. Vinodh, R. Padmavathi, D. Sangeetha, Separation of heavy metals from water samples using anion exchange polymers by adsorption process, Desalination 267 (2011) 267-276.
9. J. Liu, Y. Ma, T. Xu, G. Shao, Preparation of zwitterionic hybrid polymer and its application for the removal of heavy metal ions from water. J.Hazardous Mater., 178 (2010) 1021-1029.

10. N. Kabay, J.L. Cortina, A. Trochimczuk, M. Streat, Solvent-impregnated resins (SIRs)–methods of preparation and their applications, React. Funct. Polym. 70 (2010) 484-496.
11. S.A. Ansari, P.K. Mohapatra, M. Iqbal, J. Huskens, W. Verboom, Two novel extraction chromatography resins containing multiple diglycolamide-functionalized ligands: Preparation, characterization and actinide uptake properties, J. Chrom. A, 1334 (2014)79-86.
12. K. Onishi, T. Nakamura, S. Nishihama, K. Yoshizuka, Synergistic solvent impregnated resin for adsorptive separation of lithium ion. Ind. Eng. Chem. Res. 49 (2010) 6554-6558.
13. S. Nishihama, K. Kohata, K. Yoshizuka, Separation of lanthanum and cerium using a coated solvent-impregnated resin, Sep. Purif. Technol. 118 (2013) 511-518.
14. M.S. Hosseini, A. Hosseini-Bandegharaei, Comparison of sorption behavior of Th (IV) and U (VI) on modified impregnated resin containing quinizarin with that conventional prepared impregnated resin, J. Haz. Mater. 190 (2011) 755-765.
15. O.S. Helaly, M.A. El-Ghany, M.I. Moustafa, A.H. Abuzaid, N.A. EL-MONEM, I.M. Ismail, Extraction of cerium (IV) using tributyl phosphate impregnated resin from nitric acid medium,Tran. Nonferr. Met. Soc. 22 (2012) 206-214.
16. A. Warshawsky, J.L. Cortina, K. Jerabek, Solvent impregnated resin applications on metal separation processes. Solvent Extr. Liq. Memb. 7 (2008) 301-335.
17. A.A. Zagorodni, Ion exchange materials: properties and applications. Elsevier, (2006).

18. A.S. Suneesh, K.V. Syamala, K.A. Venkatesan, M.P. Antony, P.R. Vasudeva Rao, Chromatographic separation of americium (III) from europium (III) using alkyl diglycolamic acid, Sep. Sci. Technol. 50 (2015) 1213-1220.

19. A.S. Suneesh, K. V. Syamala, K.A. Venkatesan, M.P. Antony, P. R. Vasudeva Rao, N,N-Bis-octyldiglycolamic acid impregnated resins for americium (III)-europium (III) separation, In: Emerging Trends in Separation Science and Technology(SESTEC), D.K. Singh, P.K. Mohapatra, B.S. Tomar, A. Goswami, K.L. Ramakumar (eds). BARC, Mumbai, India. P-145

Chapter 5: Diglycolamic acid anchored on polyamine resin for the mutual separation of Eu(III) and Am(III)

This chapter describes the evaluation of diglycolamic acid anchored polyamine resin, PA-DGAH for the mutual separation of lanthanides and actinides. The effect of various parameters such as the duration of equilibration, concentrations of nitric acid, europium ion and diethylenetriaminepentaacetic acid (DTPA) in aqueous phase, on the distribution coefficient (K_d) of Am(III) and Eu(III) on PA-DGAH was studied and the results are discussed in this chapter. The conditions needed for efficient separation of americium(III) from europium(III) was optimized using DTPA and the results are discussed in this chapter.

5.1. Introduction

Methods based on solvent extraction have been extensively investigated for the mutual separation of lanthanides and actinides [1-7]. In contrast to this, the studies on the mutual separation of lanthanides and actinides using solid phase extraction are very limited. This is essentially due to the lack of availability of adsorbents suitable for lanthanide-actinide separation. Linking of ligands on a polymeric matrix could avoid the loss of ligands normally encountered in extraction chromatography and solvent extraction procedures. In fact, solid phase extraction methods are more suitable for the separation of small concentration of actinides from the feed solution, as in the present case [8-11]. However, extensive studies have been reported in literature on the separation of toxic heavy metal ions from wide variety of aqueous feeds using solid phase extraction [12-15]. In addition, solid phase adsorbents have also been employed for the separation of actinides from aqueous solutions [16-21]. For instance, Sabbarwal *et al.* [16] studied the extraction behavior of U(VI) and Pu(IV) from nitric acid medium on phosphinic acid anchored resins. Maheswari *et al.* [19] synthesized p-amino-N,N-dihexyl-acetamide anchored resin and studied the extraction behavior of U(VI) from nitric acid medium. Robert Selvan *et al.* [21] reported oxy-acetamide anchored Merrifield resin for the separation of trivalent actinides and lanthanides from nitric acid medium. However, the studies on the mutual separation of lanthanides and actinides by solid phase adsorbents are very limited. In this context, a diglycolamic acid anchored polymeric resin (PA-DGAH) for the mutual separation of lanthanides and actinides has been studied. Details of the synthesis and characterization of PA-DGAH are discussed in section 2.3.4 of chapter 2.

5.2. Kinetics of extraction

Rate of uptake of Am(III) (or Eu(III)) was studied by equilibrating 0.05 g of adsorbent with 10 mL of nitric acid (0.001 M to 0. 1 M), spiked with^{241}Am(III) tracer (or $^{(152+154)}$Eu(III) in the case of Eu(III) study). Separate experiments were performed for 5 minutes to 360 minutes. Aliquots were drawn from the aqueous phase before and after equilibration. From the initial activity and the activity measured at various intervals of time the percentage of Am(III) (or Eu(III)) extracted was calculated. The rate of uptake of Am(III) and Eu(III) by PA-DGAH at various pH values is shown in figure 5.1. It can be seen that the percentage of extraction of Am(III) and Eu(III) increases with increase in the duration of equilibration. After four hours of equilibration, the changes in percentage of extraction of Am(III) and Eu(III) in PA-DGAH are insignificant. Therefore, for all extraction studies the resin and aqueous phases were equilibrated for about seven hours to ensure equilibrium was established. A couple of models have been considered for fitting the kinetics of extraction. They are the pseudo-first order model and the pseudo-second order model. Equation for pseudo-first order model and pseudo-second order model are showed in equation 5.1 and 5.2. Detailed derivations of these equations are provided in section 2.4.2.2 of experimental section.

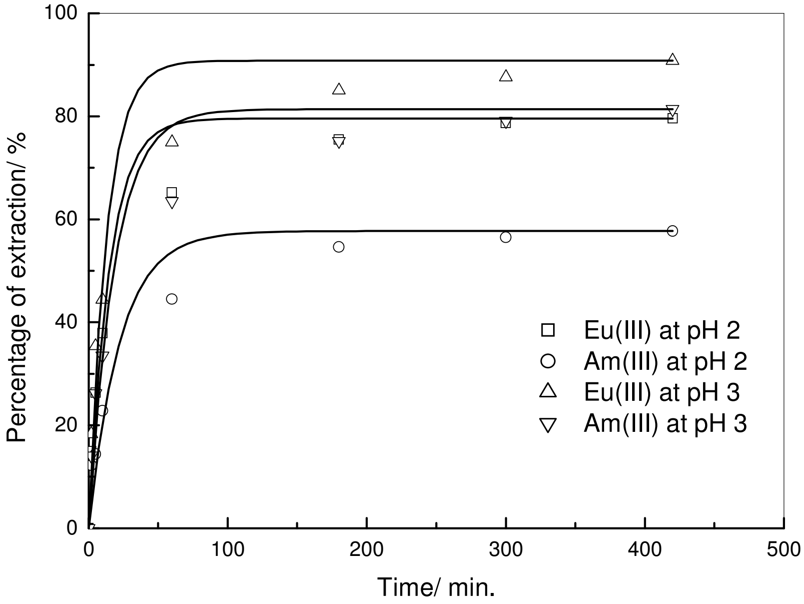

Figure 5.1. Variation in the percentage extraction of Eu(III) and Am(III) as a function of time, fitted by using pseudo-first order rate equation. Adsorbent phase: PA-DGAH (0.05 g), Aqueous Phase: HNO_3 (10 mL) at pH 2 and 3, spiked with $^{(152+154)}$Eu(III) or ^{241}Am(III) tracer.

$$q_t = q_e\left(1 - e^{-k_1 t}\right) \tag{5.1}$$

$$q_t = \frac{q_e^{2}\, k_2\, t}{1 + q_e\, k_2\, t} \tag{5.2}$$

Non linear regression of the experimental data using equation 5.1 and 5.2 results in a determination of rate constants k_1 and k_2. The fitting of the experimental kinetic data using equation 5.1 is shown in figure 5.1 and that using equation 5.2 is shown in figure 5.2. The fitting constants and statistical parameters are tabulated in table 5.1. The R^2 values are more and χ^2 values are low for second order fitting. This indicates that the data were described well by the pseudo-second order rate equation 5.2 (figure 5.2). From table 5.1, it can be seen that the rate constants (k_1 and k_2) increase with increase of pH and the magnitude of rate constant is more for Eu(III) extraction. This could be due to the strong affinity of O-donor ligand (present in PA-DGAH) towards the hard acid metal ion Eu(III) as compared to Am(III) ion [26].

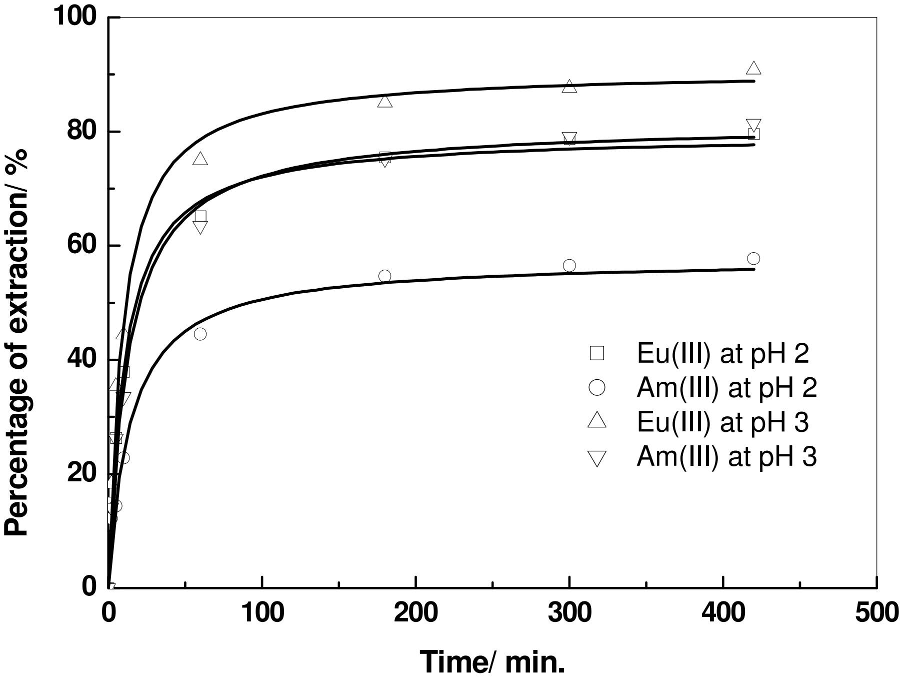

Figure 5.2. Variation in the percentage extraction of Eu(III) and Am(III) as a function of time, fitted by using pseudo-second order rate equation. Adsorbent phase: PA-DGAH (0.05 g), Aqueous Phase: HNO_3 (10 mL) at pH 2 and 3, spiked with $^{(152+154)}$Eu(III) or ^{241}Am(III) tracer.

Table 5.1. Rate constants (k_1 and k_2) obtained by non-linear regression of the kinetics of extraction using equations 5.1 and 5.2.

Metal ion	**k_1/ min^{-1}.**						**k_2/ L. mol^{-1}. min^{-1}.**					
	pH 2 /10^{-2}	**χ^2**	**R^2**	**pH 3** /10^{-2}	**χ^2**	**R^2**	**pH 2** /10^{-3}	**χ^2**	**R^2**	**pH 3** /10^{-3}	**χ^2**	**R^2**
Eu(III)	6.8	32.14	0.9676	7.7	50.60	0.9584	1.2	2.84	0.9971	1.2	6.32	0.9948
Am(III)	4.4	23.06	0.9568	5.3	48.81	0.9524	1.0	5.53	0.9896	0.9	0.99	0.9936

5.3. Extraction of Am(III) and Eu(III) in PA-DGAH.

Distribution coefficients of the metal ions Eu(III) or Am(III) were determined by equilibration experiments (please see section 2.4.2.1 of chapter 2). The method involved equilibration of 0.05 g of the adsorbent with 10 mL of the aqueous phase (nitric acid at concentration varied from 0.001 M to 0.5 M) spiked with the corresponding radiotracers (~10^{-4} M of ^{241}Am tracer was used for Am(III) and $^{(152+154)}$Eu tracer was used for Eu(III)) in 20 mL stoppered test-tubes. The variation in the distribution coefficient of Am(III) and Eu(III) as a function of nitric acid concentration is shown in figure 5.3. The adsorbent PA-DGAH is a cation exchanger. It can been seen that the distribution coefficient of both metal ions decreases with increase in the concentration of nitric acid, indicating the involvement of cation exchange mechanism operating for the extraction of these metal ions in PA-DGAH. Therefore, extraction of Am(III) or Eu(III) by PA-DGAH is expected to release 3 moles of H^+ ions for the extraction of a mole of trivalent metal ion, according to equation 5.3, shown below.

$$\mathrm{M^{3+}_{eq} + 3\,PA\text{-}DGAH_{sor} \Leftrightarrow \{(PA\text{-}DGA)_3M\}_{sor} + 3\,H^+_{aq}} \tag{5.3}$$

where $PA\text{-}DGAH_{sorb}$ is the adsorbent phase and the $PA\text{-}DGA$ is the proton dissociated form of the adsorbent. The equilibrium constant for the above reaction is given by

$$K = \frac{a_{\{(PA-DGA)_3M\}_{sor}}\ \mathrm{a}^3_{\mathrm{H^+_{aq}}}}{\mathrm{a}_{\mathrm{M^+_{aq}}}\ \ \mathrm{a}^3_{\mathrm{(PA\text{-}DGAH)}_{sor}}} \tag{5.4}$$

However for very dilute solutions as in the present case $a_{M(NO_3)_3} = [\mathrm{M(NO_3)}_3]$

$$a_{\mathrm{(PA-DGA)_3M}_{sor}} = [(\mathrm{P}A - \mathrm{DGA})_3\mathrm{M}_{sor}]\,\gamma_{\mathrm{(PA-DGA)}_3M_{sor}} \tag{5.5}$$

$$a_{\mathrm{(PA-DGAH)}_{sor}} = [\mathrm{P}A - \mathrm{DGAH}]_{\mathrm{sor}}\ \gamma_{\mathrm{(PA-DGAH)}_{sor}} \tag{5.6}$$

Therefore,

$$\mathrm{K} = \frac{[(\mathrm{P}A - \mathrm{DGA})_3\mathrm{M}_{sor}]\,\gamma_{\mathrm{(PA-DGA)}_3M_{sor}}\ \ \mathrm{a}^3_{\mathrm{HNO}_{3_{aq}}}}{[\mathrm{M(NO_3)_3}][\mathrm{P}A - \mathrm{DGAH}]^3_{\mathrm{sor}}\ \gamma^3_{\mathrm{(PA-DGAH)}_{sor}}} \tag{5.7}$$

$$K = K' \frac{\left[(PA-DGA)_3 M_{sor}\right] \; a^3_{HNO_{3aq}}}{\left[M(NO_3)_3\right]\left[PA-DGAH\right]^3_{sor}} \tag{5.8}$$

where $K' = \dfrac{\gamma_{(PA-DGA)_3 M_{sor}}}{\gamma^3_{(PA-DGAH)_{sor}}}$ and $K_d = \dfrac{\left[(PA-DGA)_3 M_{sor}\right]}{\left[M(NO_3)_3\right]}$

Therefore, $$K = K' \frac{K_d \; a^3_{HNO_{3aq}}}{\left[PA-DGAH\right]^3_{sor}} \tag{5.9}$$

Since the amount of PA-DGAH taken for equilibration is constant, the variation of K_d with H^+ ion in aqueous phase is given by equation 5.10.

$$\log K_d = \log K_2 - 3 \log a_{HNO3aq} \tag{5.10}$$

where $K_2 = \dfrac{K\left[PA-DGAH\right]^3_{sor}}{K'}$ is a constant.

Therefore, the logarithmic plot of K_d against $a_{H^+_{aq}}$ should result in a straight line with a slope of -3. The variation of K_d against $a_{H^+_{aq}}$ is shown in figure 5.3. Linear regression analysis of the extraction data results in a slope of -2 for both Eu(III) and Am(III) extraction in PA-DGAH, instead of the expected slope of -3. This indicates that PA-DGAH releases two moles of H^+ ions for the extraction of a mole of Eu(III) or Am(III). However, the observed slope of -2 is similar to the extraction behavior of Am(III) and Eu(III) reported in the solution of diglycolamic acid present in *n*-dodecane by solvent extraction mode [see section 3.4 of chapter 3]. It was reported that trivalent metal ions extraction in diglycolamic acid results in the co-extraction of nitrate from the aqueous phase. Accordingly, the extraction of Am(III) and Eu(III) in PA-DGAH could be represented as

$$M^{3+}_{eq} + NO^-_{aq} + 2\,PA\text{-}DGAH_{sor} \Leftrightarrow \left\{(PA\text{-}DGA)_2 M(NO_3)\right\}_{sor} + 2\,H^+_{aq} \tag{5.11}$$

To confirm the participation of nitrate ion and the validity of equation 5.11, the effect of sodium nitrate in aqueous phase on the extraction of Am(III) and Eu(III) was studied. The results on the variation of K_d as a function of activity of sodium nitrate is shown in figure 5.4. It can be seen that the distribution coefficient of Am(III) and Eu(III) increases with increase in the concentration of sodium nitrate, indicating participation of nitrate ion in the extraction. Linear regression analysis of the extraction data results in the slope of 1, confirms the validity of equation 5.11, for the extraction of Am(III) and Eu(III) in PA-DGAH [26].

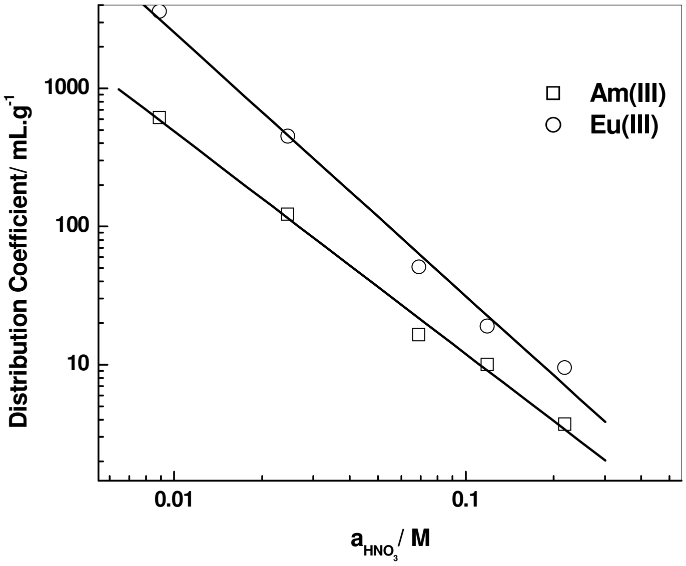

Figure 5.3. Variation in the distribution coefficients of Am(III) and Eu(III) as a function of concentrations of HNO_3. Adsorbent phase: PA-DGAH (0.05 g), Aqueous phase: Nitric acid at various concentrations (10 mL), spiked with $^{(152+154)}$Eu(III) or ^{241}Am(III) tracer.

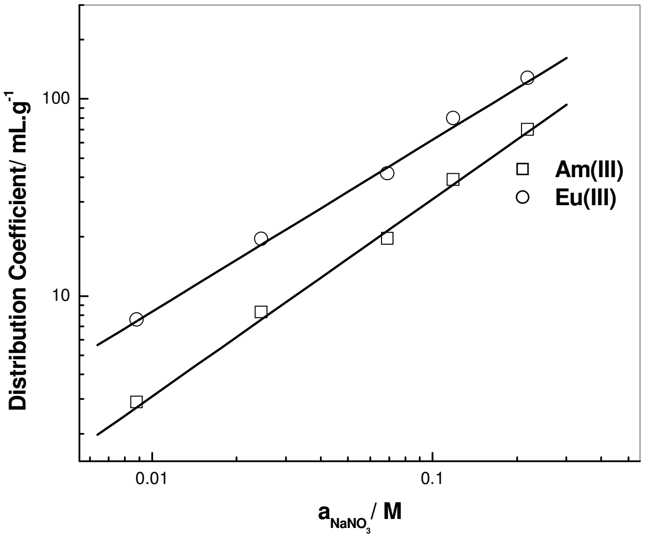

Figure 5.4. Variation in the distribution coefficient of Am(III) and Eu(III) as a function of concentrations of $NaNO_3$. Adsorbent phase: PA-DGAH (0.05 g), Aqueous phase: Sodium nitrate at various concentrations (10 mL), spiked with $^{(152+154)}$Eu(III) or ^{241}Am(III) tracer.

5.4. Extraction isotherm

Eu(III) adsorption capacity of PA-DGAH was measured by equilibrating 0.05 g of the adsorbent with 10 mL of nitric acid solution containing various quantities of europium nitrate spiked with $^{(152+154)}$Eu(III) tracer, for two hours. Aliquots were collected from the aqueous phase before and after extraction. The amount of Eu(III) sorbed was measured from the initial and final activity values. The extraction isotherm of Eu(III) in PA-DGAH is shown in figure 5.5. The loading of Eu(III) in PA-DGAH increases with increase in the amount of Eu present in the aqueous phase. The loading of Eu(III) also increases with increase of pH of aqueous phase. The experimental data can be fitted to Langmuir [23] or Freundlich [24, 25] isotherms of the form given by equation 5.12 and 5.13 respectively.

$$q_{sor} = \frac{K_L\, b\, q_{sol}}{1 + K_L\, q_{sol}} \tag{5.12}$$

$$q_{sor} = K_F\, [q_{sol}]^{\beta} \tag{5.13}$$

where q_{sol} is the amount of Eu(III) present in aqueous phase at equilibrium (in mg/L), q_{sor} is the amount of metal ion loaded in adsorbent phase at equilibrium (in mg/g), K_L (in L/mg) and K_F (in L/g) are the Langmuir and Freundlich constants, b is the apparent extraction capacity (in mg/g) and β (0 < β <1) is a measure of heterogeneity of the adsorbent [24]. The Langmuir and Freaundlich constants can be related to the energy of adsorption and therefore it is regarded as the measure of affinity of the metal ion towards the adsorbent. When β=1, the adsorbent is said to be homogeneous and all the adsorption sites are indistinguishable with respect to energy of adsorption. From Langmuir adsorption isotherm (equation 5.12), it can be shown that $q_{sorb} \to b$ at high concentration of metal ions in aqueous phase, that is at high q_{sol} values. Non-linear regression of the experimental data using equation 5.12 and 5.13 are shown in figure 5.5. The regression coefficients and χ^2 values are tabulated in table 5.2. Based on the χ^2 and R^2 values, it can be seen from figure 5.5 that the experimental data are described well by Langmuir adsorption isotherm. From Langmuir fitting the apparent extraction capacity of Eu(III) in PA-DGAH was determined to be 27.6 mg/g and 12 mg/g at pH 3 and 2 respectively [26].

Table 5.2. Apparent extraction capacity of Eu(III), Langmuir and Freundlich constants obtained by non-linear regression of the extraction data using equations 5.12 and 5.13.

Feed condition	Fitting models							
	Langmuir				Freundlich			
	b/ mg.g^{-1}	K_L/ L.mg^{-1}	χ^2	R^2	β/ mg.g^{-1}	K_F/ L.mg^{-1}	χ^2	R^2
pH 2	12.3	0.01	0.51	0.9696	0.40	0.91	0.08	0.9951
pH 3	27.6	0.013	0.87	0.9912	0.41	2.0	5.26	0.9473

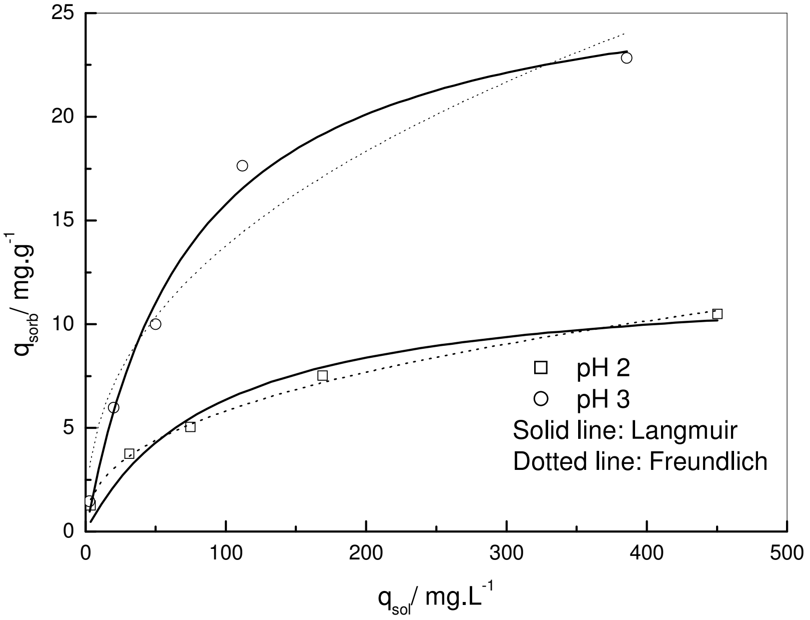

Figure 5.5. Langmuir and Freundlich adsorption isotherms for the extraction of Eu(III) from nitric acid medium. Adsorbent phase: PA-DGAH (0.05 g), Aqueous Phase: Europium nitrate (10 mL) at pH 2 and 3, spiked with $^{(152+154)}$Eu(III) tracer.

5.5. Effect of DTPA and separation factor

DTPA is an aqueous soluble N-donor ligand preferentially complexes with Am(III) and retains Am(III) in aqueous phase as compared to Eu(III) during extraction. The use of DTPA as aqueous complexing agent for increasing the separation factor of Eu(III) over Am(III) has been reported by several researchers [2, 3]. Figure 5.6 shows the distribution coefficient of Eu(III) and Am(III) in PA-DGAH at pH 3. In the absence of DTPA the separation factor (quotient of K_d of Eu(III) and K_d of Am(III)) achieved for the extraction of these metal ions is very small (~4 to 5). The distribution coefficient of both the metal ions decreases with increase in the concentration of DTPA. However, the distribution coefficient of Am(III) decreases more, since Am(III) forms a stronger complex with N-donor DTPA. This results in the increase of separation factor of Eu(III) over Am(III) with the increase in the concentration of DTPA. The separation factor increases from ~4 in the absence of DTPA to the value of 45 at DTPA concentration of 0.05 M. Further increase in DTPA concentration does not change the separation factor to any significant extent. Therefore, it is desirable to use 0.03 to 0.05 M DTPA for the separation of Eu(III) from Am(III) from dilute nitric acid medium [26].

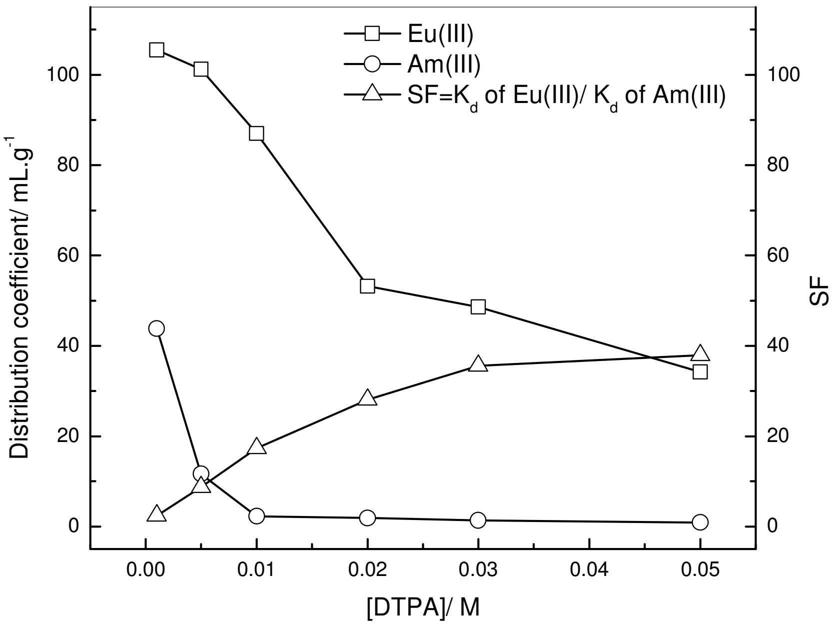

Figure 5.6. Variation in the distribution coefficients of Am(III) and Eu(III) as a function of concentrations of DTPA. Adsorbent phase: PA-DGAH (0.05 g), Aqueous phase: DTPA at various concentrations (10 mL), spiked with $^{(152+154)}$Eu(III) or ^{241}Am(III) tracer, at pH 3.

5.6. Effect of other trivalent lanthanide ions

Since the actual feed solution for lanthanide-actinide separation is composed of some other lanthanides (Ln(III)) also in addition to Eu(III), the distribution coefficients of some lanthanides in PA-DGAH at pH 3 was also determined. The distribution coefficients of Ln(III) are shown in figure 5.7. It can be seen that, the distribution coefficients of lanthanides increase from lanthanum to dysprosium. This could be due to the enhanced complexation of the ligand (PA-DGAH) towards lanthanides from La to Dy [27]. The lanthanide contraction decreases the ionic radii of trivalent lanthanides from La(III) to Dy(III) [26]. This increases the ionic potential (charge to radius ratio) of lanthanides from La(III) to Dy(III) and therefore the hard acid nature of lanthanides. Since the ligand (PA-DGAH) co-ordinates with lanthanides through oxygen donor, the distribution coefficient of lanthanides in PA-DGAH increases from Ln(III) to Dy(III). A similar extraction trend was also reported by several other researchers [28].

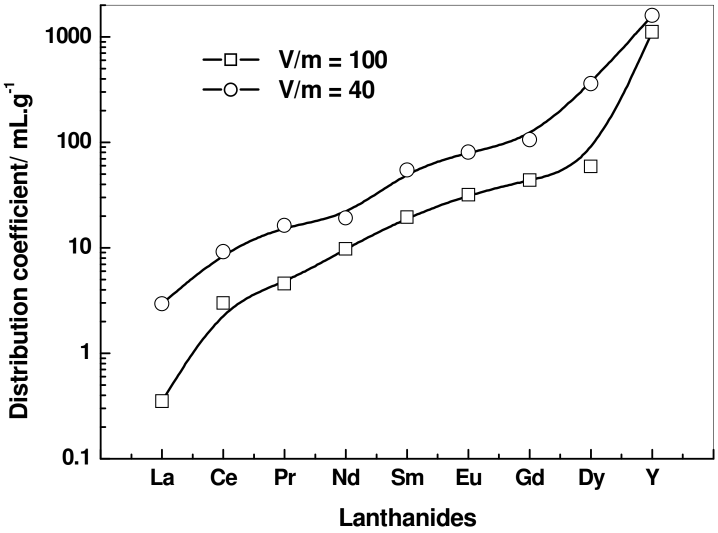

Figure 5.7. Variation in the distribution coefficient of lanthanides in PA-DGAH. Adsorbent phase: PA-DGAH (0.35 g for V/m 100 and 0.87 g for V/m 40), Aqueous phase: HNO_3 (35 mL) at pH 3 containing 0.1 g/L of each lanthanide elements.

5.7. Conclusions

A new Diglycolamic acid (PA-DGAH) anchored polyamine resin was prepared and studied for the extraction of americium(III) and europium(III) from dilute nitric acid medium. Pseudo-second order rate of extraction of Am(III) and Eu(III) was observed in

PA-DGAH and the rate constant (k_2) was determined to be 10^{-3} L.mol^{-1}.min^{-1}. The extraction equilibrium was established in four hours. The distribution coefficient of Am(III) and Eu(III) decreased with increase in the concentration of nitric acid. The slope analysis of extraction data, indicated the release of two H^+ ions for the extraction of a trivalent metal ion. The extraction was also accompanied by co-extraction of nitrate from aqueous phase. The concentration of DTPA needed for efficient separation of Am(III) from Eu(III) was optimized to be 0.03 to 0.05 M at pH 3. The study confirmed the feasibility of separating Am(III) from Eu(III) with a separation factor of ~45 by using PA-DGAH.

5.8. References

1. G.J. Lumetta, A.V. Gelis, J.C. Carter, C.M. Niver, M.R. Smoot, The actinide-lanthanide separation concept, Solvent Extr. Ion Exch. 32 (2014) 333-347.
2. K.L. Nash,The chemistry of TALSPEAK: a review of the science, Solvent Extr. Ion Exch. 33 (2015) 1-55.
3. T.S. Grimes, R.D. Tillotson, L. R. Martin. Trivalent lanthanide/actinide separation using aqueous-modified TALSPEAK chemistry, Solvent Extr. Ion Exch. 32 (2014) 378-390.
4. A. V. Gelis, G.J. Lumetta, Actinide Lanthanide Separation Process, ALSEP, Ind. Eng. Chem. Res. 53 (2014) 1624-1631.
5. A.T. Johnson, K.L. Nash, Mixed monofunctional extractants for trivalent actinide/lanthanide separations: TALSPEAK-MME. Solvent Extr. Ion Exch. 33 (2015) 642-655.
6. H.H. Dam, D.N. Reinhoudt, W. Verboom, Multicoordinate ligands for actinide/lanthanide separations, Chem. Soc. Rev. 36 (2007) 367-385.

7. C. Ekberg, A. Fermvik, T. Retegan, G. Skarnemark, M.R.S Foreman, M.J. Hudson, S. Englund, M. Nilsson, An overview and historical look back at the solvent extraction using nitrogen donor ligands to extract and separate An(III) from Ln(III), Radiochim. Acta. 96 (2008) 225-233.
8. E.P. Horwitz, R. Chiarizia, H. Diamond, R.C. Gatrone, S.D. Alexandratos, A.Q. Trochimczuk, D.W. Crick, Uptake of metal ions by a new chelating ion-exchange resin. part 1: acid dependencies of actinide ions, Solvent Extr. Ion Exch. 11 (1993) 943 – 966
9. K.N. Sabharwal, PR Vasudeva Rao, M. Srinivasan, Extraction of actinides by bifunctional phosphinic acid resin, Solvent Extr. Ion Exch. 12 (1994) 1085-1101.
10. K.A. Venkatesan, D.K. Patre, K.N. Sabharwal, T.G. Srinivasan, P.R. Vasudeva Rao, Kinetics of uranium extraction by macroporous bifunctional phosphinic acid resin, Solvent Extr. Ion Exch. 18 (2000) 551 – 565.
11. R. Chiarizia, E.P. Horwitz, K.A. D'Arcy, S.D. Alexandratos, A.W. Trochimzuk, Uptake of Actinides and other Ions by Dipiosil, A New Silica based Chelating Ion Exchange Resin in Ion Exchnge Developments and Applications, Ed. J.A. Greig. Proceedings of IEX, The Royal Society of Chemistry, UK, 1996, p 321
12. P. Bingjun, B. Pan, W. Zhang, L. Lv, Q. Zhang, S. Zheng, Development of polymeric and polymer-based hybrid adsorbents for pollutants removal from waters, Chem. Eng. J. 151 (2009) 19-29.
13. M. Chanda, K. F. O'driscoll, G. L. Rempel, Ligand exchange sorption of arsenate and arsenite anions by chelating resins in ferric ion form: II. Iminodiacetic chelating resin Chelex 100, React. Polymers, Ion Exchangers, Sorbents 8 (1988) 85-95.

14. Y., Erdem, B. F. Senkal, N. Bicak, Poly (acrylamide) grafts on spherical polyvinyl pyridine resin for removal of mercury from aqueous solutions, React. Funct. Polym. 65 (2005) 121-125.
15. B.B. Adhikari, M. Kanemitsu, H. Kawakita, K. Ohto, Synthesis and application of a highly efficient polyvinylcalix [4] arene tetraacetic acid resin for adsorptive removal of lead from aqueous solutions, Chem. Eng. J. 172 (2011) 341-353.
16. K.N. Sabharwal, PR. Vasudeva Rao, M. Srinivasan, Extraction of actinides by bifunctional phosphinic acid resin, Solvent Extr. Ion Exch. 12 (1994) 1085-1101.
17. K.A.Venkatesan, D.K. Patre, K.N. Sabharwal, T.G. Srinivasan, P.R. Vasudeva Rao, Kinetics of uranium extraction by macroporous bifunctional phosphinic acid resin, Solvent Extr. Ion Exch. 18 (2000) 551 – 565.
18. R. Chiarizia, E.P. Horwitz, K.A. D’Arcy, S.D. Alexandratos, A.W. Trochimzuk, Uptake of Actinides and other Ions by Dipiosil, A New Silica based Chelating Ion Exchange Resin in Ion Exchnge Developments and Applications, Ed. J.A. Greig. Proceedings of IEX, The Royal Society of Chemistry, UK, 1996, p 321
19. M. A. Maheswari, M. S. Subramanian, Amide Grafted Amberlite XAD-16 Polymer for the Selective and Sequential Separation of U (VI) and Th (IV) from Acidic Waste Effluents, Solvent Extr. Ion Exch. 23 (2005) 249-263.
20. Q. Cao, Y. Liu, C. Wang, J. Cheng, Phosphorus-modified poly (styrene-co-divinylbenzene)–PAMAM chelating resin for the adsorption of uranium (VI) in aqueous, J.Hazard. Mater. 263 (2013) 311-321.
21. B. Robert Selvan, T. Prathibha, K. A. Venkatesan, M. P. Antony, and P. R. Vasudeva Rao, A new 2-oxy-N, N-dioctylacetamide grafted resin for the separation of trivalent actinides from nitric acid medium, Radiochim. Acta 103 (2015) 91-99.

22. D.J. Chaiko, G.F. Vandegrift, A thermodynamic model of nitric acid extraction by tri-n-butyl phosphate. Nucl. Tech. 82 (1988) 52-59.
23. E.H Smith, Modeling batch kinetics of cadmium removal: by a recycled iron adsorbent, Sep. Sci. Technol. 33 (1998) 149-168.
24. G. Sposito, Derivation of the Freundlich equation for ion exchange reactions in soils, Soil Sci. Soc. Am. J. 44 (1980) 652-654.
25. K.A. Venkatesan, T. G. Srinivasan, and P. R Vasudeva Rao, Cobalt-extraction studies on dithiocarbamate grafted on silica gel surface, Colloids Surf., A 180 (2001) 277-284.
26. A.S. Suneesh, K.V. Syamala, K.A. Venkatesan, M.P. Antony, P.R. Vasudeva Rao, Diglycolamic acid anchored on polyamine matrix for the mutual separation of Eu (III) and Am (III), Radiochim. Acta 104 (2016) 11-21.
27. G.G.S. Subrahmanian, K. V. Syamala, A.S. Suneesh, K.A. Venkatesan, M.P. Antony, Extraction behavior of lanthanides in diglycolamic acid functionalized-polyamine matrix, In: Emerging Trends in Separation Science and Technology (SESTEC-2016), IIT Guwahati, India, May 17-21, 2016, A.C.Deb, S. Sodaye, M.S.Murali, T. Banarjee, P.K. Mohapatra, K.L.Ramakumar (eds), pp-58
28. K. Shimojo, H. Naganawa, J. Noro, F. Kubota, M. Goto, Extraction behavior and separation of lanthanides with a diglycol amic acid derivative and a nitrogen-donor ligand, Anal. Sci. 23 (2007) 1427-1432. 8.

Chapter 6: Silica functionalized diglycolamic acids for Ln(III)-An(III) mutual separation

This chapter deals with the development of a novel silica functionalized adsorbent, silica diglycolamic acid (Si-DGAH) for the mutual separation of Eu(III) and Am(III). The effect of various parameters such as duration of equilibration, concentrations of nitric acid, europium ion and diethylenetriamine-pentaacetic acid (DTPA) in aqueous phase on the distribution coefficient (K_d) of Am(III) and Eu(III) on Si-DGAH was studied. The conditions needed for efficient separation of americium(III) from europium(III) were optimized using DTPA.

6.1. Introduction

Inorganic oxides such as silica gel can be tuned to task specific adsorbent by modifying the surface of silica gel with the specific organic compounds that can form a strong complex with metal ion of interest [1-6]. These organofunctionalized inorganic materials (OFIM) form a strong co-ordinate complex with target metal ions. Thus the selectivity and extractability would be expected to be higher for OFIMs. These organo functionalized inorganic adsorbents are extremely proven candidates for the selective separation of toxic and radiotoxic metal ions [7-14]. OFIM offers advantages such as simple method of operation, robustness, regenerating ability, and improved radiation and chemical stability. The concept of surface modification of the co-polymer existed since the very early development of ion exchange resins [15-17]. The advantage of linking the metal ion specific ligands on to the polymer matrix generally prevents the loss of extractant encountered in solvent extraction and extraction chromatography procedures. The OFIMs are superior adsorbents than polymeric or organic adsorbents. This is due to the fact that employment of the organic solid supports for the treatment of aqueous wastes suffers from the drawbacks such as swelling, and chemical degradation [4, 5] etc. In fact, this problem is more severe during the treatment of radioactive wastes, where the organic matrix undergoes radiolysis leading to extensive degradation of resin [18, 19]. Another advantage of using inorganic solid support over organic is that it can be vitrified or ceramized to unleachable solid form for final disposal of spent radioactive solid supports [20]. Grafting the metal ion specific ligands on to the inorganic solid supports involves carrying out organomodification on the surface of the silica gel to covalently link the task-specific moieties on silica gel. The adsorbent prepared in this method contains 5-10% of organics on the inorganic matrix. Thus, the silica support containing diphosphonic acid groups, called as Diphosil, was developed by Chiarizia *et.al* [21] and studied for the separation of actinides from acidic solution. Naturally occurring organic materials such as humic and fulvic acid was attached to silica by Bulman *et.al* [22] and the potential of this material to extract transuranium elements from acidic solution was demonstrated.

Venkatesan *et al.* studied the removal of Hg(II) and radiocobalt from aqueous waste solutions using dithiocarbamate grafted on silica gel (Si-dtc) [23, 24]. The organomodified adsorbent, Si-dtc, showed excellent selectivity for the separation of mercury from aqueous wastes containing wide-variety of ligands. Venkatesan *et al.* [25] also prepared a silica gel grafted with organic complexing moieties such as amine, amide and benzamide functional groups and studied for the extraction of uranium from aqueous solution. Their studies clearly indicated that the amine grafted silica gel was well suited for the pre-concentration of uranium from neutral and carbonate solution containing large amount of sodium ion, especially for the recovery of uranium from sea water.

In this chapter, we report the synthesis of diglycolamic acid functionalized silica gel (Si-DGAH) for the separation of Am(III) and Eu(III) from aqueous nitric acid medium, for the first time. The effect of various parameters such as duration of equilibration, concentrations of nitric acid, europium ion and diethylenetriamine-pentaacetic acid (DTPA) in aqueous phase on the distribution coefficient (K_d) of Am(III) and Eu(III) on Si-DGAH was studied. The conditions needed for efficient separation of americium(III) from europium(III) were optimized using DTPA. Detailed synthetic scheme for the preparation of Si-DGAH is described in section 2.3.5 of chapter 2. Structure of Si-DGAH is showed in figure 6.1.

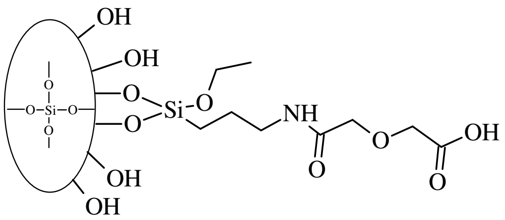

Figure 6.1. Structure of Si-DGAH

6.2. Rate of adsorption of Am(III) and Eu(III)

The kinetics of Am(III) (or Eu(III)) adsorption was studied by the batch equilibration of 0.05 g of the adsorbent with 10 ml of nitric acid solution (0.001 M to 0.1 M) spiked with ^{241}Am(III) (or $^{(152+154)}$Eu(III)) tracer at 298 K. The equilibration was stopped at a pre-fixed interval of time. The solution phase radioactivity was measured after equilibration. From the initial activity and the activity measured at various intervals of time the percentage of Am(III) (or Eu(III)) adsorbed was calculated. The rate of uptake of Am(III) and Eu(III) by Si-DGAH at different concentrations of nitric acid is shown in figure 6.2. Rapid adsorption of Am(III) or Eu(III) is observed in the initial stages of equilibration followed by the establishment of equilibrium occurring within 30 minutes.

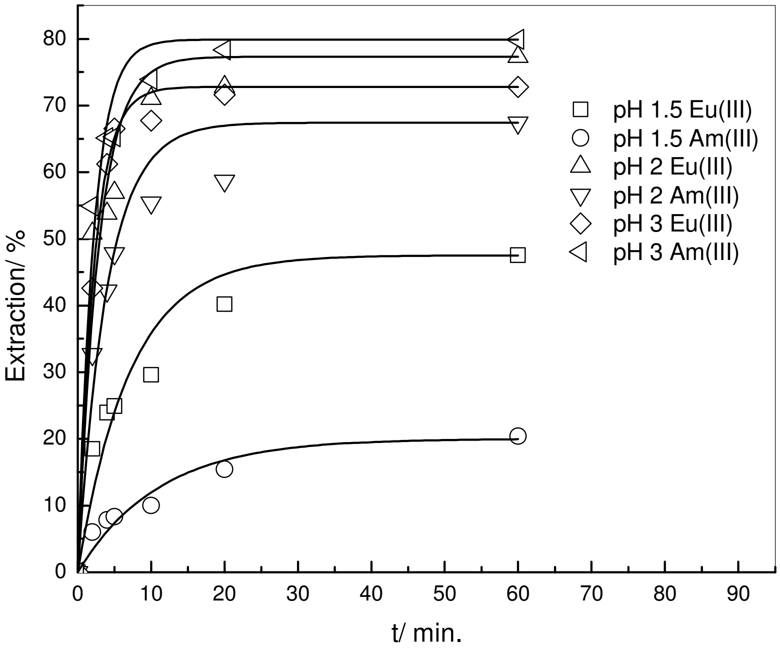

Figure 6.2. Variation in the percentage extraction of Eu(III) and Am(III) as a function of time, fitted with pseudo-first order rate equation. Adsorbent phase: Si-DGAH (0.05 g), Aqueous phase: HNO$_3$ at pH 1.5,2 and 3, spiked with $^{(152+154)}$Eu(III) or ^{241}Am(III) tracer.

A couple of models have been considered for fitting the kinetics of extraction. They are the pseudo-first order model and the pseudo-second order model. Equation for pseudo-first order model and pseudo-second order model are showed in equation 6.1 and 6.2. Detailed derivations of these equations are provided in section 2.4.2.1 of experimental section.

$$q_t = q_e\left(1 - e^{-k_1 t}\right) \tag{6.1}$$

$$q_t = \frac{q_e^{\,2}\, k_2\, t}{1 + q_e\, k_2\, t} \tag{6.2}$$

Non linear regression of the experimental data using equation 6.1 and 6.2 results in a determination of rate constants k_1 and k_2. The fitting of the experimental kinetic data using equation 6.1 is shown in figure 6.2 and that using equation 6.2 is shown in figure 6.3. The fitting constants and statistical parameters are tabulated in table 6.1 and table 6.2. The R^2 values are more and χ^2 values are low for second order fitting. This indicates that the data were described well by the pseudo-second order rate equation 6.2 (figure 6.3). From table 6.1, it can be seen that the rate constants (k_1 and k_2) increase with increase of pH and the magnitude of rate constant is more for Eu(III) extraction. This could be due to the strong affinity of O-donor ligand (present in Si-DGAH) towards the hard acid metal ion Eu(III) as compared to Am(III) ion.

Table 6.1. Rate constant (k_1) of sorption of Eu(III) and Am(III) fitted using the equation 6.1

Metal ion	**k_1/ min^{-1}.**								
	pH 1.5	**χ^2**	**R^2**	**pH 2**	**χ^2**	**R^2**	**pH 3**	**χ^2**	**R^2**
Eu(III)	0.1405	23.75	0.8028	0.3507	40.81	0.9405	0.4504	3.71	0.9941
Am(III)	0.0908	3.38	0.8876	0.2502	24.71	0.9503	0.4605	20.69	0.9703

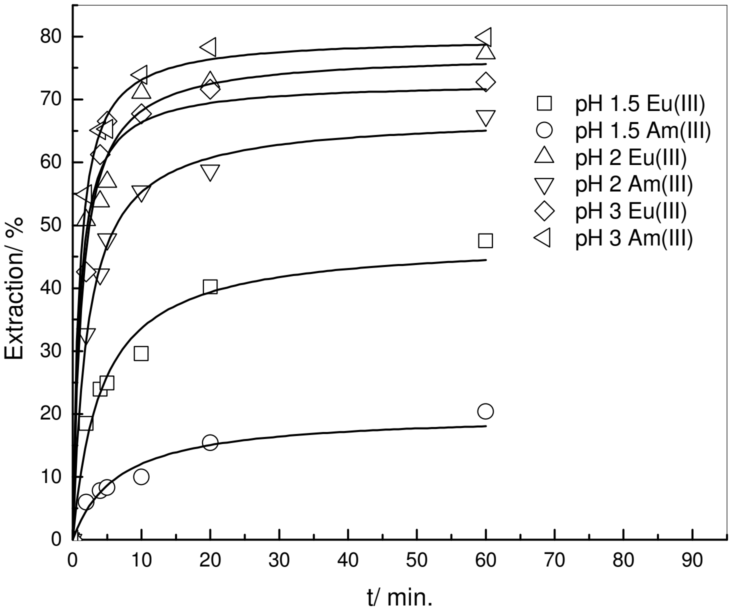

Figure 6.3. Variation in the percentage extraction of Eu(III) and Am(III) as a function of time, fitted with pseudo-second order rate equation (equation 6.2). Adsorbent phase: Si-DGAH (0.05 g), Aqueous phase: HNO_3 at pH 1.5,2 and 3, spiked with $^{(152+154)}$Eu(III) or ^{241}Am(III) tracer.

Table 6.2. Rate constant (k_2) of sorption of Eu(III) and Am(III) fitted using the equation 6.2.

Metal ion	k_2/ L.mol^{-1}.min^{-1}.								
	pH 1.5	χ^2	R^2	pH 2	χ^2	R^2	pH 3	χ^2	R^2
Eu(III)	0.0050	6.11	0.9743	0.0096	10.78	0.9842	0.0141	14.40	0.9789
Am(III)	0.0075	1.97	0.9544	0.0067	2.13	0.9957	0.0134	1.74	0.9974

6.3. Adsorption studies of Am(III) and Eu(III)

In order to test the adsorption behavior of Am(III) and Eu(III) by Si-DGAH, experiments were conducted by equilibrating 0.05 g of adsorbent with 10 mL of aqueous phase spiked with $^{(152+154)}$Eu or ^{241}Am tracer at 298 K. The mixture was taken in a 20 mL capacity stoppered glass-tube and rotated in upside-down rotation (50 rpm) for a specified period of time. The concentration of nitric acid in aqueous phase was varied from 0.001 M to 0.5 M. After 2 hrs of equilibration, an aliquot was taken from aqueous phase and the radioactivity of $^{(152+154)}$Eu or ^{241}Am was measured using a well-type NaI(Tl) scintillation counter. The distribution coefficient (K_d) was computed from the radioactivity measurement of aqueous phase using the method shown in section 2.4.2 chapter 2. The variation in the distribution coefficient of Am(III) and Eu(III) as a function of nitric acid concentration is shown in figure 6.4.

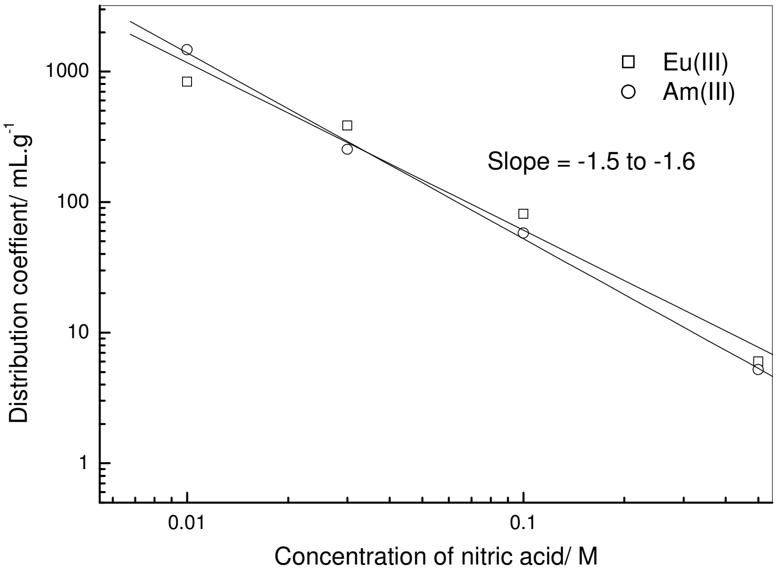

Figure 6.4. Variation in the distribution ratios of Eu(III) and Am(III) as a function of concentrations of HNO_3. Adsorbent phase: Si-DGAH (0.05 g), Aqueous phase: Nitric acid at various concentrations (10 mL), spiked with $^{(152+154)}$Eu(III) or ^{241}Am(III) tracer.

It is observed that the distribution coefficient of both Eu(III) and Am(III) decreases with increase in the concentration of nitric acid, indicating the involvement of cation exchange mechanism. The adsorbent, Si-DGAH, contains acidic functional moieties (-COOH) on the surface of silica gel. Therefore, Si-DGAH is a cation exchanger. If the extraction is governed only by cation exchange mechanism, the sorption of Am(III) and

Eu(III) on Si-DGAH could be represented by the equilibrium reaction shown in equation 6.3.

$$\mathrm{M^{3+}_{aq}} + 3\,\mathrm{Si\text{-}DGAH_{Sor}} \Leftrightarrow \{(\mathrm{Si\text{-}DGA})_3\mathrm{M}\}_{\mathrm{sor}} + 3\,\mathrm{H_{aq}}^{+} \qquad (6.3)$$

where Si-DGAH$_{sor}$ is the adsorbent phase and Si-DGA is the proton dissociated form of the adsorbent. The equilibrium constant for the above reaction is given by

$$\mathrm{K} = \frac{[(\mathrm{Si\text{-}DGA})_3 M]_{\mathrm{sor}}\,[\mathrm{H^+}]^3_{\mathrm{aq}}}{[\mathrm{M^{3+}}]_{\mathrm{aq}}\,[\mathrm{Si\text{-}DGAH}]^3_{\mathrm{sor}}} \qquad (6.4)$$

$$\mathrm{K} = \frac{K_d\,[\mathrm{H^+}]^3_{\mathrm{aq}}}{[\mathrm{Si\text{-}DGAH}]^3_{\mathrm{sor}}} \qquad (6.5)$$

where K$_d$ is defined as $\mathrm{K}_d = \frac{[(\mathrm{Si-DGA})_3\mathrm{M}]_{\mathrm{sor}}}{[\mathrm{M^{3+}}]_{\mathrm{aq}}}$

Since the amount of Si-DGAH taken for equilibration is constant, the variation of K$_d$ with H$^+$ ion in aqueous phase is given by equation 6.6.

$$\log \mathrm{K_d} = \log \mathrm{K_1} - 3 \log [\mathrm{H^+}]_{\mathrm{aq}} \qquad (6.6)$$

where K$_1$ (= K [Si-DGAH]$^3_{sor}$) is a constant. Thus, the logarithmic plot of K$_d$ against [H$^+$]$_{aq}$ should result in a straight line with slope of -3. The variation of K$_d$ as a function of [H$^+$]$_{aq}$ is shown in figure 6.4. Linear regression of the distribution data yields a slope of -1.5 to -1.6 instead of -3 for both the metal ions. This indicates the release of approximately two moles of H$^+$ ions for the extraction of one mole of Am(III) or Eu(III). The behavior observed in the present study is similar to the extraction behavior of Am(III) or Eu(III) reported in a solution of diglycolamic acid present in n-dodecane, in liquid-liquid extraction mode as described in section 2.4 of chapter 3 (see section 3.4). It was learned from chapter 3 that, the extraction of Am(III) and Eu(III) was accompanied by the release of two moles of H$^+$ ions only from diglycolamic acid, and co-extraction of one mole of NO$_3^-$ ions from aqueous phase. Based on those results, the extraction of Am(III) and Eu(III) could be represented by the equilibrium reaction shown in equation 6.7. To confirm the validity of the extraction mechanism shown in equation 6.7, the effect of nitrate ion in aqueous phase on the distribution coefficient of Am(III) was studied and the results are shown in figure 6.5. It can be seen that the K_d of Am(III) increases with increase in the concentration of nitrate ion leading to a slope value of +1.2. This observation confirms the participation of a nitrate ion for the extraction of Am(III) and also confirmed the validity of equation 6.7 for extraction.

$$\mathrm{M}^{3+}_{\mathrm{aq}} + 2\,\mathrm{Si\text{-}DGAH}_{\mathrm{sor}} + \mathrm{NO}^{-}_{3\,\mathrm{aq}} \Leftrightarrow \{\mathrm{M}\,(NO_3)(Si-DGA)_2\}_{sor} + 2\mathrm{H}^{+}_{\mathrm{aq}} \qquad (6.7)$$

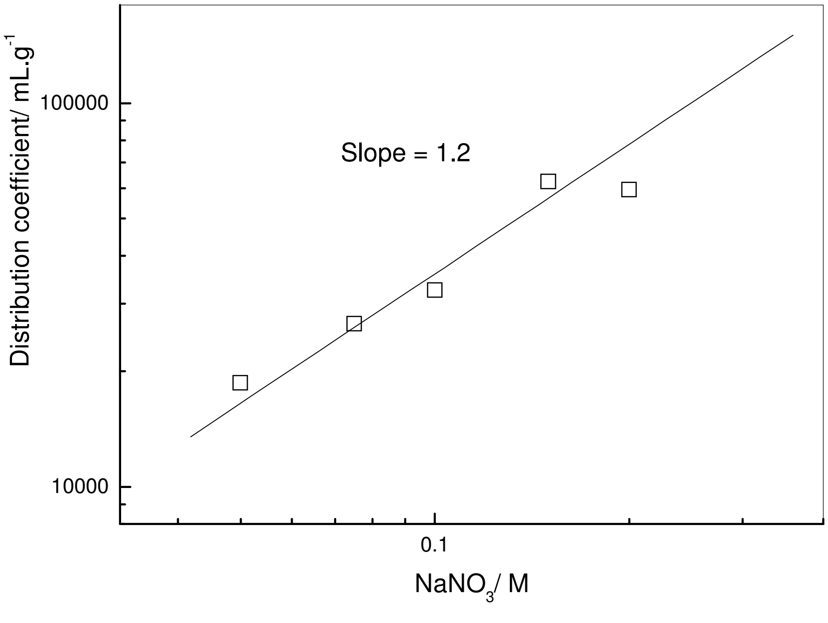

Figure 6.5. Variation in the distribution ratios of Am(III) as a function of concentrations of NaNO$_3$. Adsorbent phase: Si-DGAH (0.05 g), Aqueous phase: sodium nitrate at various concentrations (10 mL), spiked with ^{241}Am(III) tracer.

6.4.Langmuir Adsorption model

Equilibrium isotherm data for the extraction of Eu(III) by Si-DGAH was analysized by Langmuir adsorption model. For this experiment, batch experiments were conducted at 298 K by equilibrating 0.05 g of the adsorbent with 10 mL of nitric acid solution containing various quantities of europium nitrate spiked with $^{152+154)}$Eu(III) tracer. After two hours of equilibration, the initial and final radioactivity was measured and the amount of Eu(III) sorbed was calculated. Amount of Eu(III) adsorbed to Si-DGAH was modelled by linear form of Langmuir adsorption model. The linear form of Langmuir adsorption equation is shown in equation 6.8.

$$\frac{C_f}{C_s} = \frac{1}{K_L\, b} + \frac{C_f}{b} \tag{6.8}$$

where C_f is the equilibrium concentration of metal ion (mg/L), C_s is the amount of metal ion sorbed on Si-DGAH (mg/g), K_L is the Langmuir adsorption constant (L/mg) and b (mg/g) is the sorption capacity. Figure 6.6 shows the plot of C_f/C_s against C_f for the sorption of Eu(III) in Si-DGAH. Linear regression of the extraction data results in a sorption capacity of 4.4 mg/g and Langmuir adsorption coefficient, K_L = 0.0170 L/mg pH 2.

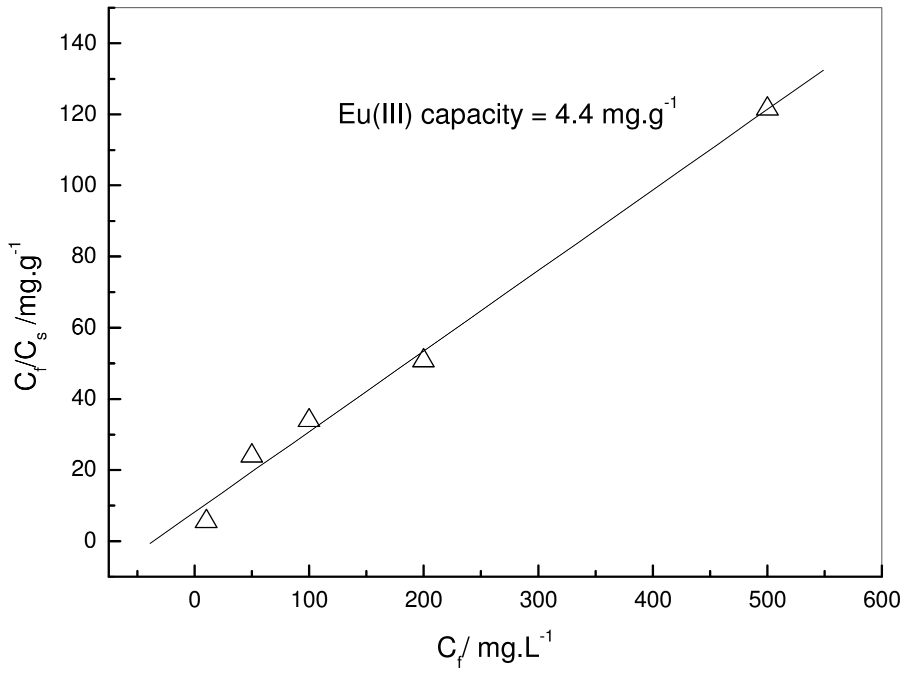

Figure 6.6. Langmuir adsorption isotherm for the sorption of Eu(III) at 298 K. Adsorbent phase: Si-DGAH (0.05 g), Aqueous phase: europium nitrate at pH 2, spiked with $^{(152+154)}$Eu(III) tracer.

6.5. Ion exchange capacity: Column studies

Ion exchange capacity of the adsorbent under dynamic condition was assessed by column chromatography. About 1 g of the adsorbent was initially immersed in water and loaded into a glass column of radius 0.5 cm. The adsorbent bed was conditioned with 50 ml of nitric acid adjusted to pH 3 (or other desired pH). The experimental feed solution was composed of $EuNO_3$ solution (1 mg/mL), spiked with $^{(152+154)}$Eu(III) tracer (50 mL) at a pH of 3 (or other desired pH) was passed at a flow rate of 2 mL/min. The effluent was collected in a 100 mL standard flask. After passing 50 mL of the feed solution, the nitric acid solution at pH 3 (or other desired pH) was also passed in to the column. The effluent was collected in the same flask. From the ratioactivity measurements of the feed and effluent, the amount of Eu(III) sorbed by the Si-DGAH was determined. Table 6.3 shows the Eu(III) sorption capacity of Si-DGAH determined under column conditions at pH 1.5, 2 and 3. It can be seen that the sorption capacity increases from 0.5 mg/g to 44.3 mg/g with the increase of pH from 1.5 to 3. This could be due to the increase in the dissociation of –COOH groups present in Si-DGAH with increase of pH, leading to higher sorption of Eu(III). This result is in good agreement with extraction mechanism shown in equation 6.7. It is interesting to note that the sorption capacity determined by column method at pH 2 (8.2 mg/g) is in close agreement with the sorption capacity determined from Langmuir adsorption isotherm (5 mg/g). The marginal difference in the capacities obtained in these two methods could be due to the efficient sorption of Eu(III) in column method.

Table 6.3. Ion exchange capacity (mg.g^{-1}) of the adsorbent as a function of pH. Amount of the adsorbent loaded: 1 g of Si-DGAH. Feed: 49 mL of EuNO$_3$ (1 mg/mL), spiked with $^{(152+154)}$Eu(III)+50 mL of HNO$_3$ adjusted to desired pH.

Feed solution pH	Ion exchange capacity/ mg.g^{-1}
1.5	0.5
2	8.2
3	44.3

6.6. Effect of DTPA and separation factor.

Figure 6.6 shows the variation of distribution coefficients of Eu(III) and Am(III) as a function of DTPA in Si-DGAH at pH 2. In the absence of DTPA the separation factor (quotient of K_d of Eu(III) and K_d of Am(III)) achieved for the extraction of these metal ions is very small (~1 to 3, not shown in figure 6.7). The TALSPEAK process and several other methods reported in literature [26] employed diethylenetriamminetetraacetic acid (DTPA) as aqueous complexing agent for facilitating the mutual separation of lanthanides and actinides. Since DTPA forms a complex with Am(III) in preference to Eu(III), the studies were carried out in the presence of DTPA to retain Am(III) in the aqueous phase and to enhance the separation factor of Eu(III) over Am(III). Figure 6.7 shows the variation in the distribution coefficient of Eu(III) and Am(III) in Si-DGAH studied as a function of DTPA concentration. As expected the distribution coefficient of both metal ions decreases with increase in the concentration of DTPA. However, the distribution coefficient of Am(III) decreases more. This results in increase in the separation factor of Eu(III) over Am(III) with the increase in the concentration of DTPA. At pH 2, the separation factor increases from ~1 in the absence of DTPA to the value of ~10 at 0.05 M DTPA concentration. Further increase in DTPA concentration lowers the distribution coefficient of both metal ions to a very small value making the adsorbent inextractable. Therefore, it is desirable to use 0.05 M DTPA for the separation of Eu(III) from Am(III) from dilute nitric acid medium with the separation factor of 12. Based on this separation factor, it is quite possible to separate the actinide Am(III) from Eu(III) present in aqueous solution [27, 28].

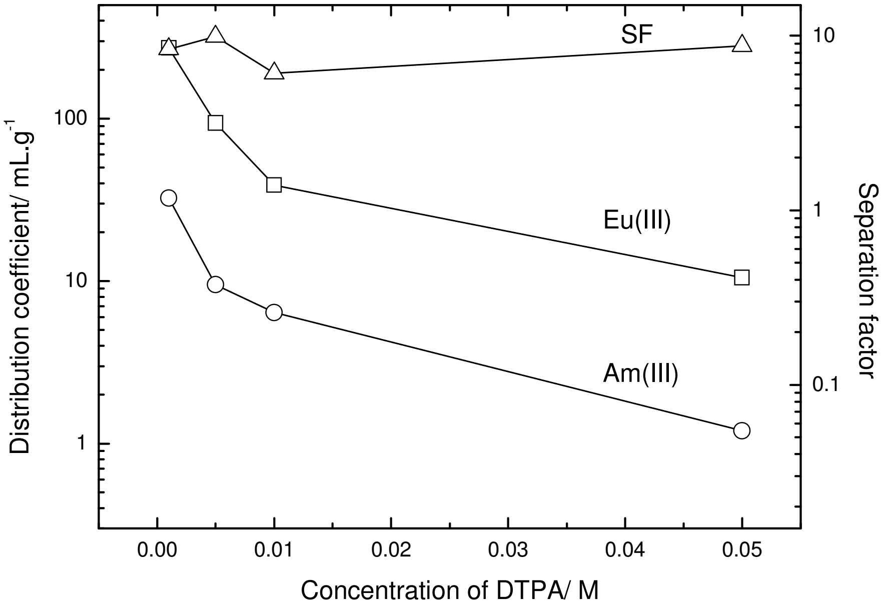

Figure 6.7. Variation in the distribution coefficient of Eu(III) and Am(III) in Si-DGAH as a function of DTPA concentration. Adsorbent phase: Si-DGAH (0.05 g), Aqueous phase: DTPA at pH 2 (10 mL), spiked with $^{(152+154)}$Eu(III) or ^{241}Am(III) tracer

6.7. Conclusions

A novel diglycolamic acid functionalized silica gel (Si-DGAH) was prepared and studied for the separation of americium(III) and europium(III) from dilute nitric acid medium. The TG-DTA, SEM-EDX and elemental analysis carried out on the adsorbent, confirmed the presence of diglycolamic moieties (1.2 mmol/g) on the surface of silica gel. Rapid adsorption of Am(III) and Eu(III) was observed in the initial stages of adsorption followed by the establishment of equilibrium occurring within 30 minutes. The distribution coefficient of Am(III) and Eu(III) decreased with increase in the concentration of nitric acid. The rate of adsorption increased with increase of pH and the rate of adsorption of both Am(III) and Eu(III) were well described by pseudo-second order kinetic models. Based on the slope analysis, the extraction of Am(III) and Eu(III) was accompanied by the co-extraction of a nitrate ion and release two H^+ ions to aqueous phase. The DTPA concentration needed for the mutual separation of Am(III) from Eu(III), was optimized to be 0.05 M at pH 2. The study confirmed the possibility of using Si-DGAH for the separation of trivalent f-block elements from dilute nitric acid medium [27, 28].

6.8. References

1. T. Shimada, K. Aoki, Y. Shinoda, T. Nakamura, N. Tokunaga, S. Inagaki, T. Hayashi, Functionalization of silica gel with akylsilanes. A new method of covalent attachment of organic functional groups on silica gel, J. Am. Chem. Soc. 125 (2003) 4688 – 4689
2. J.J. Pesek, M. Matyska, R,R. Abuelafiya, Chemically Modified Surfaces: Recent Developments, Royal Society of Chemistry, Cambridge, 1996.
3. R.P.W. Scott, Silica gel and bonded phases-Their production properties and use in LC, Wiley, New York, 1993.
4. E.F. Vansant, P. Van Der Voort, K. C. Vranken, Characterization and chemical modification of the silica surface, Elsevier, Amsterdam, 1995.
5. C.V.K. Sharma, A.J. Hessheiser, A. Clearfield, Novel materials based on self assembly of organophosphonic acids, Polyhedron 20 (2001) 2095 – 2104
6. A. Zhang, W. Wang, Z. Chai, E. Kuraoka, Modification of a novel macroporous silica-based crown ether impregnated polymeric composite with 1-dodecanol and its adsorption for some fission and non-fission products contained in high level liquid waste, Eur. Polym. J. 44 (2008) 3899-3907.
7. K.A. Venkatesan, V. Sukumaran, M. P. Antony, P. R. Vasudeva Rao, Extraction of uranium by amine, amide and benzamide grafted covalently on silica gel. J. Radioanal. Nucl. Chem. 260 (2004) 443-450

8. G. E. Fryxell, W. Chouyyok, R.D.Rutledge, Design and synthesis of chelating diamide sorbents for the separation of lanthanides, Inorg. Chem. Commun. 14(6) (2011) 971–974.
9. A.R.Cestari, C.Airoldi, Chemisorption on thiol–silicas: divalent cations as a function of pH and primary amines on thiol–mercury adsorbed, J. Colloid. Interface Sci. 195 (1997) 338 – 342.
10. P.W. Naik, P.S. Dhami, S.K. Misra, U. Jambunathan, J.N. Mathur, Use of organophosphorus extractants impregnated on silica gel for the extraction chromatographic separation of minor actinides from high level waste solutions. J. Radioanal. Nucl. Chem. 257 (2003) 327-32.
11. Y. Wei, A. Zhang, M. Kumagai, M. Watanabe, N. Hayashi, Development of the MAREC process for HLLW partitioning using a novel silica-based CMPO extraction resin. J. Nucl. Sci. Technol. 41 (2004) 315-22.
12. S.Y. Kim, Y. Xu, T. Ito, Y. Wu, T. Tada, K. Hitomi, E. Kuraoka, K. Ishii, A novel partitioning process for treatment of high level liquid waste using macroporous silica-based adsorbents. J. Radioanal. Nucl. Chem. 295 (2013) 1043-50.
13. A. Zhang, E. Kuraoka, M. Kumagai, Removal of Pd (II), Zr (IV), Sr (II), Fe (III), and Mo (VI) from simulated high level liquid waste by extraction chromatography utilizing the macroporous silica-based polymeric materials. Sep. Purif. Technol. 50 (2006) 35-44.
14. A. Zhang, W. Wang, Z. Chai, M. Kumagai, Separation of strontium ions from a simulated highly active liquid waste using a composite of silica-crown ether in a polymer. J. Sep. Sci. 31 (2008) 3148-3155.
15. A. Warshawaky, “Chelating Ion Exchangers”, in Ion Exchange and Sorption Processes in Hydrometallurgy” M. Streat and D.Naden (eds), Critical Reports on Applied

Chemistry, Vol. 19, John Wiley & Sons (for the Society of Chemical Industry), (1987) p-166

16. R.S.S. Murthy, D.E. Ryan, Preconcentration of copper, cadmium, mercury and lead from sea and tap water samples on a dithiocarbamatecellulose derivative, Anal. Chim. Acta 140 (1982) 163 – 169.
17. E.P. Horwitz, R. Chiarizia, H. Diamond, R.C. Gatrone, S.D. Alexandratos, A.Q. Trochimczuk, D.W. Crick, Uptake of metal ions by a new chelating ion-exchange resin. part 1: acid dependencies of actinide ions, Solvent Extr. Ion Exch. 11 (1993) 943 – 966
18. L. R. Van Loon, W. Hummel, Radiolytic and chemical degradation of strong acidic ion-exchange resins : Study of the ligands formed, Nucl. Tech. 128 (1999) 359 – 371
19. R. Chiarizia, E.P. Horwitz, Radiolytic stability of some recently developed ion exchange and extraction chromatographic resins containing diphosphonic acid groups, Solvent Extr. Ion Exch. 18 (2000) 109-132.
20. F. Frizon, C. Cau-dit-Coumes, Cementation of ILW ion exchange resins: Impact of sulfate ions released by radiolysis on hydrated matrix, J. Nucl. Mater. 359 (2006) 162–173.
21. R. Chiarizia, E.P. Horwitz,, K.A. D'Arcy, S.D. Alexandratos, A.W. Trochimzuk, Uptake of Actinides and other Ions by Dipiosil, A New Silica based Chelating Ion Exchange Resin: In Ion Exchnge Developments and Applications, Ed. J.A. Greig. Proceedings of IEX, The Royal Society of Chemistry, UK, (1996) pp-321
22. R.A. Bulman, Gyula Szabo, R.F.Clayton C.R.Clayton, Investigations of the uptake of transuranic radionuclides by humic and fulvic acids chemically immobilized on silica gel and their competitive release by complexing agents, Waste Manage.17 (1997) 191 – 199.

23. K.A Venkatesan, T.G Srinivasan, P.R Vasudeva Rao, Removal of complexed mercury from aqueous solutions using dithiocarbamate grafted on silica gel. Sep. sci. Technol. 37(6) (2002) 1417-1429.
24. K.A. Venkatesan, T.G. Srinivasan, P.R. Vasudeva Rao, Cobalt-extraction studies on dithiocarbamate grafted on silica gel surface, Colloid. Surf. A 180 (2001) 277–284.
25. K.A. Venkatesan, V. Sukumaran, M.P. Antony, P.R. Vasudeva Rao, Extraction of uranium by amine, amide and benzamide grafted covalently on silica gel. J. Radioanal. Nucl. Chem. 260 (2004) 443-450.
26. M. Nilsson, K.L. Nash, A review of the development and operational characteristics of the TALSPEAK process, Solvent Extr. Ion Exch. 25 (2007) 665–701.
27. A.S. Suneesh, K.V. Syamala, K.A. Venkatesan, M.P. Antony, P.R. Vasudeva Rao, Diglycolamic acid modified silica gel for the separation of hazardous trivalent metal ions from aqueous solution, J. Colloid Inter. Sci. 438 (2015) 55-60.
28. A.S. Suneesh, K. V. Syamala, K.A. Venkatesan, M.P. Antony, P. R. Vasudeva Rao, A novel glycolamic acid functionalized silica for the separation of americium (III) from europium (III), In: Emerging Trends in Separation Science and Technology(SESTEC), D.K. Singh, P.K. Mohapatra, B.S. Tomar, A. Goswami, K.L. Ramakumar (eds). BARC, Mumbai, India. P-33

Chapter 7: Magnetic solid phase separation for the mutual separation of lanthanides and actinides

This chapter describes the evaluation of two different magnetic adsorbents iron oxide functionalized diglycolamic acid (Fe-DGAH) and its thio derivative (Fe-SDGAH). The effect of various parameters such as the duration of equilibration and concentrations of nitric acid, europium ion, and diethylenetriaminepentaacetic acid (DTPA) in the aqueous phase on the distribution coefficient (K_d) of Am(III) and Eu(III) on Fe-DGAH is explained in detail. The conditions needed for efficient separation of Am(III) from Eu(III) were optimized using DTPA. The magnetic separation of the particles from the aqueous phase was demonstrated.

7.1. Introduction

Magnetic solid phase extraction (MSPE) is an advanced method for the separation of hazardous metal ions from aqueous wastes [1-9]. In MSPE technique, the magnetic particles (MPs) are added to the waste solution to adsorb the target metal ion. The MPs are then separated from the solution by means of an external magnetic force [1, 2]. The separated MPs are then immersed in a stripping solution for recovery of metal ions from the adsorbed surface. A typical magnetic separation is illustrated in figure 7.1. However, the iron oxide magnetic particle alone does not exhibit the required selectivity for separations. To improve the selectivity of MSPE, the surfaces of magnetic particles are chemically transformed with metal-ion specific ligands by organo modification reaction. This is usually carried out by silylation of magnetic particles by reacting with organosilane, which is followed by chemically linking the task-specific ligands on the silanol surface [1, 2]. The procedure for such organo modification is described elsewhere [5-11].

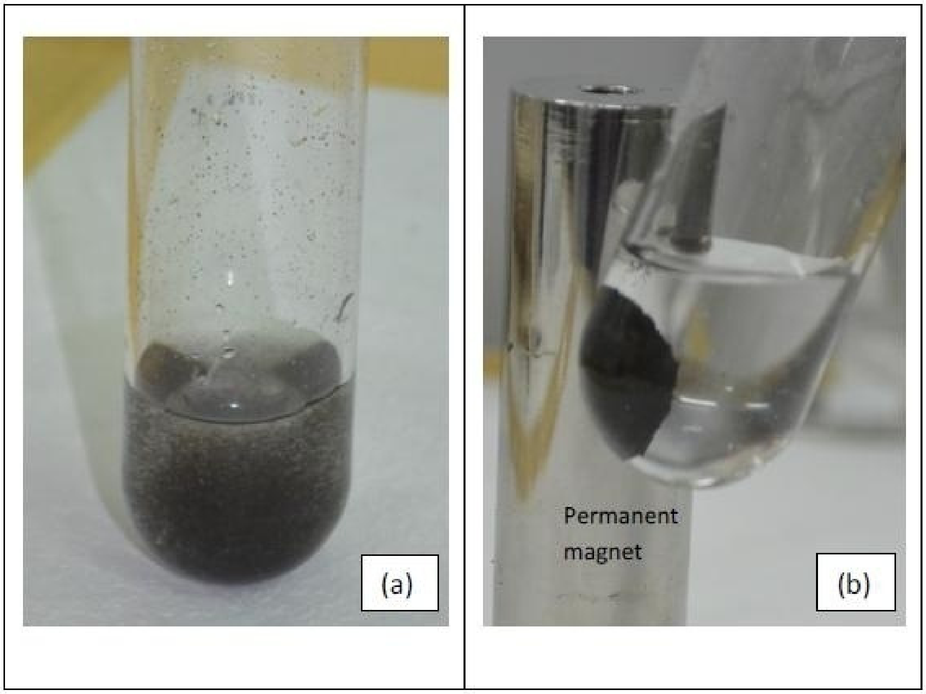

Figure 7.1. Separation of the magnetic particles by a permanent magnet. (a) The magnetic particles are dispersed in the solution obtained after equilibration. (b) Separation of magnetic particles achieved by using permanent magnet.

MSPE offers several advantages for the treatment of nuclear waste as compared to the conventional solid phase extraction [1-9]. Since this method uses the application of external magnetic field, the particle size of the adsorbent can be lowered to as low as the nano meter-size for efficient and rapid extraction of metal ions from waste solution. In addition, there is no need for packing of MPs in column as it is usually operated in batch mode and the phase separation is quickly achieved by external magnetic field [1, 2]. From the waste management point of view, the spent adsorbent can be either vitrified or converted to unleachable ceramic waste form, for final disposal of the spent contaminated iron oxide particles. Since the organo modified material contains only 10% of organics on the inorganic solid matrix, the swelling and radiolytic degradation usually encountered with organic solid supports or resins during the treatment of radioactive waste is negligible with use of MSPE [10].

Several authors have studied the separation of toxic and radiotoxic metal ions from aqueous wastes using magnetic particle functionalized with metal ion specific ligands. In this context, Zhang *et al.* [11] prepared thiol modified iron oxide composite materials for the removal of mercury(II) from pH 5-7 solutions. These adsorbents showed excellent selectivity for mercury with good recyclability options. Suleiman *et al.* [12] also studied bismuth thiol based iron oxide magnetic particles for the pre-concentration of Cr, Cu and Pb for analytical applications. Ngomsik*et al.* [13] has studied citrate functionalized magnetic iron oxide particles for the selective extraction of Eu(III), La(III), Ni(II) and Co(II) from dilute nitric acid medium. Yang *et al.* [14] has studied magnetic modified chitosan for the selective recovery of cadmium from aqueous solution. Wei Wu *et al.* [15] studied the adsorption of Cr(III) by using Fe_3O_4-ZrO_2 particles. Recently, Wu *et al.* [16] studied the separation behavior of chromium(III) by lanthanum by using magnetic solid phase extraction technique. The authors reported efficient extraction of trivalent lanthanum on 2-ethylhexylphosphoric acid (DEPHA) functionalized iron oxide - composites.

In view of the advantages of MSPE, we have synthesized two different types of magnetic adsorbents containing diglycolamic acid functional group such as iron oxide functionalized diglycolamic acid (Fe-DGAH) and its thio derivative (Fe-SDGAH). The adsorbents are synthesized by chemical modification of iron oxide. Among the various oxides, Fe_3O_4 has been popularly used as magnetic adsorbent because of its enhanced ferromagnetic behavior. Fe_3O_4 is prepared by co-precipitation of Fe^{3+} and Fe^{2+} salt. As prepared Fe_3O_4 surface contains several Fe-OH groups. The surface of Fe_3O_4 is later modified by a process involving hydrolysis and condensation process between Fe_3O_4 and an alkoxy silane. The third step involved for the synthesis is the organo modification of the surface-Si-OH with the organic attachment. The ligand of interest is initially attached to an organo silane and was anchored on to the Fe-Si by esterification process. The general synthetic scheme involved in the synthesis of a magnetic adsorbent is illustrated in figure 7.2.

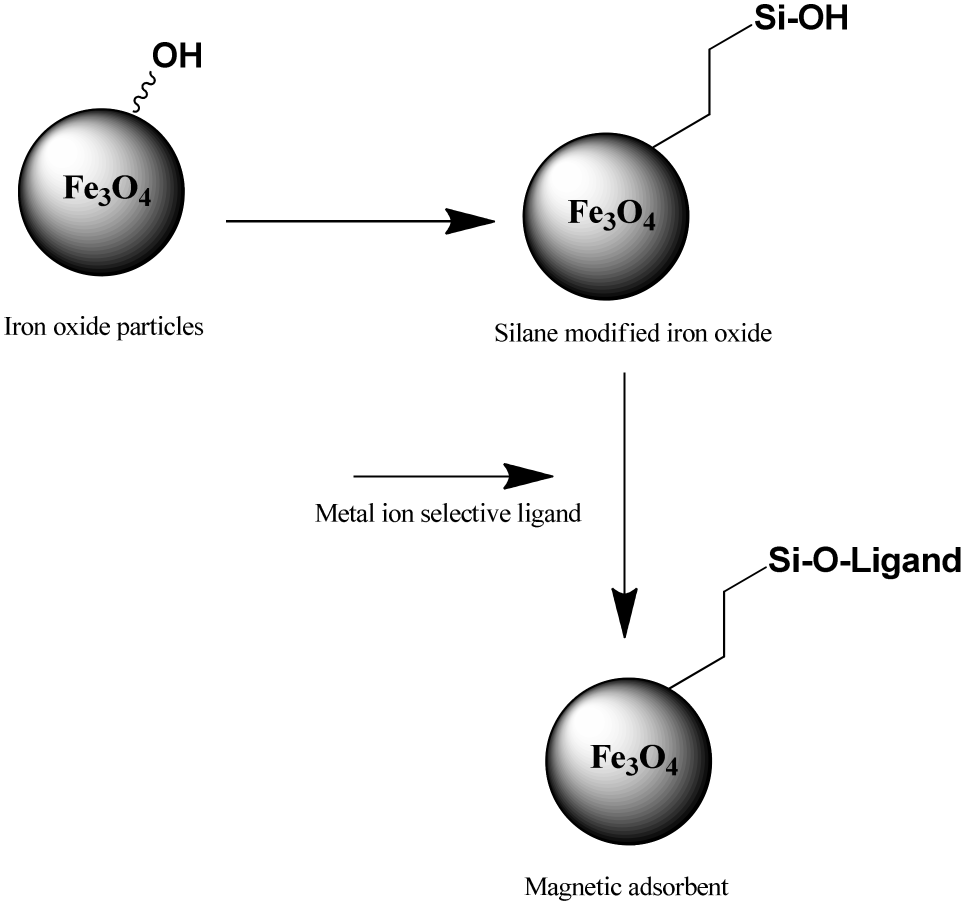

Figure 7.2. General scheme for the synthesis of a magnetic adsorbent.

Detailed synthetic procedures and characterizations of Fe-DGAH and Fe-SDGAH are explained in experimental section.

7.2. Kinetics of extraction of Am(III) and Eu(III)

The kinetics of Am(III) (or Eu(III)) sorption was studied by batch equilibration of 0.05 g of the adsorbent with 10 ml of nitric acid solution (0.001 M to 0.1 M) spiked with

^{241}Am(III) (or $^{(152+154)}$Eu(III)) tracer at 298 K. The equilibration was stopped at pre-fixed intervals of time. The solution phase radioactivity was measured after the separation of the magnetic particles by using a permanent magnet. From the initial activity and the activity measured at various intervals of time the percentage of Am(III) (or Eu(III)) sorbed was calculated by equation 2.3 of chapter 2 (section 2.4.2). The rate of uptake of Am(III) and Eu(III) by Fe-DGAH and Fe-SDGAH at pH 2 are shown in Fig 2 and Figure 3 respectively. Rapid sorption of Am(III) or Eu(III) is observed in the initial stages of equilibration followed by the establishment of equilibrium occurring within 1 h. Therefore, all the equilibration experiments were performed for 2 h for ensuring the establishment of equilibrium. After 2 h of equilibration, the changes in percentage of extraction of Am(III) and Eu(III) in Fe-DGAH is insignificant. A couple of models have been considered for fitting the kinetics of extraction. They are the pseudo-first order model and the pseudo-second order model. Equation for pseudo-first order model and pseudo-second order model are showed in equation 1 and 2. Detailed derivations of these equations are provided in section 2.4.2.1 of experimental section.

$$q_t = q_e\left(1 - e^{-k_1 t}\right) \tag{7.1}$$

$$q_t = \frac{q_e^{\,2}\, k_2\, t}{1 + q_e\, k_2\, t} \tag{7.2}$$

Non linear regression of the experimental data using equation 7.1 and 7.2 results in a determination of rate constants k_1 and k_2. The fitting of the experimental kinetic data using equation 7.1 is shown in figure 7.3 and that using equation 7.2 is shown in figure 7.4. The fitting constants and statistical parameters are tabulated in table 7.1. The R^2 values are more and χ^2 values are low for second order fitting. This indicates that the data were described well by the pseudo-second order rate equation 7.2 (figure 7.4). From table

7.1, it can be seen that the rate constants (k_1 and k_2) increases with increase of pH and the magnitude of rate constant is more for Eu(III) extraction. This could be due to the strong affinity of O-donor ligand (present in Fe-DGAH) towards the hard acid metal ion Eu(III) as compared to Am(III) ion.

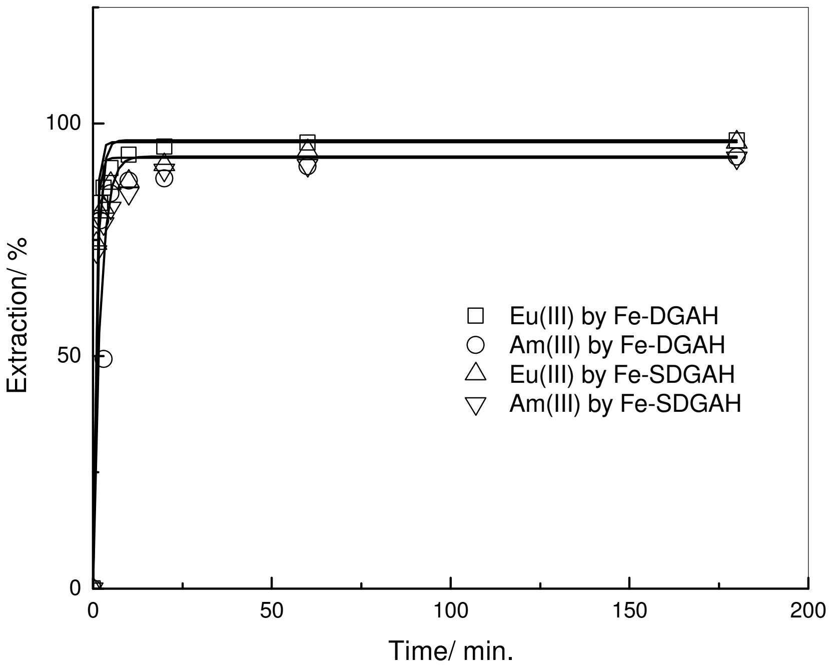

Figure 7.3. Variation in the percentage extraction of Eu(III) and Am(III) as a function of time, fitted by using pseudo-first order rate equation. Adsorbent phase: Fe-SDGAH (0.05 g), Aqueous Phase: HNO_3 at pH 3, spiked with $^{(152+154)}$Eu(III) or ^{241}Am(III) tracer.

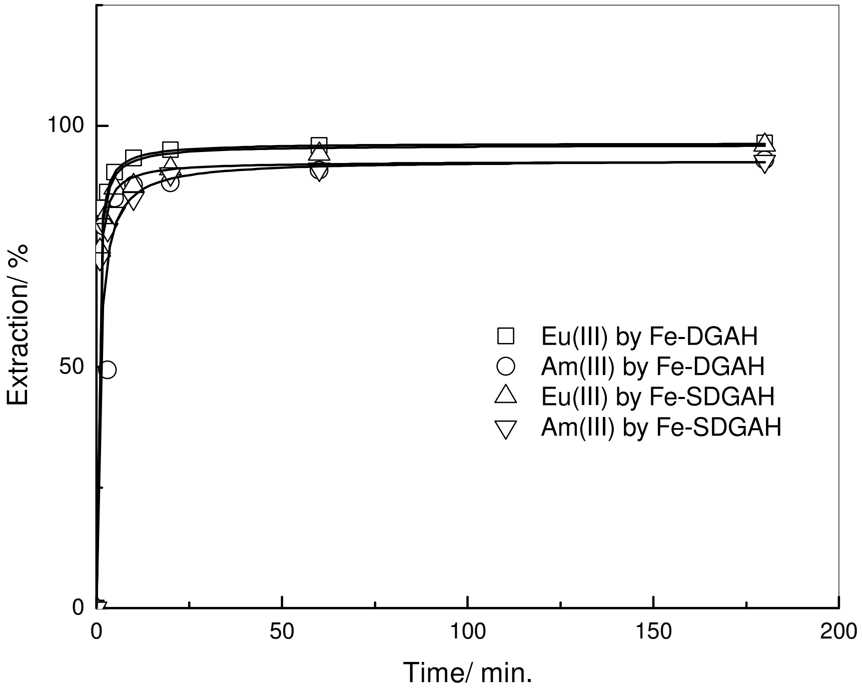

Figure 7.4. Variation in the percentage extraction of Eu(III) and Am(III) as a function of time, fitted by using pseudo-second order rate equation. Adsorbent phase: Fe-SDGAH (0.05 g), Aqueous Phase: HNO_3 at pH 3, spiked with $^{(152+154)}$Eu(III) or ^{241}Am(III) tracer.

Table 7.1. Rate constants (k_1 and k_2) obtained by non-linear regression of the kinetics of extraction using equations 7.1 and 7.2.

Metal ion	**k_1/ min^{-1}.**						**k_2/ L. mol^{-1}. min^{-1}.**					
	Fe-DGAH	**χ^2**	**R^2**	**Fe-SDGAH**	**χ^2**	**R^2**	**Fe-DGAH**	**χ^2**	**R^2**	**Fe-SDGAH**	**χ^2**	**R^2**
Eu(III)	0.88	7.92	0.9925	1.37	8.09	0.9520	0.03	0.06	0.9999	0.028	10.07	0.9899
Am(III)	0.49	140.69	0.8635	1.41	0.12	0.9426	0.01	108.78	0.8944	0.03	11.03	0.9878

7.3. Effect of nitric acid

Effect of nitric acid was investigated by equilibrating 0.05 g of adsorbent with 10 mL of aqueous phase spiked with $^{(152+154)}$Eu or ^{241}Am tracer at 298 K. The mixture was taken in a 20 mL capacity stoppered glass-tube and rotated in upside-down rotation (50 rpm) for a specified period of time. The concentration of nitric acid in aqueous phase was varied from 0.001 M to 0.1 M. After 2 hrs of equilibration, the dispersed magnetic particles were settled by external magnetic field. An aliquot was taken from aqueous phase. Details of the experimental are discussed in experimental section 2.4.2. The variation in the distribution coefficient of Am(III) and Eu(III) as a function of nitric acid concentration in aqueous phase is shown in figure 7.5. It can be seen from figure 7.5 that the K_d values of Am(III) and Eu(III) of both Fe-DGAH and Fe-SDGAH decreased with increase of concentrations of nitric acid.

Since the Fe-DGAH, is a chelating-type acidic cation exchanger, the distribution coefficient of both Eu(III) and Am(III) decreases with increase in the concentration of nitric acid. Therefore, the extraction of trivalent metal ion in Fe-DGAH could be represented by the equilibrium reaction shown in equation 7.3. The adsorbent phase is indicated by a bar over the acronym.

$$\mathrm{M_{aq}^{3+}} + 3\,\overline{\mathrm{Fe\text{-}DGAH}} \Leftrightarrow \overline{\{(\mathrm{Fe\text{-}DGA})_3 M\}} + 3\,\mathrm{H_{aq}}^{+} \tag{7.3}$$

where $\overline{\mathrm{Fe\text{-}DGAH}}$ is the adsorbent phase and $\overline{\mathrm{Fe\text{-}DGA}}$ is the proton dissociated form of the adsorbent. The equilibrium constant for the above reaction is given by

$$\mathrm{K} = \frac{\left[\overline{(\mathrm{Fe\text{-}DGA})_3 M}\right][\mathrm{H}^+]_{\mathrm{aq}}^3}{[\mathrm{M}^{3+}]_{\mathrm{aq}}\left[\overline{\mathrm{Fe\text{-}DGAH}}\right]^3} \tag{7.4}$$

$$K = \frac{K_d\,[\mathrm{H}^+]^3_{\mathrm{aq}}}{\left[\overline{\mathrm{Fe\text{-}DGAH}}\right]^3} \qquad (7.5)$$

where K_d is defined as

$$K_d = \frac{\left[\overline{(\mathrm{Fe\text{-}DGA})_3 M}\right]}{[\mathrm{M}^{3+}]_{\mathrm{aq}}}$$

Since the amount of Fe-DGAH taken for equilibration is constant, the variation of K_d with H^+ ion concentration in aqueous phase is given by equation 7.6.

$$\log K_d = \log K_1 - 3 \log [\mathrm{H}^+]_{\mathrm{aq}} \qquad (7.6)$$

where K_1 $(= K\,\overline{[\mathrm{Fe\text{-}DGAH}]^3})$ is a constant. Thus, the logarithmic plot of K_d against $[H^+]_{aq}$ should result in a straight line with slope of -3. The variation of K_d as a function of $[H^+]_{aq}$ is shown in figure 7.5. Linear regression of the distribution data yields a slope of -2 instead of -3 for both the metal ions. This indicates the release of two moles of H^+ for the extraction of one mole of Am(III) or Eu(III). This behavior could be explained by the extraction of hydrolyzed specie ($Am(OH)^{2+}$ or $Eu(OH)^{2+}$) on Fe-DGAH. However, the observed behavior is similar to the extraction behavior of Am(III) and Eu(III) reported in a solution of thiodiglycolamic acid present in n-dodecane reported in liquid-liquid extraction mode [17,18]. It was shown that Am(III) and Eu(III) extraction in organic phase was accompanied by the release of two moles of H^+ ions from diglycolamic acid and co-extraction of one mole of NO_3^- ions from aqueous phase. Based on those results, the extraction of Am(III) and Eu(III) in the present case could be represented by the equilibrium reaction shown in equation 7.7. To verify the validity of the extraction mechanism shown in equation 7.7, the effect of nitrate ion in aqueous phase on the distribution coefficient of Am(III) was studied and the results are shown in figure 7.6. It can be seen that the K_d of Am(III) increases with increase in the concentration of nitrate ion leading to a slope value of 1, which confirms the participation of a nitrate ion for the extraction of Am(III).

$$M^{3+}_{aq} + 2\,\overline{Fe\text{-}DGAH} + NO^{-}_{3\,aq} \Leftrightarrow \overline{\{M(NO_3)(Fe-DGA)_2\}} + 2H^{+}_{aq} \qquad (7.7)$$

Fe-SDAH also exhibits a similar extraction behavior. Variation in the distribution coefficients of Eu(III) and Am(III) as a function of nitric acid concentration is showed in figure 7.5. It is observed that the distribution coefficient of both Eu(III) and Am(III) decreases with increase in the concentration of nitric acid. It can also be seen that, Fe-SDGAH extracts Am(III) preferentially over to Eu(III), whereas Fe-DGAH exhibits Eu(III) selectivity (as seen in figure 7.5).

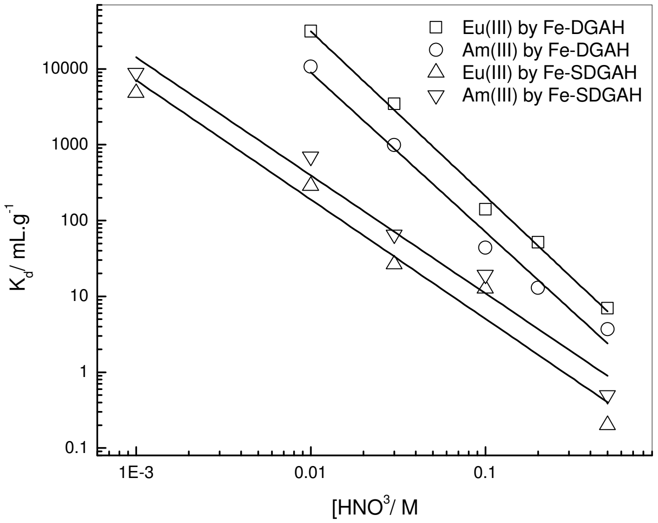

Figure 7.5. Variation in the distribution ratios of Eu(III) and Am(III) as a function of concentrations of nitric acid. Adsorbent phase: Fe-DGAH or Fe-SDGAH (0.05 g), Aqueous phase: [HNO_3] at various concentrations (10 mL), spiked with $^{(152+154)}$Eu(III) or ^{241}Am(III) tracer.

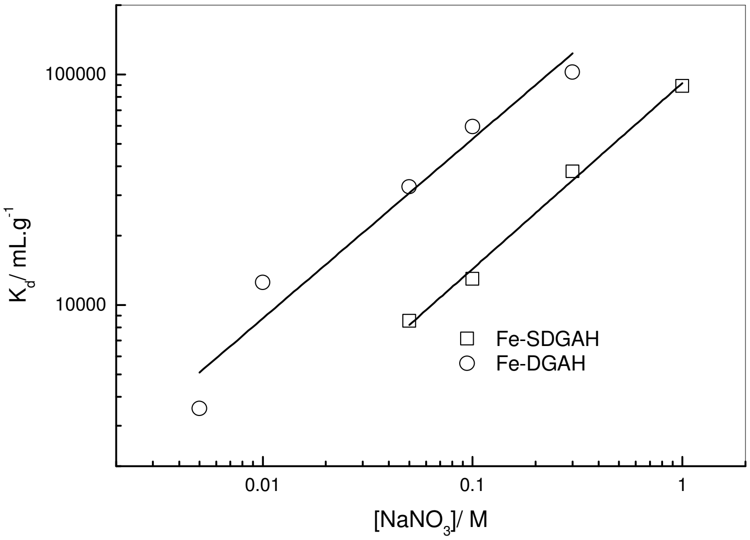

Figure 7.6. Variation in the distribution coefficient of Am(III) as a function of concentrations of NaNO$_3$. Adsorbent phase: Fe-DGAH or Fe-SDGAH (0.05 g), Aqueous phase: Sodium nitrate at various concentrations (10 mL) at pH 3, spiked with ^{241}Am(III) tracer.

7.4. Langmuir Adsorption model

Equilibrium isotherm data for the extraction of Eu(III) by Fe-DGAH (or by Fe-SDGAH) was analysized by Langmuir adsorption model. For this experiment, batch experiments were conducted at 298 K by equilibrating 0.05 g of the adsorbent with 10 mL of nitric acid solution containing various quantities of europium nitrate spiked with $^{152+154)}$Eu(III) tracer. After two hours of equilibration, the initial and final radioactivity was measured and the amount of Eu(III) sorbed was calculated. Amount of Eu(III) adsorbed to Fe-DGAH was modelled by linear form of Langmuir adsorption model. The linear form of Langmuir adsorption equation is shown in Eq.7.8.

$$\frac{C_f}{C_s} = \frac{1}{K_L\, b} + \frac{C_f}{b} \qquad (7.8)$$

where C_f is the equilibrium concentration of metal ion (mg/L), C_s is the amount of metal ion sorbed on Fe-DGAH (mg/g), K_L is the Langmuir adsorption constant (L/mg) and b (mg/g) is the sorption capacity. Figure 7.7 and 7.8 shows the plot of C_f/C_s against C_f for the sorption of Eu(III) in Fe-DGAH and Fe-SDGAH respectively. Linear regression of the extraction data results in a sorption capacity of various adsorbents are also showed in the figure. It can be seen that the adsorption capacity of Fe-DGAH is very high at pH 2 (~56.15). However, Fe-SDGAH exhibited an adsoption capacity of 11.8 at pH 2.

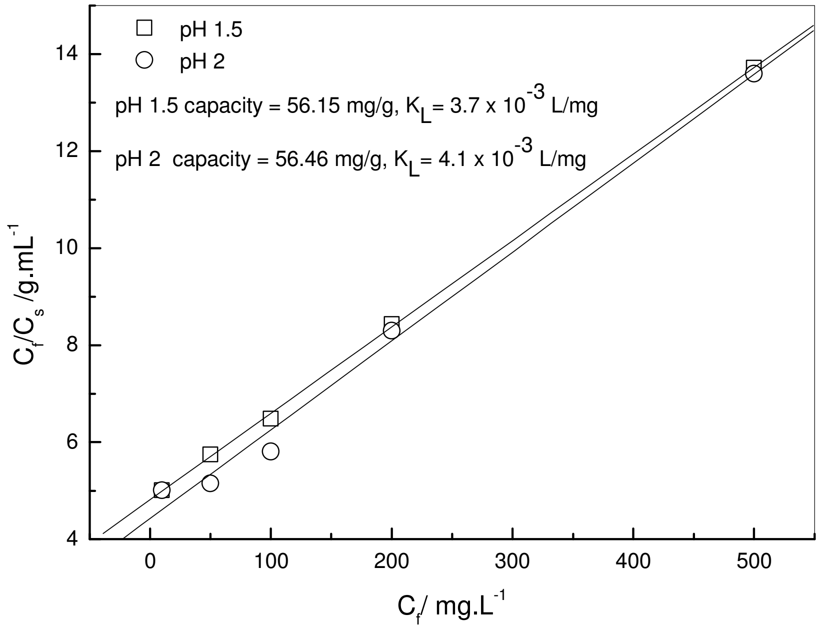

Figure 7.7. Langmuir adsorption isotherm for the sorption of Eu(III) at 298 K. Adsorbent phase: Fe-DGAH (0.05 g), Aqueous Phase: Europium nitrate at pH 1.5 & 2, spiked with $^{(152+154)}$Eu(III) tracer.

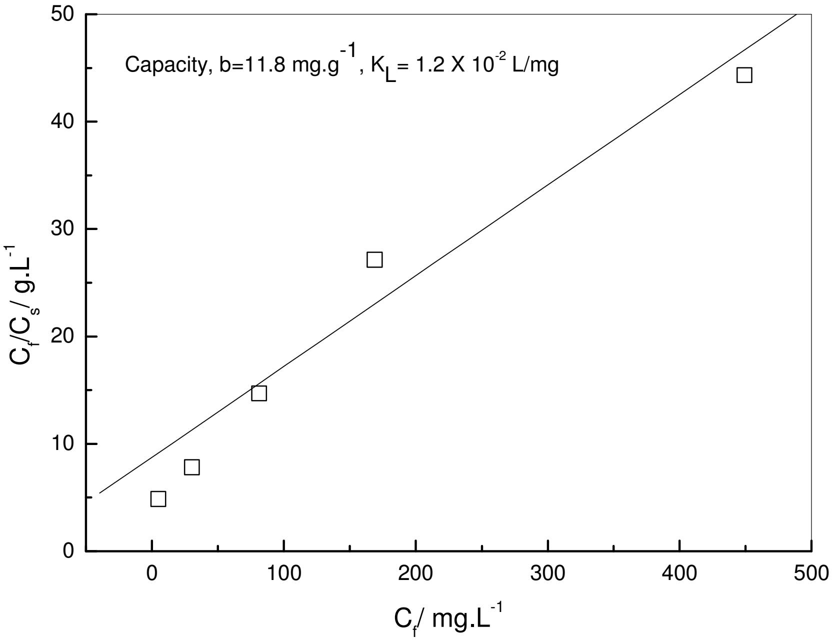

Figure 7.8. Langmuir adsorption isotherm for the sorption of Eu(III) at 298 K. Adsorbent phase: Fe-SDGAH (0.05 g), Aqueous Phase: Europium nitrate at pH 2, spiked with $^{(152+154)}$Eu(III) tracer.

7.5. Effect of DTPA and separation factor.

From figure 7.5, it was learned that Fe-DGAH showed selectivity towards Eu(III) and Fe-SDGAH showed selectivity towards Am(III). Eu(III) selectivity of Fe-DGAH could be due to the presence of –COOH group present in Fe-DGAH. Therefore, use of Am(III) selective soft donor complexing agents in the aqueous phase can improve the Eu(III)/Am(III) separation in the case of Fe-DGAH. Table 7.2 shows the distribution ratios of Eu(III) and Am(III) in Fe-DGAH at pH 1.5 and 2. In the absence of DTPA the separation factor (quotient of K_d of Eu(III) and K_d of Am(III)) achieved for the extraction of these metal ions is very small (~1 to 3). The TALSPEAK process and several other methods reported in literature [17, 18] employed diethylenetriamminetetraacetic acid (DTPA) as aqueous complexing agent for facilitating the mutual separation of lanthanides and actinides. Since DTPA forms a complex with Am(III) in preference to Eu(III), the extractions carried out in the presence of DTPA facilitates the retention of Am(III) in the aqueous phase and thus enhances the separation factor of Eu(III) over Am(III).

Table 7.2 also shows the distribution ratios of Eu(III) and Am(III) in Fe-DGAH studied as a function of DTPA concentration. It is also interesting to note that the distribution ratio of Eu(III) and Am(III) increases with increase of pH in the presence of DTPA. It can be expected that the dissociation of DTPA increases with increase of pH and retain both Am(III) and Eu(III) in aqueous phase. However, it seems that the acid dissociation of Fe-DGAH increases to a greater extent as compared to DTPA dissociation. A similar behavior was also reported in TALSPEAK process, when HDEHP was used as solvent instead of Fe-DGAH [13, 41]. Since Fe-DGAH is involved in the extraction Eu(III) and Am(III), the distribution ratio of both these metal ions increases with increase of pH even in the presence of DTPA.

As expected the distribution ratio of both metal ions decreases with increase in the concentration of DTPA. However, the distribution ratio of Am(III) decreases more. This results in increase in the separation factor of Eu(III) over Am(III) with the increase in the concentration of DTPA. At pH 2, the separation factor increases from ~1 in the absence of DTPA to the value of 150 at 0.05 M DTPA concentration. Further increase in DTPA concentration lowers the distribution ratio of both metal ions to very small values making the adsorbent in-extractable. Therefore, it is desirable to use 0.05 M DTPA for the separation of Eu(III) from Am(III) from dilute nitric acid medium with the separation factor of 150 [19].

Table 7.2. Variation in the distribution coefficient of Eu(III) and Am(III) in Fe-DGAH as a function of DTPA concentration. Adsorbent phase: Fe-DGAH (0.05 g), Aqueous phase: [DTPA] at pH 1.5 and 2, spiked with $^{(152+154)}$Eu(III) or ^{241}Am(III) tracer.

[DTPA]/ M	Distribution coefficient/ mg.L^{-1}				SF	
	Eu(III)		**Am(III)**		**pH**	
	pH 1.5	**pH 2**	**pH 1.5**	**pH 2**	**1.5**	**2**
0	2951	20803	956	15841	3.1	1.3
0.001	2155	4150	536	89	4	46.6
0.005	991	1190	187	26	5.3	45.8
0.05	194	190	37	1.2	5.2	158.3

7.6. Desorption studies

Studies were conducted to understand the optimum conditions required for the quantitative recovery of loaded metal ions (Am(III) or Eu(III)) from the adsorbent phase (Fe-DGAH or Fe-SDGAH).

The adsorbent was initially loaded with Am(III) (or Eu(III)) and the loaded Am(III) (or Eu(III)) were removed by using 0.5 M HNO_3. For example, loading of Am(III) in Fe-SDGAH was carried out equilibrating 0.05 g of the adsorbent with 10 ml of nitric acid solution at pH 3 spiked with ^{241}Am(III) tracer at 298 K for 2 hours. After equilibration, the aqueous phase removed quantitatively. From the measurement of radioactivity of ^{241}Am(III) present in aqueous phase, the amount of Am(III) loaded in the adsorbent was determined. The adsorbent was then contacted with 10 mL of 0.5 M nitric acid. The equilibration was carried out for 30 minutes. An aliquot was taken from aqueous phase and radioactivity of Am(III) present in aqueous phase was determined. The aqueous phase was then removed and contacted again with the fresh aqueous phase of 0.5 M nitric acid (10 mL). This procedure was repeated until the Am(III) was recovered quantitatively. A similar experiment was performed for Eu(III) recovery.

The cumulative stripping of Eu(III) and Am(III) from the adsorbent phase is shown in figure 7.9. It can be seen that the cumulative recovery of Eu(III) and Am(III) increases with increase in the number of contacts of the stripping solution. More than 99.9% of Eu(III) and Am(III) can be recovered in 4 to 5 contacts using 0.5 M nitric acid. A similar experiment performed for Fe-DGAH revealed that all the loaded Am(III) and Eu(III) can be stripped within 3-4 contacts [19].

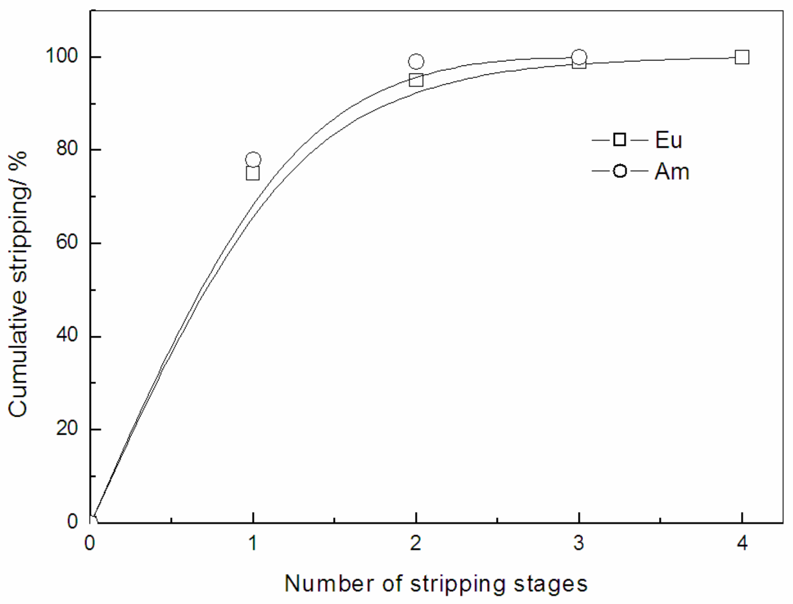

Figure 7.9. Cumulative recovery of Eu(III) and Am(III) from the loaded adsorbent. Adsorbent phase: Fe-SDGAH, Stripping solution: 0.5 M HNO_3.

7.7. Adsorbent recycling

Reuse and recycling of the adsorbent is one of the important parameters needed for actual applications. In this context the distribution coefficient of Am(III) was determined during extraction and stripping for 5 cycles. The results are shown in table 7.3 (for Fe-DGAH) and table 7.4 (for Fe-SDGAH). It can be seen that the adsorbent can be recycled more than five times without any change in the distribution coefficient of Am(III) during extraction and stripping. This result confirms that the diglycolamic acid anchored on to the adsorbent is stable toward nitric acid and it can be reused more than five times [19, 20].

Table 7.3. Distribution coefficient (K_d) of Am(III) during recycling studies. Conditions for extraction: Adsorbent phase: Fe-DGAH (0.05 g), Aqueous Phase: HNO_3 at pH 3, spiked with ^{241}Am(III) tracer. Conditions for Stripping: Adsorbent phase: Fe-SDGAH (0.05 g), Aqueous Phase: 0.5 M HNO_3

Recycling stages	K_d/ mL/g, during extraction	K_d/ mL/g, during stripping
1	8231	0.5
2	8150	0.6
3	8282	0.8
4	8094	0.9
5	7982	1.1

Table 7.4. Distribution coefficient (K_d) of Am(III) during recycling studies. Conditions for extraction: Adsorbent phase: Fe-SDGAH (0.05 g), Aqueous Phase: HNO_3 at pH 3, spiked with ^{241}Am(III) tracer. Conditions for Stripping: Adsorbent phase: Fe-SDGAH (0.05 g), Aqueous Phase: 0.5 M HNO_3

Recycling stages	K_d/ mL/g, during extraction	K_d/ mL/g, during stripping
1	6021	2.2
2	5985	2.1
3	5864	1.8
4	5908	2.0
5	5958	0.98

7.8. Conclusions

The magnetic adsorbents Fe-DGAH and Fe-SDGAH were synthesized and characterized by TG-DTA, SEM-EDX and XRD. Extraction behavior of Am(III) and Eu(III) was studied by using Fe-DGAH and Fe-SDGAH. Rapid sorption of Am(III) and Eu(III) was observed in the initial stages of sorption followed by the establishment of equilibrium occurring within 2 h. The distribution ratio of Am(III) and Eu(III) decreased with increase in the concentration of nitric acid. It was also observed that Fe-DGAH showed higher selectivity towards Eu(III) whereas Fe-SDGAH showed higher selectivity towards Am(III). The rate of sorption increased with increase of pH. Based on the slope analysis of extraction data, two H^+ ions were released for the extraction of a trivalent metal ion and the other charge of the cation seems to be compensated by the co-extraction of nitrate from aqueous phase. DTPA was employed as an aqueous complexing agent for improving the separation factor of Eu(III)/Am(III) by using Fe-DGAH. The concentration of DTPA needed for efficient separation of Am(III) from Eu(III), was optimized (0.05 M DTPA at pH 2) and the study confirmed the feasibility of separating Am(III) from Eu(III) with a separation factor of ~150 by using Fe-DGAH.

7.9. References

1. K. A. Arteaga, J.A. Rodriguez, E. Barrado. Magnetic solids in analytical chemistry. Anal. Chim. Acta 674 (2010) 157–165.
2. G. Giakisikli, A.N. Anthemidis, Magnetic materials as sorbents for metal/metalloid preconcentration and/or separation. A review. Anal. Chim. Acta 789 (2013) 1–16.
3. Y. Liu, M. Chen, H. Yongmei, Study on the adsorption of Cu (II) by EDTA functionalized Fe_3O_4 magnetic nano-particles. Chem. Eng. J. 218 (2013) 46–54.
4. L.L. Vatta, J. Kramer, K.R. Koch, Diethylenetriamine Functionalized Silica Coated Magnetite Nanoparticles for Selective Palladium Ion Extraction from Aqueous Solutions. Sep. Sci. Technol. 42 (2007) 1985–2002.
5. M. E. Mahmoud, M.S. Abdelwahab, E.M. Fathallah, Design of novel nano-sorbents based on nano-magnetic iron oxide–bound-nano-silicon oxide–immobilized-triethylenetetramine for implementation in water treatment of heavy metals. Chem. Eng. J. 223 (2013) 318–327.

6. A. Afkhami, R. Norooz-Asl, Removal, preconcentration and determination of Mo(VI) from water and wastewater samples using maghemitenanoparticles, Colloids Surf., A 346 (2009) 52–57.
7. L. Chen, Y. Huang, L. Huang, B. Liu, G. Wang, S. Yu, S. Characterization of Co(II) removal from aqueous solution using bentonite/iron oxide magnetic composites, J. Radioanal. Nucl. Chem. 290 (2011) 675–684.
8. P.H. Towler, J.D. Smith, D.R. Dixon, Magnetic recovery of radium, lead and polonium from seawater samples after preconcentration on a magnetic adsorbent of manganese dioxide coated magnetite. Anal. Chim. Acta 328 (1996) 53–59.
9. D. Wu, Y. Sun, Q. Wang, Adsorption of lanthanum (III) from aqueous solution using 2-ethylhexyl phosphonic acid mono-2-ethylhexyl ester-grafted magnetic silica nanocomposites, J. Hazard. Mater. 260 (2013) 409– 419.
10. W. Lutze, R.C. Ewing, Radioactive waste forms for future, North-Holland, Oxford, 1988.
11. S. Zhang, Y. Zhang, J. Liu, Q. Xu, H. Xiao, X. Wang, H. Xu, J. Zhou, Thiol modified Fe_3O_4@SiO_2 as a robust, high effective, and recycling magnetic sorbent for mercury removal, Chem. Eng. J. 226 (2013) 30–38.
12. J. S. Suleiman, B. Hu, H. Peng, C. Huang, Separation/preconcentration of trace amounts of Cr, Cu and Pb in environmental samples by magnetic solid-phase extraction with Bismuthiol-II-immobilized magnetic nanoparticles and their determination by ICP-OES, Talanta. 77 (2009) 1579–1583.
13. A. F. Ngomsik, A. Bee, D. Talbot, G. Cote, Magnetic solid–liquid extraction of Eu(III), La(III), Ni(II) and Co(II) with maghemite nanoparticles, Sep. Purif. Technol. 86 (2012) 1–8.

14. G. Yang, L. Tang, X. Lei, G. Zeng, Y. Cai, X. Wei, Y. Zhou, S. Li, Y. Fang, Y. Zhang, Cd(II) removal from aqueous solution by adsorption on α-ketoglutaric acid-modified magnetic chitosan, Appl. Surf. Sci., 292 (2014) 710-716.
15. Y.W. Wu, J. Zhang, J. Liu, L. Chen, Z.L. Deng, M.X. Han, X.S. Wei, A.M. Yu, H.L. Zhang, Fe_3O_4@ZrO_2 nanoparticles magnetic solid phase extraction coupled with flame atomic absorption spectrometry for chromium(III) speciation in environmental and biological samples, Appl. Surf. Sci., 258 (2012) 6772-6776.
16. D. Wu, Y. Sun, Q. Wang, Adsorption of lanthanum (III) from aqueous solution using 2-ethylhexyl phosphonic acid mono-2-ethylhexyl ester-grafted magnetic silica nanocomposites, J. Hazard. Mater. 260 (2013) 409– 419.
17. M. Nilsson, K.L. Nash, A review of the development and operational characteristics of the TALSPEAK process, Solvent Extr. Ion Exch. 25 (2007) 665–701.
18. A.S. Suneesh, R. Kumaresan,S. Rajeswari, P.K. Nayak, K.V. Syamala, K.A. Venkatesan, M.P. Antony, P.R. Vasudeva Rao, Development and demonstration of americium (III)-europium (III) separation using diglycolamic acid, Sep. Sci. Technol. 48 (2013) 1998-2006.
19. A.S. Suneesh, R. Jain, K.A. Venkatesan, M.P. Antony, BM Bhanage, P.R. Vasudeva Rao, Novel Diglycolamic Acid Functionalized Iron Oxide Particles for the Mutual Separation of Eu (III) and Am (III), Solv. Extr. Ion Exch.33 (2015) 656-670.
20. A.S. Suneesh, R. Jain, K.A. Venkatesan, M.P. Antony, BM Bhanage, P.R. Vasudeva Rao, Magnetic Assisted Separation of Trivalent F-Elements from Dilute Nitric Acid Medium, Sep. Sci. Technol. 50 (2015) 2041-2050.

Chapter 8: Summary and scope of future studies

This chapter summarizes the results of the studies aimed at the development of diglycolamic acid class of extractants having desirable properties for the mutual separation of trivalent actinides from trivalent lanthanides and vice-versa. Several alkyldiglycolamic acids have been synthesized and studied to examine the feasibility of using them for the mutual separation of trivalent lanthanides and actinides by liquid-liquid extraction as well as solid-liquid extraction route. In all the experiments Am(III) was used as a representative element for actinide and Eu(III) was used as a representative element for lanthanide. The summary of results is described below.

8.1. Development of bis(2-ethylhexyl)diglycolamic acid and bis(2-ethylhexyl)thio diglycolamic acid for Ln(III)-An(III) by liquid-liquid extraction mode

The extractants, bis(2-ethylhexyl)diglycolamic acid (HDEHDGA) and bis(2-ethylhexyl)thiodiglycolamic acid (HDEHSDGA), developed in the present study are promising candidates for the mutual separation of lanthanides and actinides. Both HDEHDGA and HDEHSDGA can be conveniently dissolved in a traditional diluent, n-dodecane, for studying the liquid-liquid extraction behavior of Am(III) and Eu(III). HDEHDGA showed selectivity for europium (III) in the presence of DTPA in aqueous phase, whereas, the thio-derivative showed superior selectivity for americium(III) in the presence of TPEN in organic phase. Based on the slope analysis of extraction data, two molecules of HDEHDGA or HDEHSDGA were involved in the extraction of trivalents, with the other charge on the cation was compensated by nitrate ion. Among these extractants, HDEHSDGA shows the potential of separating actinides from lanthanides in a single contact with a separation factor of ~2600 at pH 3. Though, HDEHSDGA offered high separation factors of the order of ~3000, HDEHDGA was chosen for the mixer-settler demonstration run owing to the fact that sulfur containing extractants are less stable towards high nitric acid and radiation background.

A method was also developed for the demonstration of mutual separation of Am(III) and Eu(III) from dilute nitric acid medium by using a solution of 0.1 M HDEHDGA/n-DD. Unlike the other lanthanide-actinide separating extractants in use, HDEHDGA was made up of CHON- atoms and compatible with a nuclear diluent, n-dodecane. Quantitative extraction of Am(III) and Eu(III) was achieved in 2-3 contacts with the use of 0.1 M HDEHDGA/n-DD, at pH 3. Under this condition, the co-extraction of unwanted metal ions such as Zr(IV) and Ru(III) was negligible. The conditions needed for the selective recovery of Am(III) from the loaded organic phase was optimized. By using 0.01 M DTPA-0.025 M CA at pH 1.5, more than 96% of Am(III) could be recovered from the loaded organic phase after 20-stages in a mixer-settler. However, the stripping of Eu(III) was only 2%. The results, therefore, confirmed the feasibility of using HDEHDGA/n-DD for the mutual separation of Eu(III) and Am(III) from nitric acid medium.

8.2. Development of Tulsion ADS 400 resin impregnated alkyldiglycolamic acid for the mutual separation of Ln(III)-An(III)

The alkyl derivatives of diglycolamic acid with alkyl group varied from butyl to decyl group were prepared and studied for the mutual separation of Am(III) and Eu(III) by extraction chromatography. The glycolamic acids were impregnated on Tulsion ADS 400 and the extraction behavior of Eu(III) and Am(III) in the impregnated resin was studied as a function of various parameters. While the separation factor of Eu(III) over Am(III) remained at ~2 in the absence of DTPA, the separation factor increased to ~15 when 0.005 M DTPA was present in aqueous phase. Based on the optimized conditions, the column study was performed for chromatographic separation. The study confirmed the feasibility of using octyl diglycolamic acid impregnated resin for the mutual separation of Eu(III) and Am(III) by extraction chromatography.

8.3. Polyamine resin anchored with diglycolamic acid for the mutual separation of Ln(III)-An(III)

Diglycolamic acid (PA-DGAH) anchored polyamine matrix was prepared and studied for the extraction of americium(III) and europium(III) from dilute nitric acid medium. Pseudo-second order rate of extraction of Am(III) and Eu(III) was observed in PA-DGAH and the rate constant (k_2) was determined to be 10^{-3} L.mol^{-1}.min^{-1}. The extraction equilibrium was established in four hours. The distribution coefficient of Am(III) and Eu(III) decreased with increase in the concentration of nitric acid. The slope analysis of extraction data, indicated the release of two H^+ ions for the extraction of a trivalent metal ion. The extraction was also accompanied by co-extraction of nitrate from aqueous phase. The concentration of DTPA needed for efficient separation of Am(III) from Eu(III) was optimized to be 0.03 to 0.05 M at pH 3. The study confirmed the feasibility of separating Am(III) from Eu(III) with a separation factor of ~45 by using PA-DGAH.

8.4. Silica functionalized diglycolamic acids for Ln(III)-An(III) mutual separation

A novel diglycolamic acid functionalized silica gel (Si-DGAH) was prepared and studied for the separation of americium(III) and europium(III) from dilute nitric acid medium. The TG-DTA, SEM-EDX and elemental analysis carried out on the adsorbent, confirmed the presence of diglycolamic moieties (1.2 mmol/g) on the surface of silica gel. Rapid adsorption of Am(III) and Eu(III) was observed in the initial stages of adsorption followed by the establishment of equilibrium occurring within 30 minutes. The distribution coefficient of Am(III) and Eu(III) decreased with increase in the concentration of nitric acid. The rate of adsorption increased with increase of pH and the first order rate constant was determined to be 0.20 min^{-1} for Am(III) and 0.32 min-1 for Eu(III) at pH 2. Based on the slope analysis, the extraction of Am(III) and Eu(III) was accompanied by the co-extraction of a nitrate ion and release two H^+ ions to aqueous phase. The DTPA concentration needed for the mutual separation of Am(III) from Eu(III), was optimized to be 0.05 M at pH 2. The study confirmed the possibility of using Si-DGAH for the separation of trivalent f-block elements from dilute nitric acid medium.

8.5. Magnetic assisted extraction for the mutual separation of lanthanides and actinides

A couple of magnetic solid phase adsorbents Fe-DGAH and Fe-SDGAH were synthesized and studied for separating trivalent lanthanides and actinides. The magnetic adsorbents were characterized by TG-DTA, SEM-EDX and XRD. The results confirmed the presence of diglycolamic moieties on iron oxide particles. Rapid sorption of Am(III) and Eu(III) was observed in the initial stages of sorption followed by the establishment of equilibrium occurring within 2 h. The distribution ratio of Am(III) and Eu(III) decreased with increase in the concentration of nitric acid. It was also observed that Fe-DGAH showed higher selectivity towards Eu(III) whereas Fe-SDGAH showed higher selectivity towards Am(III). The rate of sorption increased with increase of pH. Based on the slope analysis of extraction data, two H^+ ions were released for the extraction of a trivalent metal ion and the other charge of the cation compensated by the co-extraction of nitrate from aqueous phase. DTPA was employed as an aqueous complexing agent for improving the separation factor of Eu(III)/Am(III) by using Fe-DGAH. The concentration of DTPA needed for efficient separation of Am(III) from Eu(III), was optimized (0.05 M DTPA at pH 2) and the study confirmed the feasibility of separating Am(III) from Eu(III) with a separation factor of ~150 by using Fe-DGAH.

8.6. Scope for future studies

The diglycolamic acid, HDEHDGA, was studied for the extraction of actinides, lanthanides, other fission products, and corrosion products from citric acid medium as well as from fast reactor fuel simulated HAW. On the basis of batch studies a demonstration experiment was carried out with actual fast reactor HAW. However, HDEHSDGA was examined only for the extraction of limited number of metal ions. The extraction behaviors of other metal ions which are likely to be present in HAW need to be studied for HDEHSDGA. Demonstration of mutual separation of Eu(III) and Am(III) was studied by using diglycoloamic acid impregnated resins. More studies need to carry out with simulated and actual HAW to establish a separation method for the mutual separation of lanthanides and actinides by using diglycolamic acid impregnated resins. Similarly, other solid phase reagents such as polyamine diglycolamic acid (PA-DGAH), silica diglycolamic acid (Si-DGAH) and iron oxide functionalized diglycolamic acid (Fe-DGAH) etc have been studied for understanding the extraction behavior of lanthanides, actinides etc. However, detailed studies of the extraction of metal ions from actual fast reactor HAW need to be studied. In this context, more studies need to be carried out for establishing a solid phase extraction based mutual separation of lanthanides and actinides. Similarly, use of iron oxide functionalized diglycolamic acid for the magnetic solid phase separation (MSPS) has been established in laboratory scale only. Therefore, more studies are required to develop a large scale demonstration facility by using MSPS technique.

The present thesis aimed at developing novel diglycolamic acid based extractants and solid phase reagents for the mutual separation of lanthanides and actinides. No attempt was made to understand the radiation and chemical stability of the reagents, and nature of possible degradation products. The radiation stability under various exposures and the hydrolytic stability can also be studied.

It was observed that the extractive properties largely varied with alkyl chains attached to the diglycolamic acid. Therefore, it is imperative to investigate the fundamental property of diglycolamide that governs the extraction behavior. In order to understand the physical and extractive properties of diglycolamic acid based extractants, knowledge about metal-ligand complexation at molecular level is essential for getting an insight in to those observations. Moreover, such molecular level approach would help in designing and developing the advanced solvents that minimize the drawbacks of the present extractants. Molecular dynamics (MD) simulations have been extensively employed for understanding the conformations of organic molecules and insights of solvent extraction and solid phase separations. No attempt was made to investigate metal–ligand complexation phenomenon by molecular dynamics calculations. Therefore, MD simulations on diglycolamic acid and DFT calculations on the co-ordination behavior of actinides with diglycolamic acids can be studied in future.

GLOSSARY

ADSs	Accelerated driven subcritical systems
AHWR	Advanced Heavy Water Reactors
An	Actinide
APTS	Triethoxytriaminopropylsilane
Bq/L	Becquerel per litre
BTBP	6,6’-bis(5,6-dialkyl- [1,2,4]-triazin-3-yl)-2,2’-bipyridine
BTP	2,6-bis-(1,2,4-triazine-3-yl)pyridines
BWR	Boiling water reactor
CA	Citric acid
$CDCl_3$	Deuterated $CHCl_3$
CHNS	Carbon, Hydrogen, Nitrogen, Sulfur analyser (Elemental analyser)
CMPO	Octyl,phenyl N,N-diisopropylcarbomylmethylphosphine oxide
δ	Chemical Shift value of NMR
n-DD	*n*-Dodecane
DGA	Alkyl diglycolamides
DGAA	Diglycolamic acid
DIDPA	Di-*iso*-decylphosphoric acid
DIPB	1,4-Di-*iso*-propylbenzene
D_M	Distribution ratio of metal ions
DPAH	dithiophosphinic acid
DTPA	Diethylene triaminepentaacetic acid
DTG	Derivative of thermogravimetry
DVB	Divinylbenzene
EDTA	Bis(ethylenediaminetetraacetic acid)
EDX	Energy Dispersive X-ray
FBR	Fast Breeder Reactors
FBTR	Fast Breeder Test Reactor
Fe-DGAH	Iron oxide (Fe_3O_4) particle functionalized with diglycolamic acid
Fe-SDGAH	Iron oxide (Fe_3O_4) particle functionalized with thiodiglycolamic acid

FP	Fission products
FTIR	Fourior transformation infra red spectrospcopy
GANEX	Group actinide extraction
GWe	Giga Watt (electrical)
HAW	High-active waste
HDBDGA	N,N-Dibutyldiglycolamic acid
HDDDGA	N,N-Didecyldiglycolamic acid
HDEHDGA	Bis(2-ethylhexyl)diglycolamic acid
HDEHP	N,N-diethylhexylphosphoric acid
HDEHSDGA	Bis(2-ethylhexyl)thiodiglycolamic acid
HDHDGA	N,N-Dihexyldiglycolamic acid
HDODGA	N,N-Dioctyldiglycolamic acid
HpGe	High pure germanium
HSAB	Hard and Soft Acids and Bases
ICP-OES	Inductively coupled plasma-optically emission spectrometry
JCPDS	Joint Committee on Powder Diffraction Standards (XRD standards)
KAMINI	KAlpakkam MINI reactor
K_d	Distribution coefficient of metal ions
keV	Kilo electron volts
LIX 63	5,8-Diethyl-7-hydroxy-6-dodecanone oxime
LIX 64	2-Hydroxy-5-dodecylbenzophenone oxime
Ln	Lanthanide
LWR	Light water reactor
MA	Minor actinide
MeV	Million electron volts
MP	Magnetic particles
MSPS	Magnetic Solid phase Separation
MW_t	Mega watt (thermal)
NaI(Tl)	Sodium iodide (Thalium) analyser
NMR	Nuclear magnetic resonance spectrum
OFS	Organofunctionalized adsorbents
P&T	Partitioning and transmutation

PA-DGAH	Polyamine resin modified diglycolamic acid
PHWR	Pressurized Heavy Water Reactors
PUREX	Plutonium Uranium Reduction EXtraction
PWR	Pressurized water reactor
SANEX	Selective actinide extraction
SEM	Scanning Electron Microscopy
SF	Separation factor
Si-DGAH	Silica anchored diglycolamic acid
SIRs	Solvent impregnated resins
SNF	Spent nuclear fuel
SPE	Solid phase extractants
TALSPEAK	Trivalent Actinide Lanthanide Separation by Phosphorus Extractants from Aqueous Komplexes
TBP	Tri-n-butyl phosphate
TEHDGA	N,N,N’,N’-tetra-2-ethylhexyldiglycolamide
TEOS	Tetraethoxysilane
Terpy	2,2’,6’,2”-terpyridine
TG-DTA	Thermogravimetric-Differential thermal analyzer
TODGA	N,N,N’,N’-tetra-octyldiglycolamide
TOPO	Tri-octylphosphine oxide
TPEN	tetrakis(2-pyridylmethyl)ethylenediamine
TPTZ	2,4,6-tripyridyl-1,3,5-triazine
TRUEX	Transuranic extraction
TRUSPEAK	Transuranic extraction-transuranium elements extraction by phosphours based reagents from aqueous Komplexing agents
TTA	Thenoyltrifluoro acetone
XRD	X-ray diffraction